10.13147/SOE.2025.15

DISSERTATION FOR DOCTORAL (PHD) DEGREE

Indic Boris

University of Sopron

Faculty of Wood Engineering and Creative Industries

Sopron, Hungary

2025

10.13147/SOE.2025.15

10.13147/SOE.2025.15

DISSERTATION FOR DOCTORAL (PhD) DEGREE

University of Sopron
Faculty of Wood Engineering and Creative Industries,
József Cziráki Doctoral School of Wood Sciences and Technologies

Comparative transcriptomic studies of plant - *Armillaria* interactions

in
Material Science and Technology
PhD Program: Fibre- and Nanotechnologies

Author: Indic Boris
Supervisor: Dr. Sipos György

Sopron, Hungary
2025

10.13147/SOE.2025.15

Comparative transcriptomic studies of plant - *Armillaria* interactions

Dissertation for doctoral (PhD) degree
University of Sopron József Cziráki Doctoral School
of Wood Sciences and Technologies
Fibre- and Nanotechnologies programme

Written by:

Indic Boris

Made in the framework of Fibre- and Nanotechnologies programme

of the József Cziráki Doctoral School, University of Sopron

Supervisor: Dr. Sipos György
I recommend for acceptance (yes / no)

(signature)

The candidate reached …..... % at the complex exam,

Sopron, ...
Chairman of the Examination Board

As assessor I recommend the dissertation for acceptance (yes/no)

First assessor (Dr. .....) yes/no
(signature)

Second assessor (Dr. .....) yes/no
(signature)

(Possible third assessor (Dr. .....) yes/no
(signature)

The candidate reached .....% in the public debate of the dissertation

Sopron,

.....
Chairman of the Assessor Committee

Qualification of the doctoral (PhD) degree ….....

.....
Chairman of the University Doctoral
and Habilitation Council (UDHC)

10.13147/SOE.2025.15

DECLARATION

I, the undersigned **Indic Boris** by signing this declaration declare that my PhD thesis entitled **"Comparative transcriptomic studies of plant - Armillaria interactions"** was my own work; during the dissertation I complied with the regulations of Act LXXVI of 1999 on Copyright and the rules of the doctoral dissertation prescribed by the Cziráki József Doctoral School, especially regarding references and citations.[1]

Furthermore, I declare that during the preparation of the dissertation I did not mislead my supervisor(s) or the programme leader with regard to the independent research work.

By signing this declaration, I acknowledge that if it can be proved that the dissertation is not self-made or the author of a copyright infringement is related to the dissertation, the University of Sopron is entitled to refuse the acceptance of the dissertation.

Refusing to accept a dissertation does not affect any other legal (civil law, misdemeanour law, criminal law) consequences of copyright infringement.

Sopron, ... 20....

……..

PhD candidate

[1] **Act LXXVI of 1999** Article 34 (1) Anyone is entitled to quote details of the work, to the extent justified by the nature and purpose of the recipient work, by designating the source and the author specified therein.

Article 36 (1) Details of publicly lectures and other similar works, as well as political speeches, may be freely used for the purpose of information to the extent justified by the purpose. For such use, the source, along with the name of the author, shall be indicated, unless this is impossible.

10.13147/SOE.2025.15

ACKNOWLEDGEMENTS

I extend my deepest gratitude to my supervisor, Prof. Dr. György Sipos, for his exceptional expertise, unwavering guidance, and the scientific and academic environment he provided throughout this research.

My sincere thanks also go to Dr. László Nagy, Neha Sahu, and the entire Department of Microbiology at the University of Szeged. Their collaborative spirit and generous assistance greatly facilitated my work.

I am deeply grateful to Dr. Simang Champramary, my lab buddy and now a dear friend, for his invaluable advice and support, both in the lab and beyond.

To Hana, Zsolt, Klaudia, Munif, Amelia, Doa and Effie, whom I had the privilege of befriending during my time in Sopron, thank you for being there, improving and making this experience so much more special.

To Kaja, Katrin, Mrva, Keti, Vels, Ivana, Masa, Marina, Milan, Jovana, Filip, Dusan, I am deeply grateful and blessed for having you all in my life.

I would also like to thank my family, Gaga, Benjo, baka Vinka, Cedo, Ana, and Maki, for their unwavering patience, support and encouragement.

Most importantly, I want to express my deepest gratitude to my mother for her unconditional love and the countless sacrifices she made. Her belief and hard work in me made this possible. V.t.

TABLE OF CONTENTS

LIST OF ABBREVIATIONS

Auxiliary activity family (AA)

Carbohydrate-active enzymes (CAZymes)

Carbohydrate-binding module family (CBM)

Carbohydrate-binding modules (CBM)

Carbohydrate esterases (CE)

Cell wall degradation (CWD)

Cell wall–degrading enzyme (CWDE)

Differentially expressed genes (DEGs)

Endoplasmic reticulum (ER)

Flavin adenine dinucleotide (FAD)

Glucose-methanol-choline oxidoreductase (GMC oxidoreductase)

Glycoside hydrolase (GH)

Homogentisate 1,2-dioxygenase (HGD)

Hydrogen peroxide (H_2O_2)

Multi-dimensional scaling (MDS)

Pectate lyase B (*pelB*)

Plant cell wall-degrading enzymes (PCWDEs)

Pathogen host interaction database (PHIbase)

Polycyclic aromatic hydrocarbons (PAHs)

Polysaccharide lyases (PL)

Protein disulfide isomerases (PDIs)

Reactive oxygen species (ROS)

Rice, sawdust, tomato and oranges medium (RSTO)

Roth and Shaw medium (RS medium)

White-rot (WR)

ABSTRACT

Armillaria fungi, recognized as major plant pathogens, can cause significant losses both in forestry and agriculture. They contribute to forest decline with their ability to infect living trees and by possessing formidable capabilities to decompose wood. In order to develop effective management strategies, it is crucial to understand their mechanisms for plant infection and wood decay.

By investigating the enzymatic profiles of two *Armillaria* species with contrasting lifestyles, the highly virulent pathogen *Armillaria ostoyae* and the mostly saprophytic and secondary pathogen *Armillaria borealis*, this study addresses this gap in knowledge. Key players involved in their pathogenicity strategies and wood degradation capabilities were identified by using transcriptome analysis and homology searches on cultivated strains.

Our analysis revealed species-specific variations in virulence factors, in addition to identifying a repertoire of plant cell wall degrading enzymes in both fungi. Coinciding with their more aggressive infection strategy, *A. ostoyae* exhibited a higher abundance of enzymes targeting plant cell walls, including possessing a potentially stronger lignin and pectin degradation arsenal.

Beside plant pathogenicity and wood degradation, this research also explored the mycoremediation potentials of these fungal species. Both *A. ostoyae* and *A. borealis* displayed a promising genetic repertoire for the breakdown of various monocyclic aromatic compounds that might be utilised in bioremediation of the contaminated environments.

This research provides valuable insights into virulence and wood decay mechanisms of *Armillaria* and provides the groundwork for the future studies that should ultimately lead to development of effective control strategies. Alongside this, it emphasises their possible use in bioremediation, particularly of monocyclic aromatic compounds.

1. INTRODUCTION

Forests play a vital role in maintaining ecological balance and supporting economic sustainability. However, they are constantly threatened by various environmental pressures, and soil-borne fungal pathogens like *Armillaria* species. These fungi ravage forests worldwide, causing severe root rot and ultimately leading to tree death. With a very wide host range, *Armillaria* fungi pose a significant threat to the health and diversity of forest ecosystems, resulting in substantial ecological and economic losses.

While current control methods offer limited effectiveness, recent advancements in genomics, particularly transcriptomics, offer powerful tools to unveil the secrets of these complex plant-pathogen interactions.

Leveraging these innovative tools, the present study delves into an extensive comparative genomic and transcriptomic analysis. We focused on the interactions between Norway spruce (*Picea abies*) and two *Armillaria* species representing contrasting lifestyles: the highly virulent pathogen *A. ostoyae* and the opportunistic pathogen *A. borealis*. Furthermore, to gain deeper insights into virulence variations, we employed high and low virulent isolates within each species.

Our primary goals were to identify fungal genes and pathways that play key roles in three critical aspects of the interaction:

- **Pathogenicity**: Understanding the molecular basis of the virulence of *A. ostoyae* and *A. borealis* will provide crucial knowledge for developing targeted control strategies.
- **Wood degradation**: Deciphering the mechanisms employed by these fungi to decompose wood will provide insights into its spread and potential for industrial and bioremediation applications.
- **Mycoremediation**: Investigating the potential of *A. ostoyae* and *A. borealis* in breaking down environmental toxins could open up new possibilities for bioremediation.

This study seeks to uncover the intricate relationship between these fungi and plants, offering valuable knowledge on their molecular interactions and serving as a foundation for innovative strategies to manage *Armillaria* spread and combat other plant diseases. Ultimately, this research holds the potential to contribute significantly to protecting the health and resilience of forests.

1.1. Forest ecosystems

Forests are essential ecosystems filled with life that provide habitat and sustenance to countless species. They also have a significant impact on global processes including carbon sequestration, water resource regulation, and biodiversity. However, together with natural processes including climate and soil characteristics, human activities such as deforestation, logging, and pollution upset this delicate balance, reducing forest health and making them more vulnerable to plant infections (Sands, 2013; Kelvin et al., 2015).

1.2. Plant cell wall

The plant cell wall serves as the primary defence barrier of plant cells. It is composed of cellulose, hemicellulose, pectin, lignin, and various proteins (Figure 1), and beside protecting the cell from external damage it also provides mechanical support and regulates the development of cells. Differences in structure and composition of the cell wall components among species, cell types, and developmental stages, allow for adaptation to environmental challenges (Showalter, 1993; Mansora et al., 2019). Overcoming this barrier is essential for the fungi to establish its pathogenicity and thus it is critical to understand the molecular interactions between *Armillaria* and plant cell walls.

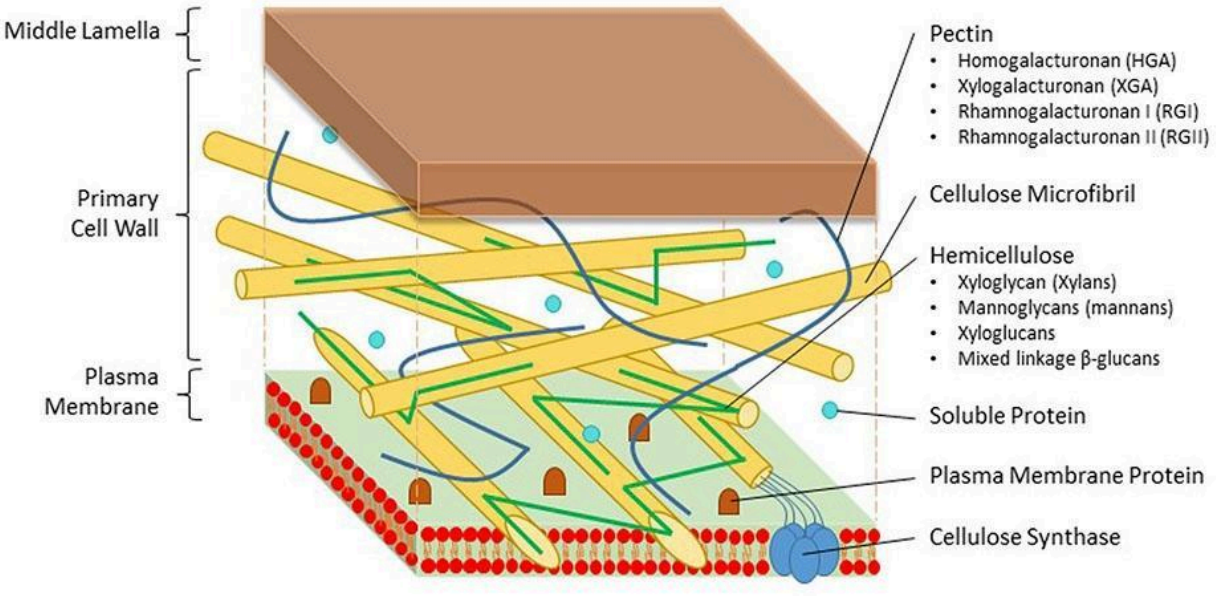

Figure 1. Structure of the plant cell wall (Loix et al., 2017)

1.3. Wood degradation

Degradation of wood is a naturally occurring process and it is a result of complex interplay of physical, chemical, and biological mechanisms. Although it is essential to the cycling of nutrients in forest ecosystems, it also affects the economic value and structural integrity of wood products (Zabel and Morrell, 2012; Goodell et al., 2020). During this process, the key components of plant cell walls undergo degradation with fungi, notably white-rot fungi, being recognized as highly efficient wood degraders. These organisms secrete a wide array of enzymes, such as cellulases, hemicellulases, and ligninases, which possess the ability to break down the complex polymers present in wood (Sánchez, 2009; Li et al., 2022). White-rot fungi exhibit particular proficiency in deconstructing lignin, the most resilient component, utilising specific enzymes like lignin peroxidases (Martinez et al., 2004; Goodell et al., 2008). The characteristic "white rot" appearance observed in deteriorated wood is a result of the degradation process by white-rot fungi.

A prominent example of a white-rot fungus is *Armillaria*, notorious for causing the destructive white root rot in plants (Schilling et al., 2021). *Armillaria* infects trees through the roots, instigating decay and eventually leading to the death of the host. Noteworthy is *Armillaria*'s capacity to degrade all of the primary constituents of the plant cell wall, which contributes to its destructive nature (Blanchette, 1991; Kirk and Cullen, 1998; Li et al., 2022).

Additionally, white-rot fungi play a significant role in the global carbon cycle, helping to break down dead wood and other plant materials in the ecosystem (Stokland et al., 2012). Understanding the intricate mechanisms employed by *Armillaria* to overcome the formidable defences of plant cell walls and degrade wood is crucial for developing effective strategies to combat this destructive pathogen.

1.4. The genus *Armillaria*

The genus *Armillaria* encompasses a diverse group of fungi notorious for causing white root rot disease in a wide range of woody plants, including trees, shrubs, and vines (Dettman and van der Kamp, 2001; Zolciak, 2007; Petchayo Tigang et al., 2020; Kedves et al., 2021). Classified within the phylum Basidiomycota, *Armillaria* fungi are easily recognizable due to their unique shoe-string-like structures called rhizomorphs (Anderson and Kohn, 1995).

Additionally, they produce large, fleshy fruiting bodies (mushrooms) often described as "honey fungi" due to their characteristic golden colour (Gonthier, 2010, Heinzelmann et al., 2019). *Armillaria* fungi are essential components of forest ecosystems due to their role as decomposers, facilitating nutrient cycling through the breakdown of plant materials (Sipos et al., 2017). However, their ability to degrade plant cell walls also positions them as significant plant pathogens (de Vries et al., 2001; Lundell et al., 2014). This dual role has far-reaching economic and ecological implications, such as reduced forest productivity, loss of biodiversity, crop damage, and heightened susceptibility to secondary infestations (Baumgartner et al., 2011; Ross-Davis et al., 2013; Heinzelmann et al., 2019; Balla et al., 2021).

1.4.1. Distribution determinants of *Armillaria* species

Armillaria species exhibit a global distribution, influenced by climate, soil conditions, host availability, and human activities (Coetzee et al., 2018). Climate plays a major role, with temperate and humid regions favouring most species, while others have adapted to drier or colder environments (Heinzelmann et al., 2019). Moisture availability, crucial for *Armillaria* growth, is strongly affected by climate. Species like *A. mellea* thrive in high moisture areas, while *A. gallica* demonstrates wider adaptability (Mihail et al., 2002). Soil conditions also influence distribution, with most species preferring well-drained soils with specific organic matter content and pH (Singh, 1983; Kile, 1993; Brazee et al., 2012). Host availability is another key factor, with most *Armillaria* species associated with forest trees, though some inhabit non-forest environments with herbaceous plants (Kile, 1993; Smith et al., 2008). Finally, human activities like logging and introducing non-native trees can alter the distribution of *Armillaria* by creating favourable conditions for their establishment and spread (Hood et al., 2001; Kubiak et al., 2017).

1.4.2. Distribution of *Armillaria* species

As highlighted earlier, *Armillaria* fungi exhibit a widespread global distribution, with variations in species richness across regions (Figure 2) (Sipos et al., 2018; Kedves et al., 2021). The diversity of *Armillaria* species is particularly prominent in East Asia, while the Southern Hemisphere generally has a lesser abundance of species (Kim et al., 2022).

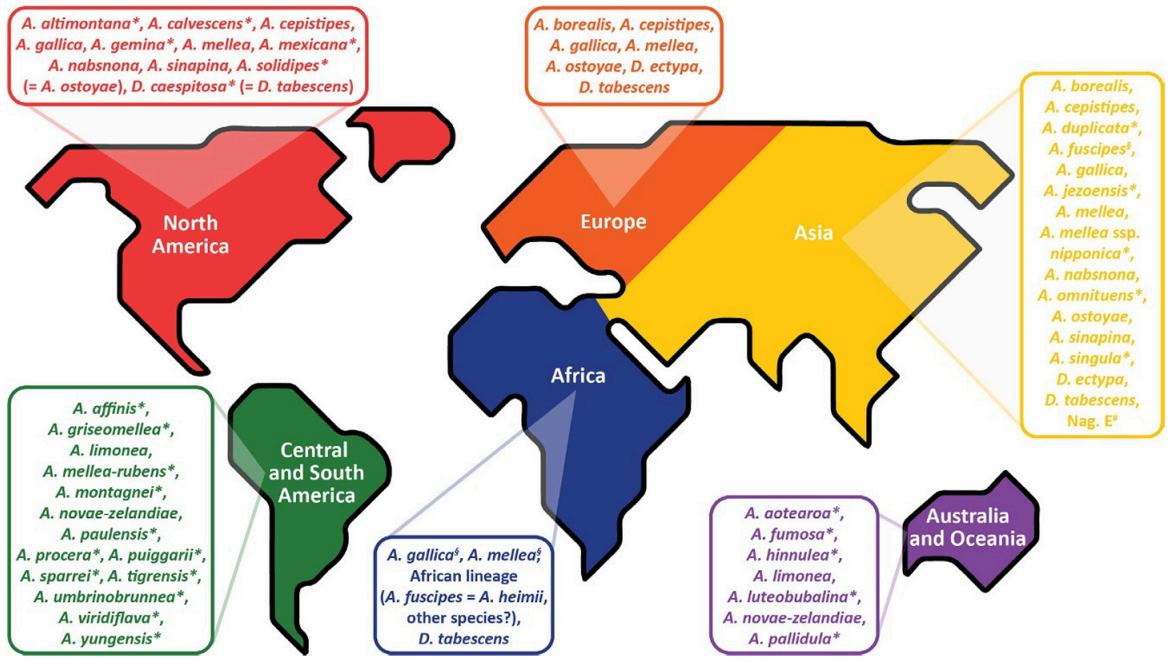

Figure 2. Geographic distribution of *Armillaria* and *Desarmillaria* species (Kim et al., 2022).

- **North America:** *Armillaria* species are found in both temperate and tropical regions. Examples include the widely distributed *A. mellea* and the large colony-forming *A. solidipes* (Bruhn et al., 2000; Kedves et al., 2021).
- **Europe:** Distribution is influenced by climate, with species like *A. gallica* found in temperate and boreal regions, and *A. ostoyae* in arid or Mediterranean areas (Koch et al., 2017; Kim et al., 2022). *A. borealis* reaches the northernmost European forests (Roll‐Hansen, 1985).
- **Asia:** At least 16 species are reported, with *A. ostoyae, A. mellea,* and *D. tabescens* considered the most significant pathogens in East Asia (Kim et al., 2022).

- **Australia:** At least seven species are present in native and introduced forests. *A. luteobubalina* dominates eucalyptus forests, while *A. novae-zelandiae* is widespread across Oceania region (Koch et al., 2017; Kim et al., 2022).
- **Africa:** Alongside endemic lineages in sub-Saharan regions, introduced species like *A. gallica* and *A. mellea* are present in South Africa (Kim et al., 2022).

1.4.3. Host preferences of *Armillaria* species

The host preferences of *Armillaria* species vary greatly, with some being generalists that infect a variety of plants while others are specialists targeting specific species (Heinzelmann et al., 2019).

In the Northern Hemisphere, *Armillaria* species can infect both conifers and hardwoods. For example, *A. mellea* tends to infect hardwoods such as oak and maple, while *A. ostoyae* prefers conifers like spruce and pine (Koch et al., 2017; Sipos et al., 2018). *A. gallica* and *A. cepistipes* are considered weaker pathogens with broader host ranges, while *A. borealis* targets both deciduous and coniferous trees (Kedves et al., 2021; Akulova et al., 2020).

Southern Hemisphere species also display diverse preferences. *A. luteobubalina* specialises in eucalyptus in Australia, while *A. novae-zelandiae* infects oaks (Kim et al., 2022). Africa's *A. fuscipes*, an opportunistic pathogen, has a broad host range including trees, shrubs, and agricultural crops (Kim et al., 2022).

1.4.4. Life cycle of *Armillaria* fungi

The life cycle of *Armillaria* fungi is complex, and in contrast to many basidiomycetes that maintain a long-lived dikaryotic vegetative state, *Armillaria* predominantly exists in a diploid state (Korhonen and Hintikka, 1974; Baumgartner et al., 2011). The life cycle commences with the dispersal of basidiospores, the sexual spores of *Armillaria*, through wind, water, or animal vectors (Koch et al., 2017). Upon landing on suitable substrates like decaying wood or host plant roots, these spores germinate and develop into diploid mycelia. This vegetative growth then gives rise to the aforementioned rhizomorphs critical for long-distance exploration and colonisation of new areas and hosts (Garbelotto, 2004; Kim et al., 2022).

Upon encountering a suitable host, *Armillaria* can adopt either a symbiotic or parasitic interaction with the plant's roots (Kedves et al., 2021). During the parasitic stage, the fungus infiltrates the living tissues of the host, extracting nutrients and causing root decay, wilting, and ultimately plant death (Gao et al., 2010). Additionally, *Armillaria* forms dense networks of rhizomorphs within the infected roots and surrounding soil, ensuring its persistence and facilitating the spread of the infection (Rishbeth, 1985).

Under favourable environmental conditions, typically cool and moist, *Armillaria* produces its fruiting bodies above ground (Baumgartner et al., 2011; Travadon et al., 2012). These basidiocarps harbour basidia, specialised structures responsible for generating the next generation of basidiospores. The release of these spores into the environment completes the cycle, enabling the dispersal of the fungus to new locations (Rishbeth, 1985; Coetzee et al., 2018). Additionally, when compatible mating types meet, *Armillaria* can undergo sexual reproduction. The process involves combining hyphae from different mating types to create a dikaryotic mycelium, which then generates new fruiting bodies and spores to continue the life cycle (Baumgartner et al., 2011). This is affected by various factors, such as environmental conditions, the host plant species, and the genetics of the fungus itself.

1.4.5. Interactions between *Armillaria* and plants

Armillaria fungi interact with plants in different ways, adapting their behaviour based on the environment and the host they encounter. Some *Armillaria* species are able to survive on both living and dead organic matter as facultative necrotrophs, while others function only as saprophytes, breaking down dead wood (Shaw and Kile, 1991; Baumgartner et al., 2011). This adaptability allows *Armillaria* to form extensive ecological networks encompassing multiple host species within a forest ecosystem (Devkota and Hammerschmidt, 2020; Kedves et al., 2021). The nature of these interactions can be categorised as pathogenic, saprophytic, or even symbiotic.

The most well-known interaction is the pathogenic one, where *Armillaria* acts as a destructive parasite of living plants. In this stage, the fungus infiltrates the root cambium of the host plant, resulting in root rot and eventually causing the plant to die. The extent of this damage is influenced by different factors, such as the particular *Armillaria* species at play, the vulnerability of the host plant, and the environmental conditions at the time (Fox, 2000;

Robinson, 2010; Baumgartner et al., 2011; Kedves et al., 2021). Following the death of the host, *Armillaria* seamlessly transitions to a saprophytic phase, decomposing the dead wood tissues and causing white rot (Baumgartner et al., 2011). This decomposition process not only contributes to nutrient cycling but also creates suitable niches for other organisms like insects and fungi to colonise.

Not all *Armillaria* species exhibit a pathogenic stage. Certain species operate only as saprophytes and are crucial in forest ecosystems as they decompose the organic material (Baumgartner et al., 2011). Additionally, there are species that form symbiotic partnerships with specific plants. For instance, *Armillaria* has been found to have mycorrhizal associations with orchid species such as *Galeola* and *Gastrodia* (Guo et al., 2016; Koch and Herr, 2021). One such example is the rare Chinese medicinal plant, *Gastrodia elata*, which relies on *Armillaria* species as essential symbionts for its survival (Zhan et al., 2020).

By acknowledging both the detrimental and beneficial roles of *Armillaria*, we can develop strategies to promote the growth and productivity of forest trees while minimising the damage caused by *Armillaria* root rot disease.

1.4.6. Diversity of the *Armillaria* genus

The *Armillaria* genus, part of the Armillarioid clade together with *Desarmillaria* and *Guyanagaster* genera, that emerged in Eurasia 51 million years ago, exhibits remarkable diversity (Koch et al., 2017; Koch and Herr, 2021). Despite challenges in classification due to morphological similarities and traditional methods' limitations, over 70 *Armillaria* species are currently identified, with many more likely undiscovered (Hanna et al., 2007; Sipos et al., 2018; Heinzelmann et al., 2019; Kedves et al., 2021). Molecular analysis using markers like internal transcribed spacer (ITS) and translation elongation factor 1α (*tef1*) reveals significant genetic variation among species (Harrington and Wingfield, 1995; Pérez-Sierra and Henricot, 2002; Sicoli et al., 2003; Maphosa et al., 2006; Keča et al., 2006; Matheny et al., 2007; Brazee et al., 2011; Heinzelmann et al., 2019). This diversity extends to ecology and biology, with *Armillaria* species displaying varied host preferences, stress responses, and interactions with other soil organisms (Kedves et al., 2021). Understanding this diversity is crucial for uncovering adaptation mechanisms, developing management strategies for *Armillaria*-related infections, and conserving rare species.

1.4.7. Infection strategies of *Armillaria* species

The infection mechanisms employed by *Armillaria* fungi are highly adaptable, allowing them to infect a diverse array of plants, including trees and herbaceous species (Kedves et al., 2021). The parasitic or saprotrophic nature of *Armillaria* species is characterised by various strategies developed to interact with host plants, influenced by factors such as host susceptibility, environmental conditions, and competition with other fungi (Baumgartner et al., 2011; Heinzelmann et al., 2019; Devkota and Hammerschmidt, 2020).

Armillaria utilises multiple strategies for breaching plant defences, including:

- **Direct penetration:** The fungus physically pierces the host's root cell wall for direct invasion (Devkota and Hammerschmidt, 2020).
- **Wound colonisation:** Existing wounds like cuts or abrasions serve as entry points for the fungus (Cleary et al., 2012).
- **Mycelial bridges:** The fungus connects nearby plants with its mycelium, facilitating infection spread (Baumgartner et al., 2011).

Beyond these infection mechanisms, *Armillaria* species deploy a sophisticated arsenal of enzymes and secondary metabolites to optimise their invasive processes. Notably, plant cell wall degrading enzymes (PCWDEs), particularly those associated with chitin-binding and pectin degradation, emerge as pivotal contributors to the pathogenicity potential of *Armillaria* species (Sipos et al., 2017).

1.5. Molecular mechanisms of *Armillaria*-plant interactions

The complex dynamics between *Armillaria* species and their plant hosts occur at the molecular level, influencing colonisation success, disease progression, and plant defence reactions (Coetzee et al., 2018). A comprehensive understanding of these mechanisms is essential for devising effective strategies against *Armillaria* diseases (Coetzee et al., 2018; Kedves et al., 2021).

The successful establishment of the fungal colonisation hinges on its capacity to overcome the plant's defence mechanisms and alter the plant's physiology to create a favourable environment for its growth and survival. A critical aspect of this offensive approach is the

utilisation of PCWDEs (Baumgartner et al., 2011). Cellulases, hemicellulases, and pectinases play crucial roles in penetrating the plant's physical barriers and facilitating fungal entry into host tissues. Additionally, *Armillaria* deploys a sophisticated array of effector proteins, acting as virulence factors that modulate the plant's immune response and physiological processes (Bauters, 2021). These effector proteins exhibit diverse functionalities, including suppressing plant immunity via targeted degradation of host defence proteins, reprogramming plant metabolism to favour fungal growth, and even promoting the formation of adventitious roots that serve as a readily available nutrient source (Kedves et al., 2021).

In response to fungal invasion, plants engage in a multi-layered defence strategy, with its significant component being the generation of reactive oxygen species (ROS) (Kedves et al., 2021). These reactive molecules function as a defensive barrier at the cellular level, causing oxidative harm to the invading fungus. Nevertheless, certain *Armillaria* species have evolved effective detoxification strategies, including enzymatic breakdown of ROS, enabling them to circumvent this defence mechanism and persist in colonising (Bradley et al., 2022).

The interaction between *Armillaria* and plants entails an intricate interplay between fungal virulence factors and the plant's defence responses, all coordinated at the molecular level. Understanding these complex molecular mechanisms is essential for devising efficient approaches to manage *Armillaria*-related diseases and mitigate their impact on agricultural and forest environments.

1.5.1. Fungal secretome

The fungal secretome, which includes all secreted proteins and related compounds, plays a crucial role in the interactions of a fungus with its surroundings (Girard et al., 2013). These molecules aid in nutrient acquisition, provide protection from unfavourable conditions, and influence interactions with other organisms. The specific repertoire of secreted proteins varies depending on the fungal lifestyle (symbiotic, saprotrophic, or pathogenic) and its species (Hess et al., 2018). Some studies suggest a link between the secretory protein profile and fungal phylogeny, rather than just lifestyle (Krijger et al., 2014).

Carbohydrate-active enzymes (CAZymes) are a specialised group of enzymes crucial for degrading and modifying carbohydrates, including plant cell wall components (Zhang et

al., 2014). *Armillaria* species, like many plant pathogens, possess a vast arsenal of CAZymes, highlighting their crucial role in the infection process (Somai-Jemmali et al., 2017; Sipos et al., 2017). The specific CAZyme profile produced by a fungus can vary depending on the stage of infection and the plant host encountered (O'Connell et al., 2012; M'Barek et al., 2015).

The CAZy database categorises these enzymes into five main families based on their function:

- **Glycoside hydrolases (GHs)** break down glycosidic bonds in complex carbohydrates.
- **Glycosyltransferases (GTs)** are enzymes that are responsible for catalysing the formation of new glycosidic bonds, which play a significant role in the synthesis of fungal cell walls and the production of extracellular polysaccharides.
- **Carbohydrate esterases (CEs)** are enzymes that modify carbohydrate structures by breaking ester linkages.
- **Auxiliary activity enzymes (AAs)** are redox enzymes that work alongside other CAZymes to break down complex carbohydrates and lignin.
- **Carbohydrate-binding modules (CBMs)** enhance the interaction between enzymes and their carbohydrate substrates.

Research indicates that the expression of specific families of CAZymes is often increased during interactions between plants and fungi, suggesting their crucial role in overcoming the physical defences of plants (Lyu et al., 2015). Genome analysis of *Armillaria* species has revealed a wide range of genes encoding CAZymes, underscoring their significance in the process of infection. Studies have demonstrated that certain CAZymes, such as endoglucanases and β-glucosidases, are upregulated during interactions with plant hosts, indicating their involvement in the breakdown of plant cell walls (Sipos et al., 2017).

Understanding the composition and function of the fungal secretome, particularly the diverse CAZyme arsenal, is crucial for deciphering the molecular mechanisms underlying *Armillaria*-plant interactions.

1.6. *Armillaria* root rot control strategies

While effective control strategies are crucial for protecting valuable plant resources, managing this disease requires a multifaceted approach, as evidenced by the limitations of current control methods.

Soil fumigation using chemicals such as methyl bromide and carbon disulfide is a widely employed practice for the cultivation of high-value crops (Baumgartner et al., 2011; Kedves et al., 2021). However, the effectiveness of this approach varies depending on soil characteristics and the severity of diseases present (Robinson and Smith, 2001). Additionally, there are growing concerns about the potential negative impacts of these chemicals on human health, the environment, and the surrounding microbiome, prompting the need to explore alternative strategies (Baumgartner et al., 2011; Heinzelmann et al., 2019).

Silvicultural practices such as clear-cutting, selective cutting, replanting, and thinning may not be effective in eliminating *Armillaria* from forest ecosystems due to the fungus' ability to colonise woody debris (Chen et al., 2019; Kedves et al., 2021). While removing stumps and roots (inoculum removal) can control the disease, this approach can be expensive, time-consuming, and prone to recurrence due to persistent underground rhizomorphs (Robinson and Smith, 2001). Chemical fungicides offer another option, but their high cost, labour intensity, and potential environmental and health risks limit their widespread use (Baumgartner et al., 2011; Chen et al., 2019; Kedves et al., 2021).

Biocontrol methods utilising naturally occurring antagonistic microorganisms represent a promising alternative. Studies have shown success with *Trichoderma* species in suppressing *Armillaria* growth (Chen et al., 2019; Rees et al., 2021). However, achieving sufficient and sustained concentrations of these beneficial microbes in large-scale forest environments remains a challenge. Nonetheless, the efficacy of biocontrol agents can be highly site-specific, requiring further research to optimise their application for *Armillaria* management.

For high-value crops like grapevines, walnuts, and peaches, post-infection treatments aim to minimise yield losses. These treatments involve root collar excavation and application of commercial inoculants containing antagonistic microorganisms. Studies have demonstrated positive outcomes, including increased yield and improved vascular tissue function (Baumgartner, 2004; Baumgartner et al., 2011).

1.7. Advances in *Armillaria* studies

While traditional research has focused on plant defence responses to *Armillaria* infection, a more comprehensive understanding of the *Armillaria* infection process remains incomplete. Comparative genomics and transcriptomics studies offer powerful tools to unveil deeper understanding of the origins of pathogenicity in *Armillaria* and shed light on the complex interactions between the fungus and its plant hosts. By comparing the genomes of different *Armillaria* species and their hosts, researchers can identify genes and pathways crucial for host specificity, pathogenicity, and resistance. Additionally, transcriptomic analysis reveals the genes actively expressed during infection, providing insights into the plant's defence mechanisms and the fungus' strategies for colonisation.

Ancestral *Armillaria* species were likely non-pathogenic wood-decaying saprotrophs. This transition involved the acquisition of genes encoding various enzymes and secondary metabolites that play key roles in breaking down plant cell walls, suppressing host defences, and manipulating host metabolism. Notably, *Armillaria* genomes harbour genes for expansins and cerato-platanins, which loosen the plant cell wall, and carboxylesterases and salicylate hydroxylases, which may help the fungus detoxify plant defence compounds. Moreover, *Armillaria* displays a wide array of genes associated with secondary metabolism, which may be responsible for generating virulence factors that enhance its pathogenicity (Fox and Howlett, 2008; Collins et al., 2013; Sipos et al., 2017).

The analysis of the *A. mellea* genome unveiled an unexpectedly large genome size and an extensive repertoire of carbohydrate-active enzymes, reminiscent of those found in Basidiomycota and Ascomycota species (Collins et al., 2013). Subsequent comparative genomic studies on other *Armillaria* species confirmed unusually large genomes, suggesting extensive genome duplications and diversification events. These expansions resulted in an enrichment of genes specific to rhizomorph development, plant cell wall degradation (particularly pectin degradation), and putative pathogenicity factors (Collins et al., 2013; Sipos et al., 2017).

The classification of *Armillaria*'s mechanism for wood decay has also generated debate within the scientific community. Certain studies classify *Armillaria* as a white-rot fungus due to the detection of lignin-degrading enzymes (Collins et al., 2013, 2017; Floudas et al., 2015), while others emphasise a reduced presence of these enzymes in comparison to standard

white-rot fungi (Sipos et al., 2017, 2018). Additionally, some studies suggest that *Armillaria* primarily targets cellulose, hemicellulose, and pectin components, leaving lignin relatively untouched during early stages of decay (Campbell, 1932; Schwarze, 2007). This ambiguity underscores the limitations of the traditional white-rot/brown-rot classification system.

1.8. Potential of armillarioids in mycoremediation

Mycoremediation, a bioremediation technique utilising fungi and their enzymatic arsenal, offers a promising approach for cleaning up polluted environments (Barr and Aust, 1994; Kulshreshtha et al., 2014). Among the diverse fungal groups, white-rot fungi, like *Armillaria* species, are particularly adept at degrading complex organic pollutants due to their potent enzymatic machinery.

Armillaria exhibits a diverse range of enzymes, including laccases, cytochrome P450 monooxygenases, FAD monooxygenases, cutinases, peroxidases, hydrolases, and antioxidants (Akhtar and Mannan, 2020). These enzymes play a crucial role in degrading lignin, but their versatility has a potential to extend beyond natural substrates, making them valuable tools for mycoremediation applications.

Research has shown promising results for using armillarioids in various remediation scenarios. Yildirim et al. (2018) demonstrated the effectiveness of *Desarmillaria tabescens* in breaking down malathion pesticides in liquid media, suggesting its potential for wastewater treatment. Rigling et al. (2006) explored the biosorption abilities of *Armillaria* species, finding that the rhizomorphs of *A. ostoyae* and *A. cepistipes* efficiently removed heavy metals from contaminated soils. Similarly, Xu et al. (2019) identified *A. cepistipes* as a promising candidate for remediating vanadium-contaminated environments.

Understanding the specific enzymes and protein families involved in xenobiotic degradation is crucial for optimising the use of fungi in mycoremediation. As Krijger et al. (2014) point out, a fungus's ability to thrive in challenging environments is linked to its repertoire of specialised genes and protein families. By screening armillarioid species for their xenobiotic-degrading enzyme profiles and comparing them with other fungi, we can gain valuable insights into their bioremediation potential.

2. AIMS

Armillaria fungi, like *A. ostoyae* and *A. borealis*, inflict significant damage on trees due to their potent enzymatic capabilities for plant infection and wood decay. However, our current understanding of the specific virulence factors and wood-degrading enzymes employed by these fungi remains incomplete. This knowledge gap hinders the development of targeted strategies to manage their spread and mitigate their destructive impact.

This study addresses this critical gap by employing a comparative transcriptome analysis to investigate the enzymatic profiles of *A. ostoyae* and *A. borealis*, two *Armillaria* species representing distinct ecological roles in plant-fungus interactions. *A. ostoyae* is a notorious pathogen, while *A. borealis* is a secondary pathogen, offering a unique opportunity to compare the enzymatic machinery employed by these fungi. We aim to achieve the following:

1. **To identify and functionally characterise the virulence factors employed by *A. ostoyae* and *A. borealis*:** Analysing their RNA-Seq transcriptome data and performing homology searches against known virulence factors to identify key enzymes involved in their pathogenic strategies, focusing on those that degrade plant cell walls and suppress host defences

2. **To compare the wood-degrading enzyme profiles of *A. ostoyae* and *A. borealis*:** Analysing the transcriptome data for the presence and abundance of genes encoding cellulases, hemicellulases, lignin-modifying enzymes, and pectinases. By identifying differences in their enzymatic machinery elucidate variations in wood degradation efficiency between the two species.

3. **To assess the mycoremediation potential of *A. ostoyae* and *A. borealis*:** Performing a comparative genomic analysis to evaluate the genetic repertoire of these fungi for degrading various aromatic compounds. This will provide insights into their potential for bioremediation of environments contaminated with specific pollutants.

By achieving these aims, this study will provide valuable insights into the pathogenic and wood-degrading mechanisms of *Armillaria* species. This knowledge will pave the way for developing targeted control strategies for these destructive fungi. Additionally, the findings on mycoremediation potential hold promise for utilising these fungi in environmental cleanup efforts.

3. MATERIALS AND METHODS

3.1. Stem collection and preparation

Stems of two recently cut Norway spruce (*Picea abies*) trees were used for the experiment. The trunks of the trees were cut into 10 cm segments and only those without any damage or defects were chosen. In total, 36 stems were utilised, with an equal distribution from each tree. To monitor the progress of the growth of the fungal mycelia under the bark, small "windows", measuring 1 cm × 1.5 cm, were cut halfway up the stems' bark.

The stems were divided into two groups: one group remained untreated (fresh group - F), while the other underwent sterilisation by autoclaving at 121°C and 15 psi for 15 minutes (autoclaved group - A). Non-autoclaved Norway spruce stem segments represent fresh but deteriorating wood with some remaining immune activity. Autoclaved Norway spruce stem segments represent fully dead wood, as autoclaving eliminates fungal growth and immune response, allowing us to focus on genes directly involved in wood degradation mechanisms.

To ensure the viability of spruce stem segments we implemented several measures:

- Immediate processing: the spruce stems were obtained from freshly cut Norway spruce trees, minimising the time between felling and processing.
- Sterile conditions: the stems were processed under sterile conditions to prevent contamination by external microorganisms that could interfere with the experiment.
- Nutrient supplementation: the stems were incubated in a nutrient-rich medium to provide essential elements for maintaining tissue viability and supporting fungal growth.
- Controlled environment: the incubation chamber was maintained at optimal temperature (24°C), and in dark conditions.

3.2. Fungal cultures

All *Armillaria* cultures used in the experiments originated from Switzerland and were collected between 1994 and 1998 (Heinzelmann et al., 2017). For determining potential *Armillaria* virulence and wood degrading factors, high and low virulent isolates of conifer-specific *A. ostoyae* and *A. borealis* were chosen. Details regarding the isolates used in this study are given in Table 1.

Table 1. *A. ostoyae* and *A. borealis* isolates used in this study.

Strain	Lab designation WSL	Source	Host	Year of isolation
A. borealis (Heinzelmann et al., 2017)				
A4 (low virulent)	LWF ALP 8-2	Rhizomorph	Forest dominated by *P. abies*	1994
A6 (high virulent)	PBMD Schwanden	Rhizomorph	*P. abies* (stump)	1995
A. ostoyae (Prospero et al., 2004; Heinzelmann et al., 2017)				
C2 (low virulent)	LWF LAU 10	Rhizomorph	Forest dominated by *F. sylvatica*	1998
C18 (high virulent)	PBMD 3933	Mycelial fan	*P. abies*	1995

3.3. Media and preparation of fungal cultures

In order to sustain fungal cultures prior to the start of the experiment, they were maintained in the dark on solid Roth and Shaw media (RS media) (Shaw and Roth, 1976). This rich medium, containing 40 g malt extract, 20 g dextrose, 5 g bacto peptone, and 19 g agar per 1 litre, provides fungi with all the nutrients necessary for optimal growth and development.

To maintain the viability of the cultures, reinoculation was routinely performed every 3 months. This involved transferring a small agar plug (5 mm × 5 mm) with fungal mycelia of the existing cultures to a new Petri plate containing fresh RS medium. The reinoculated cultures were then incubated aerobically in the dark, at 24 °C for approximately 3 weeks to allow them to grow and reach their maximum biomass. Plates were then transferred to cold storage at 4 °C in order to slow down the growth of the fungi and extend their lifespan. Fresh cultures of all isolates were set up before the start of the experiment.

3.4. *In vitro* stem invasion assay

For the *in vitro* stem invasion assay, 500 ml sterile plastic jars were used for growing subcortical mycelial fans. Each jar was filled with rice, sawdust, tomato and oranges (RSTO) medium (Sipos et al., 2017), a modification of RST medium (Ford et al., 2015), which was freshly made on the day of use.

First step was overlaying the bottom of each jar with 30 g rice, 15 g sawdust, 150 ml water, with each of them autoclaved separately at 121 °C and 15 psi for 15 minutes. The

moistened rice-sawdust layer was overlaid with a 1 cm top layer of homogenised orange, tomato, distilled water and 3-week old desired *Armillaria* isolates grown on RS medium.

Jars were tightly sealed with sterile lids and incubated in the dark at 24 °C for 10 days. This incubation period allowed fungal establishment and colonisation of the substrate, as well formation of mycelial "lawn" on top of the surface. After 10 days, the stem segments were placed carefully on the newly developed top mycelial layer. This allowed *Armillaria* isolates to initiate invasion of the cambial zone within the stem segments. The invasion and subsequent development of subcortical mycelial fans within the stem segments were monitored visually until mycelial front line formed in the designated openings on the stems.

3.5. Mycelia collection

Once mycelial fans were present in the openings, stem segments were carefully dissected with sterile scalpels to expose the underlying subcortical mycelial fans (Figure 3). Sections of the mycelial fans were then collected using sterile forceps. Approximately 200 mg of mycelial fan tissue was collected from each infected stem segment (three segments per treatment group). To minimise RNA degradation, collected samples were immediately flash-frozen in liquid nitrogen and stored at -80 °C until RNA extraction.

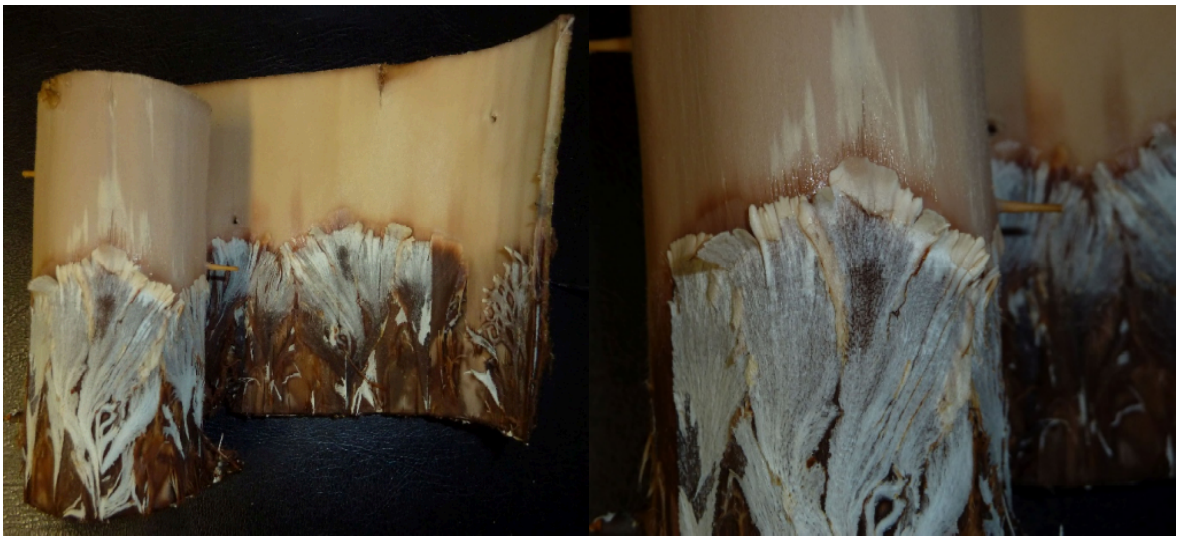

Figure 3. *Armillaria* mycelium under the bark of Norway spruce stem

Additional jars containing *Armillaria* isolates were prepared as described above, but without the inclusion of spruce stem segments. Once the top mycelial layer was formed,

Armillaria cultures were collected from the jars, frozen in liquid nitrogen stored at -80 °C in order to be used as control samples.

3.6. RNA isolation

Using sterile and pre-chilled mortar and pestle, the samples were grounded thoroughly into a fine powder in the presence of liquid nitrogen. This mechanical disruption ensured complete cell lysis and efficient RNA extraction. The addition of liquid nitrogen during homogenization minimised RNA degradation due to enzymatic activity.

RNA was extracted from the homogenised mycelial fan tissue using the RNeasy Plant Midi Kit (Qiagen Inc.) according to the manufacturer's protocol. This column-based purification system offers efficient isolation of high-quality RNA. Briefly, the homogenised tissue was lysed in a buffer containing β-mercaptoethanol to inactivate RNases. The lysate was then passed through a gDNA Eliminator column to remove any contaminating genomic DNA. The clarified lysate was subsequently loaded onto RNeasy Plant Midi Kit columns, where RNA selectively binds to the membrane while cellular debris and contaminants are washed away. On-column DNase treatment with the RNase-Free DNase Set further ensured complete removal of genomic DNA. Finally, purified RNA was eluted in RNase-free water and stored at -80 °C until further analysis.

The quantity of isolated RNA was measured using the Qubit® RNA BR Assay Kit (Thermo Fisher Scientific) on a Qubit® 4 Fluorometer according to the manufacturer's instructions. Each RNA sample was measured in triplicate to ensure accuracy and reproducibility of the results.

Three independent mycelial fan sections were collected from the stems of each group (fresh and autoclaved) and processed separately for RNA extraction and quantification, constituting biological triplicates. This approach controls for inherent biological variability between individual samples and allows for more robust and reliable data analysis.

3.7. Library preparation and sequencing

Total RNA extracted from mycelial fan samples was used for transcriptome analysis. Library preparation was performed using the NEBNext Ultra II Directional RNA Library Prep Kit for Illumina (NEB) following the manufacturer's instructions. This kit employs a directional RNA-Seq workflow, ensuring strand-specific sequencing and improving transcript mapping accuracy.

Prior to library construction, RNA samples were enriched for mRNA transcripts using RiboCop rRNA Depletion Kits (Lexogen). This step removes abundant ribosomal RNA (rRNA) molecules, which comprise a major portion of total RNA but lack coding potential. By depleting rRNA, the library becomes enriched for mRNA transcripts, leading to higher sequencing efficiency and improved coverage of protein-coding genes.

Following rRNA depletion, the enriched mRNA was fragmented into smaller pieces suitable for library construction. The fragmented RNA underwent end repair to create blunt ends and then received Illumina adapter sequences for subsequent amplification and sequencing.

Finally, the adapter-ligated fragments were amplified according to the manufacturer's protocol. This amplification step enriches the library for adapter-containing fragments and generates sufficient material for sequencing on the Illumina platform.

The quality of the prepared libraries was assessed on Agilent 4200 TapeSation System using D1000 Screen Tape (AgilentTechnologies), while the quantity was determined using the Qubit 3.0 Fluorometer.

Qualified libraries were sequenced on the NovaSeq 6000 instrument (Illumina) using a 2× 151 bp paired-end sequencing configuration. This generates high-quality, paired-end reads with a read length of 151 nucleotides from both ends of the fragmented transcripts.

3.8. Transcriptome analysis

Raw RNA-Seq reads obtained from Illumina sequencing were quality-filtered using FastQC v0.11.9 (Andrews, 2010). Reads with low quality scores or adapter sequences were

removed using Trimmomatic v0.39 (Bolger et al., 2014) to ensure optimal downstream analyses.

High-quality, trimmed reads were then aligned to the reference genomes of *Armillaria ostoyae* (NCBI genome GCA_900157425.1 version 2) and *Armillaria borealis* (JGI: *Armillaria borealis* FPL87.14 v1.0) using STAR v2.7.5a (Dobin et al., 2013).

Following alignment, the level of expression for each gene was estimated using RSEM v1.3.1 (Li and Dewey, 2011). RSEM generates an expression matrix containing the normalised counts of transcripts for each gene across all samples.

Prior to running the differential expression analysis, the gene expression counts were normalised using the trimmed mean of M values (TMM) method using edgeR v3.38.1 (Chen et al., 2016). This normalisation addresses library size biases and ensures accurate comparisons between samples. Additionally, genes with low expression levels (counts per million (cpm) < 10) were filtered out to reduce noise and improve statistical power.

Genes with at least a two-fold expression change (log2 fold change threshold) and false discovery rate (FDR) values ≤0.05 were considered statistically significant and differentially expressed.

The combined use of FDR, p-value, and two-fold filtering thresholds is crucial for identifying differentially expressed genes (DEGs) that are both statistically significant and biologically relevant:

- FDR helps limit the proportion of false discoveries among the identified significant results, thereby enhancing the credibility of the findings.
- The p-value measures the evidence against the null hypothesis, indicating whether a gene is differentially expressed. However, due to multiple testing issues, relying solely on p-values can be misleading. Therefore, coupling p-values with FDR provides more robust and reliable results.
- The two-fold change threshold ensures that only biologically meaningful changes in gene expression are considered. This threshold requires that a gene's expression level is at least doubled or halved to be deemed differentially expressed, filtering out minor changes that may not be biologically significant.

To visualise the overall patterns of gene expression across different samples, multi-dimensional scaling (MDS) was performed using the plotMDS function in the edgeR package. MDS projects high-dimensional gene expression data into a lower-dimensional space, allowing for visual exploration of similarities and differences between samples based on their gene expression profiles.

3.9. Differential expression analysis

The normalised and filtered expression matrix was then used for differential expression analysis between specific conditions (e.g., high virulent vs. low virulent) using Limma-Voom (Ritchie et al., 2015). This statistical framework accounts for technical variability and normalises data before identifying genes showing significant changes in expression between conditions. The power of the differential expression analysis was predicted using the superseq v0.0.0.99 R-package (Bass et al., 2019) to assess the likelihood of detecting significant differences before running the analysis.

3.10. Functional annotation

Significantly differentially expressed genes were further analysed to understand their potential roles in fungal-wood interactions through functional annotation.

Additionally, various tools were employed for functional annotation of genes:

- InterProScan v5.32-71.0 (Jones et al., 2014): Identified protein domains and associated Gene Ontology (GO) terms, providing insights into their potential biochemical roles.
- PANZERR (Protein ANNotation with Z-scoRE) (Törönen et al., 2018): Provided functional annotations based on protein sequence similarity and domain predictions.
- KofamScan (Aramaki et al., 2020): Assigned genes to KEGG pathways and modules for analysis of metabolic and biological processes.
- dbCAN2 (Zhang et al., 2018): Specifically characterised genes encoding carbohydrate-active enzymes (CAZymes) involved in plant cell wall degradation.

Following annotation, enrichment scores were calculated in R using Fisher's test.

3.11. Annotation of carbohydrate-active enzymes (CAZymes)

Following orthology determination and enrichment analysis for general functional insights, a specific focus was placed on carbohydrate-active enzymes (CAZymes) due to their crucial role in plant cell wall degradation and fungal-wood interactions.

For the functional annotation of genes encoding CAZymes involved in plant cell wall degradation, we employed dbCAN2 (Zhang et al., 2018). This tool was chosen for its accuracy and comprehensive database of CAZy families and their associated functions.

Additionally, Sahu et al. (2023) provided valuable data on a diverse range of plant cell wall degrading enzymes, including cellulases, xylanases, pectin lyases, pectinases, polygalacturonase, laccases, and peroxidases, along with their preferred substrates (Supplementary material 1). Specifically, we utilised information on enzyme functionalities and degradation targets from this resource to identify and retain CAZyme families with a well-established or predicted role in plant cell wall degradation for further analysis based on copy number information. This specific annotation strategy allowed for a deeper understanding of the potential mechanisms underlying fungal colonisation and degradation of wood tissues.

3.12. Candidate virulence and wood degradation gene selection

Comparative transcriptome analyses were conducted to identify candidate virulence factors associated with plant colonisation and wood degradation in *A. ostoyae* and *A. borealis*. This involved contrasting high virulence isolates (*A. ostoyae* C18/ *A. borealis* A6) with both low virulence isolates (*A. ostoyae* C2/ *A. borealis* A4) and their respective vegetative mycelial controls (*A. ostoyae* C18C and C2C/ *A. borealis* A6C and A4C) across two experimental settings:

- Analysis 1: Fresh Norway spruce stem segments (focusing on virulence factors).
- Analysis 2: Autoclaved Norway spruce stem segments (focusing on wood degradation factors).

Following the identification of DEGs through RNA-seq analysis, additional steps were taken to refine the selection of candidate genes specifically related to virulence and wood degradation:

- SignalP v5.0 (Almagro Armenteros et al., 2019) predicted the presence of signal peptides in DEG protein sequences, indicating potential secretion crucial for interaction with the plant or wood. This step created "extracellular" and "non-extracellular" subgroups.
- Subcellular localization tools like TMHMM v2 (Hallgren et al., 2022), WoLF PSORT (Horton et al., 2007), DeepLoc v1.0 (Almagro Armenteros et al., 2017), and OutCyte v1.0 (Zhao et al., 2019) were used to further refine the selection towards proteins potentially associated with the cell membrane or interacting with the host environment or wood components.
- Comparison against the Plant-Herbivore Interaction (PHI) database (Winnenburg et al., 2006) identified genes previously associated with pathogen-host interactions in other systems, leveraging existing knowledge to prioritise potentially relevant genes.

Focusing on upregulated genes, further classification categorised them as extracellularly targeted proteins based on WoLF PSORT predictions. These proteins can potentially interact directly with the plant host environment or wood components and play crucial roles in virulence or wood degradation mechanisms.

This rigorous selection process resulted in a focused set of candidate virulence and wood degradation factors categorised as extracellular proteins, providing a foundation for further investigation into their specific roles during fungal-plant interactions and wood breakdown.

3.13. Identifying potential bioremediation genes

Combined bioinformatics and comparative analysis approach was used to identify and characterise potential bioremediation genes in *A. ostoyae* and *A. borealis*. We specifically analysed gene expression data from highly and less virulent isolates grown in two contrasting environments: fresh spruce stems during active plant invasion and control conditions on nutrient-rich RS media.

First, amino acid sequences from seven *Armillaria* species, two *Desarmillaria* species, one *Guyanagaster* species, 14 white-rot basidiomycete fungi, 12 ascomycete fungi, and one Mucoromycota outlier were downloaded from the Joint Genome Institute (JGI) MycoCosm database (https://mycocosm.jgi.doe.gov/mycocosm/home) (Supplementary material 2). Species selection was guided by a literature review that focused on their biodegradation potential.

These sequences were then assigned KEGG orthology IDs using KofamScan (Aramaki et al., 2020). We then employed the Biocatalysis/Biodegradation Database (Ellis et al., 2006) for initial curation of enzyme activities related to xenobiotic degradation. Enzymes with potential relevance but lacking curation were further examined and confirmed in the KEGG database (Kanehisa and Goto, 2000). Only enzymes explicitly linked to xenobiotic degradation pathways in KEGG were selected for further analysis.

All computational analyses and comparisons were performed using R version 4.2. Phylogenetic Principal Component Analysis (PCA) was conducted with the adephylo package (v1.1-11) (Jombart et al., 2010). Enzyme copy numbers for each species were calculated and utilised to construct the PCA plot. A phylogenetic tree built from single-copy orthologs (Supplementary material 3) served as the reference for the PCA. This tree was generated using MAFFT v7 (Katoh and Standley, 2013) for sequence alignment and FastTree v2.1 (Price et al., 2010) for building the maximum-likelihood tree. Data visualisation was achieved using ggplot2.

Furthermore, MEME Suite (Bailey et al., 2015) was employed for motif analysis of identified bioremediation-related genes.

4. RESULTS

4.1. Identification of potential virulence factors (fresh stems)

4.1.1. Stem invasion

Both high and low virulent isolates of *A. ostoyae* and *A. borealis* successfully colonised non-autoclaved Norway spruce stem segments. Mycelial samples were collected soon after the fungal front reached designated openings in the segments.

High virulence *A. ostoyae* isolates successfully colonised the stem segments significantly faster than their low virulence counterparts, with an average colonisation time of 13 days compared to 19 days. *A. borealis* isolates, on average, had slower colonisation times (23 and 24 days for high and low virulence, respectively), with the high virulence isolate showing a minimal advantage. Each colonisation time represents the average of three replicates per isolate.

4.1.2. Sequencing results

RNA-Seq analysis was performed on three biological replicates for each isolate and condition, including high and low virulence isolates of *A. ostoyae* and *A. borealis* grown in fresh stems and controls. Overall, sequencing depths ranged from 20.7 to 93.7 million paired-end reads, with an average of 73% and 71% of reads mapping to transcripts in *A. ostoyae* and *A. borealis* genomes, respectively (Supplementary material 4). Mapping percentages varied across samples, with control samples generally showing higher mapping rates than fresh stem samples. Both species showed some differences in mapping percentages between high and low virulence isolates.

4.1.3. Multi-dimensional scaling analysis

MDS was used to visualise the relationships between the transcriptomic profiles of different samples. The MDS plots clearly separated the samples based on species, virulence level, and treatment (control vs. fresh stem) (Figure 4). This confirms the distinct transcriptomic signatures associated with these factors.

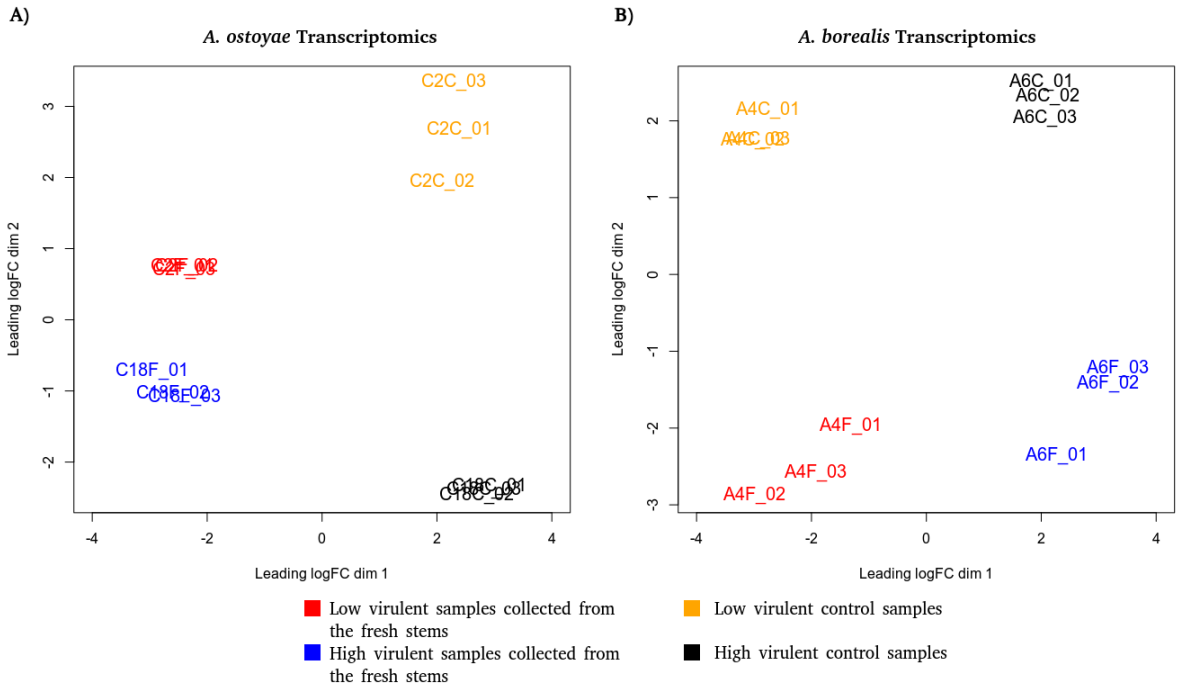

Figure 4. Multidimensional scaling of transcriptomes from *A. ostoyae* (C2: low virulent, C18: high virulent) (A) and *A. borealis* (A4: low virulent, A6: high virulent) (B). Replicates are coloured according to sample types. (C2C/C18C/A4C/A6C: control samples, C2F/C18F/A4F/A6F: samples from under the bark of fresh stems)

4.1.4. Differentially expressed genes (DEGs)

To identify potential virulence factors involved in the infection mechanism in *A. ostoyae* and *A. borealis*, we compared gene expression profiles of high and low virulence isolates grown in fresh Norway spruce stem segments to each other, as well as to their respective controls. DEGs are identified as genes that have exhibited significant up- (red) or down-regulation (blue) in one sample compared to the other (Figure 5).

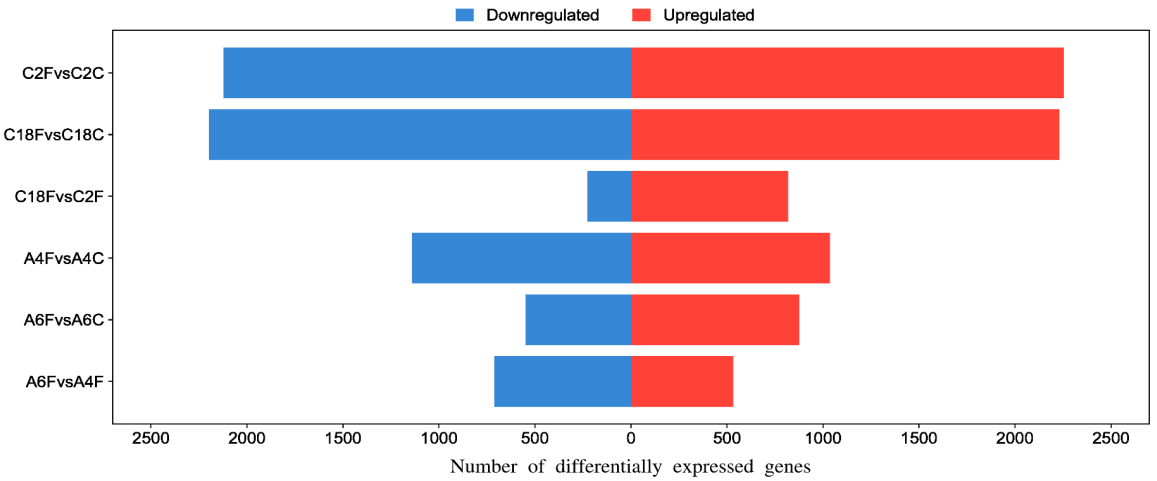

Figure 5. Comparison of up- (red) and down-regulated (blue) DEGs in *A. ostoyae* (C2: low virulent, C18: high virulent) and *A. borealis* (A4: low virulent, A6: high virulent) isolates grown in fresh Norway spruce stems (C2F/C18F/A4F/A6F) and their controls (C2C/C18C/A4C/A6C).

4.1.5. Identifying potential virulence factor candidates

To identify potential virulence factors associated with plant colonisation, we focused on upregulated genes specifically present in the stem-invasive mycelia of highly virulent isolates compared to both low virulent isolates and their respective controls (Figure 6). This two-pronged approach allowed us to identify:

- **Inducible virulence candidates**: These genes were only upregulated in highly virulent isolates compared to all other groups, potentially representing virulence-specific functions.
- **Constitutive virulence candidates**: These genes were upregulated in highly virulent isolates compared to their own controls, suggesting roles in general fitness or baseline virulence characteristics.

Among these upregulated genes, using tools like SignalP and WoLF PSORT we specifically focused on extracellularly targeted proteins as they have direct access to the plant host environment and potentially play crucial roles in virulence (Table 2).

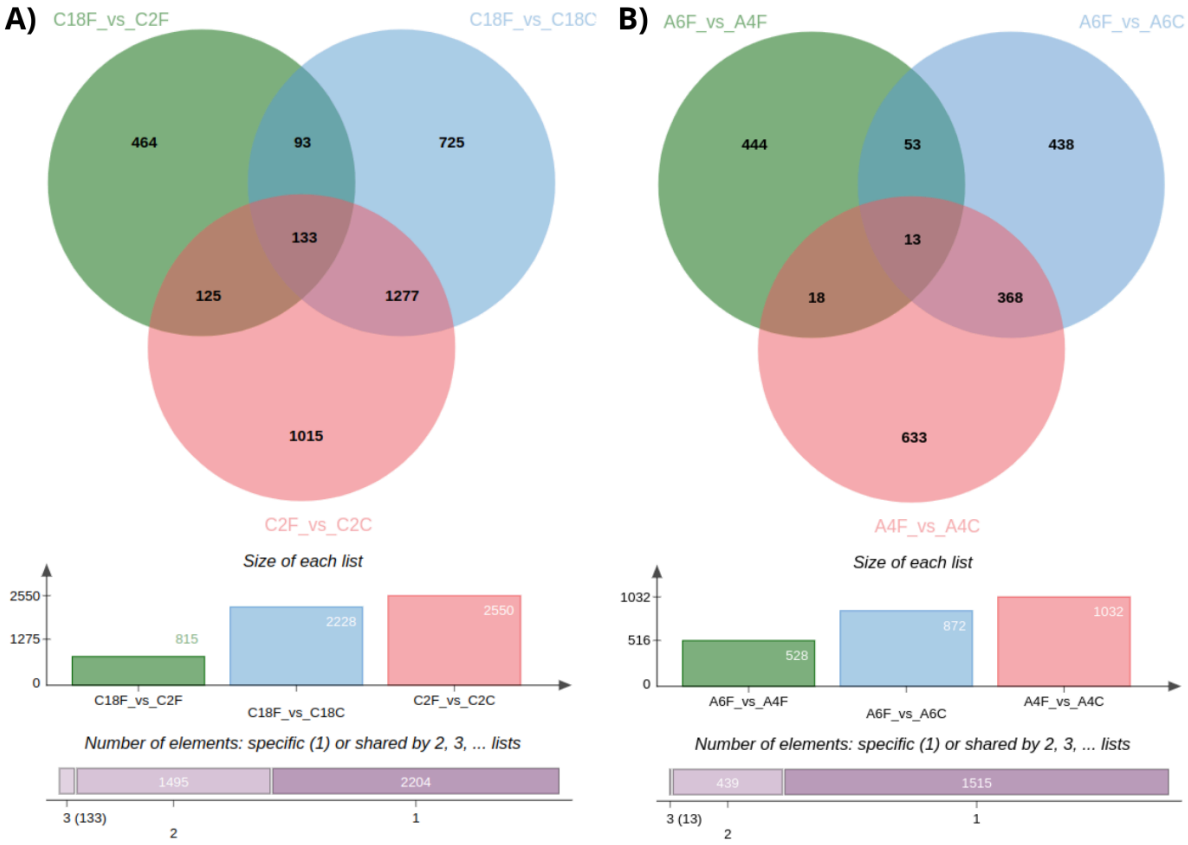

Figure 6. Overlap of upregulated genes specific to highly virulent vs. low virulent and control isolates of *A. ostoyae* (C2: low virulent, C18: high virulent) (A) and *A. borealis* (A4: low virulent, A6: high virulent) (B) incubated in fresh stems (F) or control (C) environments, with charts showing the list size and intersection size repartition located underneath the diagram.

Table 2. Summary of identified upregulated genes and secreted proteins of interest in highly virulent isolates of *A. ostoyae* and *A. borealis* incubated in fresh stems.

Species	Category	Total upregulated	Secreted proteins
***A. ostoyae* (C18F)**	Constitutive	2228	339
	Inducible	464	28
***A. borealis* (A6F)**	Constitutive	872	185
	Inducible	444	54

4.1.6. Identification and characterization of secreted proteins

Among the identified secreted proteins, carbohydrate-active enzymes (CAZymes) emerged as a prominent group with potential roles in plant cell wall degradation and fungal-wood interactions. We utilised the classification system by Sahu et al. (2023) to further classify CAZymes into two major categories:

- **Plant cell wall degrading enzymes (PCWDEs)**: Enzymes directly involved in breaking down various components of the plant cell wall, potentially facilitating fungal colonisation
- **Fungal cell wall modifying enzymes (FCW)**: Enzymes modifying fungal cell wall components potentially related to adaptation and growth within the host.

Analysis of CAZymes revealed a higher abundance of PCWDEs, particularly in the constitutive pools of highly virulent isolates of *A. ostoyae* (C18F) and *A. borealis* (A6F) (Figure 7A). Both species displayed substantial representation of enzymes targeting cellulose, hemicellulose, lignin, and pectin, key components of the plant cell wall, among the constitutive group. Notably, *A. ostoyae* exhibited a higher overall abundance of PCWDEs compared to *A. borealis* (Figure 7B). This finding suggests a potentially stronger emphasis on degrading the host plant cell wall, as further supported by the higher PCWDE:FCW ratio observed in all groups (Figure 7C).

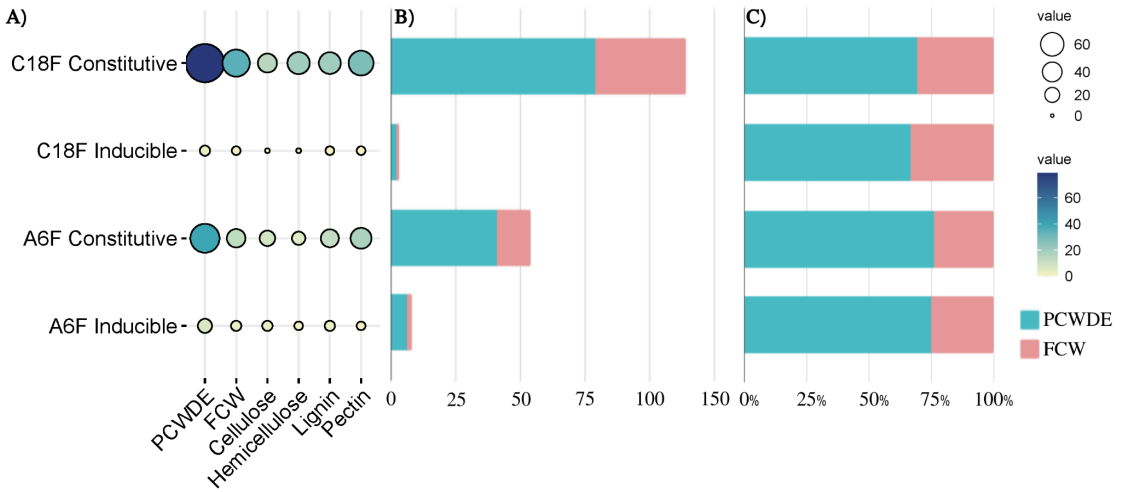

Figure 7. Count distribution of major CAZyme categories (PCWDE and FCW), classified according to Sahu et al. (2023): A) Count distribution of PCWDE, FCW, cellulose, hemicellulose, lignin and pectin degrading CAZymes among upregulated candidate DEGs of highly virulent isolates of *A. ostoyae* (C18F) and *A. borealis* (A6F) incubated in fresh stems. B) Total PCWDE and FCW counts in each group. C) PCWDE and FCW ratios in each group.

4.1.7. CAZyme profiles

Analysis of CAZyme families reveals distinct enzyme profiles between *A. ostoyae* (C18F) and *A. borealis* (A6F) (Figure 8), potentially reflecting their contrasting lifestyles and virulence strategies.

Inducible Enzymes: Both species utilise inducible enzymes to refine their virulence strategies based on encountered defences within the host plant. These inducible responses highlight their ability to adapt and overcome potential challenges during host colonisation.

- ***A. ostoyae* (C18F)**: Exhibits inducible expression of pectinase (GH105), lignin-modifying enzyme (AA3_2), and chitinase (CE4) involved in modifying the fungal cell wall.
- ***A. borealis* (A6F):** Possesses two inducible cellulases (AA9), a lignin-modifying enzyme (AA3_2), and a hemicellulases (GH35)

Species-specific constitutive enzymes: *A. ostoyae* (C18F) exhibits a more abundant and diverse constitutive PCWDEs repertoire than *A. borealis* (A6F).

***A. ostoyae* (C18F)**:

- **Cellulose**: Enzymes like AA16, GH5_5, and GH6 highlight C18F's potential for efficient cellulose breakdown.
- **Hemicellulose**: The presence of diverse hemicellulases like AA14, GH10, and GH35 indicates its potential to effectively depolymerize various hemicellulose types.
- **Lignin**: Higher abundance of AA1_1, and AA3_2 compared to *A. borealis* (A6F) suggests *A. ostoyae* (C18F) might possess a stronger ability to modify lignin.
- **Pectin**: The various pectinases, including uniquely present CBM67, GH53, PL1_7, PL26, and PL8_4, underscore *A. ostoyae's* (C18F) potential for diverse pectin degradation.

***A. borealis* (A6F):**

- **Cellulose:** Possesses a unique cellulose degrading enzyme (GH131), suggesting a potentially targeted approach compared to *A. ostoyae's* (C18F) broader capabilities.
- **Hemicellulose:** The presence of a unique enzyme (GH93) highlights potential specialisation on specific hemicellulose types within the host cell wall.
- **Pectin:** Unique pectinases (PL3_2, GH88) suggest adaptation for degrading specific pectins, potentially impacting nutrient acquisition or virulence strategies.

The observed differences in enzyme abundance and presence within the constitutive pools paints a picture of distinct baseline approaches to overcoming host defences. *A. ostoyae* exhibited a broader range of enzymes targeting various cell wall components, including cellulose, hemicellulose, lignin, and pectin. This suggests a potentially more aggressive strategy for breaching the plant cell wall and accessing host nutrients, potentially contributing to its enhanced virulence. In contrast, *A. borealis* displayed a more specific enzyme profile, potentially indicating a niche-oriented approach that might be less efficient in overcoming plant defences.

Shared constitutive enzymes: While distinct nuances emerge in the wood degradation strategies of *A. ostoyae* (C18F) and *A. borealis* (A6F), a closer look reveals a significant portion of their CAZyme repertoire is shared. These commonalities highlight convergent strategies employed by both fungi for tackling key components of the plant cell wall.

- **Cellulose**: cellulases (AA9, GH3, GH7, GH12) found abundantly across various secretion types in both species.
- **Hemicellulose**: both species utilise a diverse array of enzymes from these families (CE16, GH31, GH35, GH51) targeting various hemicellulose components like xylan, arabinoxylan, and glucuronoxylan.
- **Lignin**: while C18F exhibits higher abundance, these lignin-modifying enzymes (AA1_1, AA2, AA3_2) are present in both fungi, suggesting shared mechanisms for lignin modification during wood degradation.
- **Pectin**: Shared pectinases (CE8, CE12, GH28, GH78, PL4_1) indicate common strategies for degrading pectin.

The observed differences in abundance, inducible expression, and secretion types suggest unique nuances in their approaches to overcoming host defences and establishing themselves within the host.

Fungal cell wall modifying enzymes (FCWs):

- **Chitin**: Both species had chitinases, primarily GH18, GH20, and CBM50, with *A. ostoyae* C18F showing slightly higher abundance.

- **Glucan**: Glucanases (GH16, GH55, GH71, GH128) were present across both species and secretion types, with *A. ostoyae* (C18F) exhibiting higher abundance (e.g., GH5_15, GH17).
- **Mannan**: Both species had mannanses, mainly GH76, with *A. ostoyae* (C18F) additionally having unique constitutive mannanases (GH92 and GH125).
- **Galactan**: *A. borealis* (A6F) uniquely possesses a constitutive GH135 galactanase.

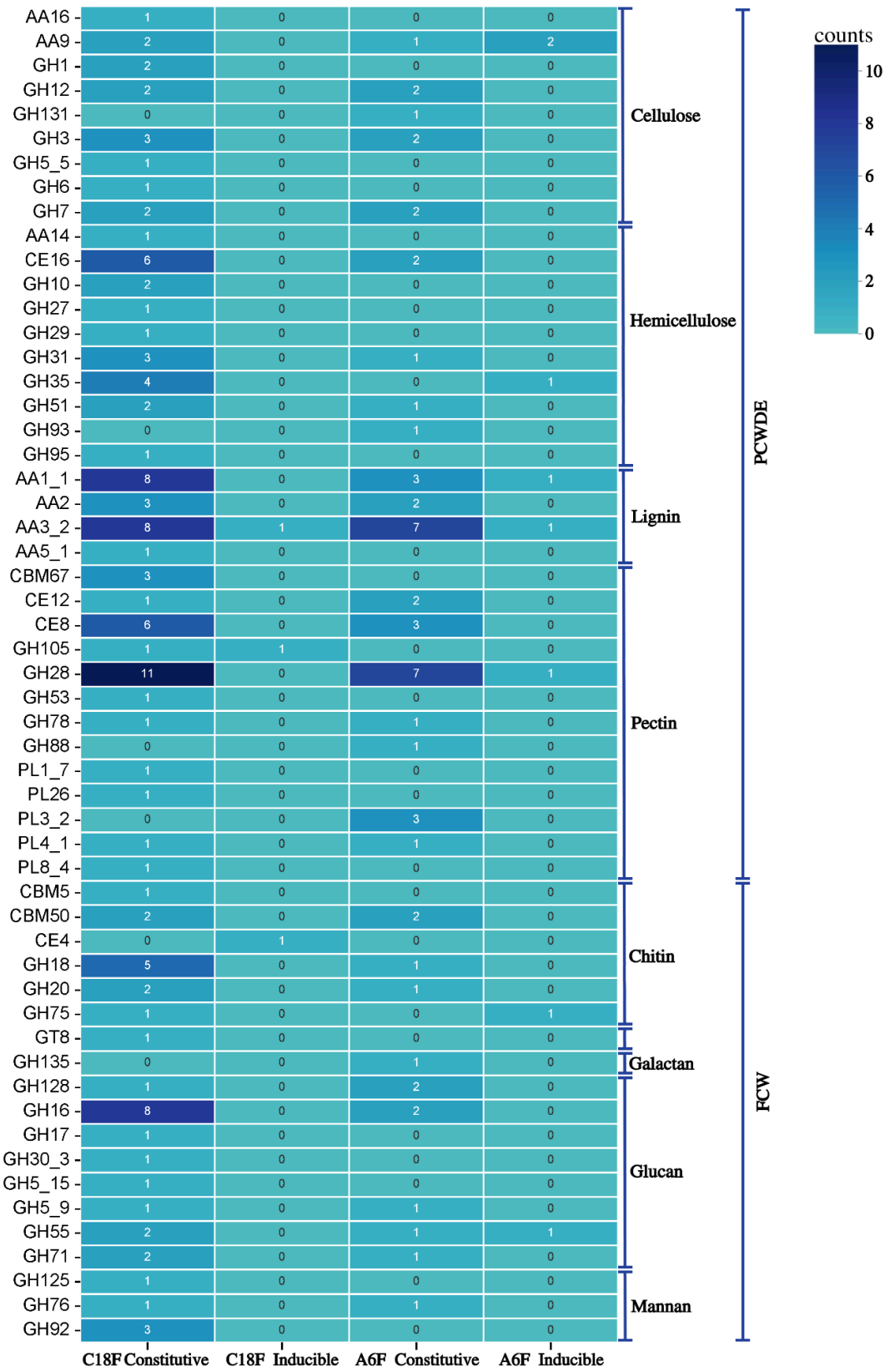

Figure 8. Distribution and abundance of CAZyme families in *A. ostoyae* (C18F) and *A. borealis* (A6F) incubated in fresh stems.

4.1.8. Non-CAZyme secretory virulence candidates

The analysis was constructed based on the InterPro annotations (IDs) of secreted proteins that were not identified as CAZymes. These annotations provide functional characterizations and categorise proteins into families based on their sequence similarity and predicted functions. By excluding CAZyme proteins, the focus is shifted towards the diverse range of non-enzymatic proteins potentially involved in virulence mechanisms (Figure 9).

Overall, *A. ostoyae* (C18F) exhibits a higher abundance of non-CAZyme secretory proteins compared to *A. borealis* (A6F) in both constitutive and inducible profiles.

Several peptidases and hydrolases are present across both species, including carboxylases (IPR002018), lysine-specific metallo-endopeptidases (IPR029463), and peptidases from various families (IPR008754, IPR001563, IPR000209).

Notably, some proteins displayed differential expression patterns. *A. ostoyae* exhibited higher constitutive abundances of enzymes like intradiol ring-cleavage dioxygenase (IPR000627), haem peroxidase (IPR019791), and guanine-specific ribonuclease (IPR000026). Conversely, *A. borealis* showed inducible expression of hydrophobins (IPR001338), constitutive expression of leucine-rich repeat (IPR001611) and four cerato-plantains (IPR010829) and a higher abundance of Kre9/Knh1 family enzymes (IPR018466).

Figure 9. Distribution and abundance of non-CAZyme secretory virulence candidates in *A. ostoyae* (C18F) and *A. borealis* (A6F) based on InterPro categories

4.1.9. Analysis of potential virulence factors against PHIbase

Utilising PHIbase (Pathogen Host Interaction Database), a comprehensive collection of experimentally validated interactions between plant pathogens and their hosts, potential virulence factors identified from both CAZyme and non-CAZyme groups were analysed, aiming to assess their relevance to *A. ostoyae* and *A. borealis* interactions with Norway spruce.

PHIbase categorises genes based on the consequence of their disruption in the pathogen. Key categories we focused on include:

- Loss of pathogenicity: Genes essential for the pathogen to cause disease. Disruption of these genes renders the fungus completely incapable of infecting the host.
- Reduced virulence: Entries where gene disruption resulted in a less severe disease phenotype compared to the wild-type strain.
- Lethal: Entries where gene disruption resulted in a non-viable fungal strain, suggesting the gene encodes an essential function.

Analysis of PHIbase identified homologs for numerous virulence factor candidates in both *A. ostoyae* and *A. borealis* (Table 3). Generally, a higher number of PHIbase homologs for *A. ostoyae* virulence factor candidates was present compared to *A. borealis*, with the majority of the identified homologs being associated with reduced virulence phenotypes.

Table 3. Distribution of PHIbase homologs for potential virulence factors

Species	Secreted proteins	Category	Loss of pathogenicity	Reduced virulence	Lethal
***A. ostoyae* (C18F)**	***CAZymes***	Constitutive	0	44	0
		Inducible	0	2	0
	non-CAZymes	Constitutive	2	28	0
		Inducible	0	5	1
***A. borealis* (A6F)**	***CAZymes***	Constitutive	0	25	0
		Inducible	0	3	0
	non-CAZymes	Constitutive	0	15	0
		Inducible	0	4	0

While PHIbase provides a valuable resource for exploring gene function across diverse pathogens, its data encompasses interactions between various pathogens and their hosts, not just plant pathogens. To specifically focus on virulence factors relevant to *A. ostoyae* and *A. borealis* interactions with Norway spruce, we further refined our analysis.

We filtered the identified PHIbase homologs to prioritise those originating from well-characterised plant pathogenic fungi. This ensured we were primarily considering genes with established roles in plant infection and disease development. Additionally, we focused on homologs confirmed as virulence or pathogenicity factors in their respective fungal species. This filtering process aimed to provide a more targeted and relevant understanding of the potential virulence factors identified in *A. ostoyae* and *A. borealis*.

By implementing this filtering strategy, we aimed to:

- **Increase specificity:** Focus on homologs with a higher likelihood of being relevant to plant-fungus interactions.
- **Enhance relevance:** Prioritise homologs with established roles in fungal virulence and pathogenicity.
- **Reduce false positives:** Minimise the influence of homologs potentially unrelated to plant disease.

The subsequent analysis (Figure 10) presents the distribution of PHIbase homologs for potential virulence factors in both constitutive and inducible pools of *A. ostoyae* (Supplementary material 5) and *A. borealis* (Supplementary material 6) after applying this filtering step. There are a total of 25 PHIbase IDs, 14 for CAZymes and 11 for non-CAZymes, identified across all functional groups and fungal species.

This refined data provides a more focused perspective on the potential roles of these factors in the fungal infection of Norway spruce. All of the selected PHIbase homologs identified in this analysis were associated with reduced virulence phenotypes in their respective fungal species.

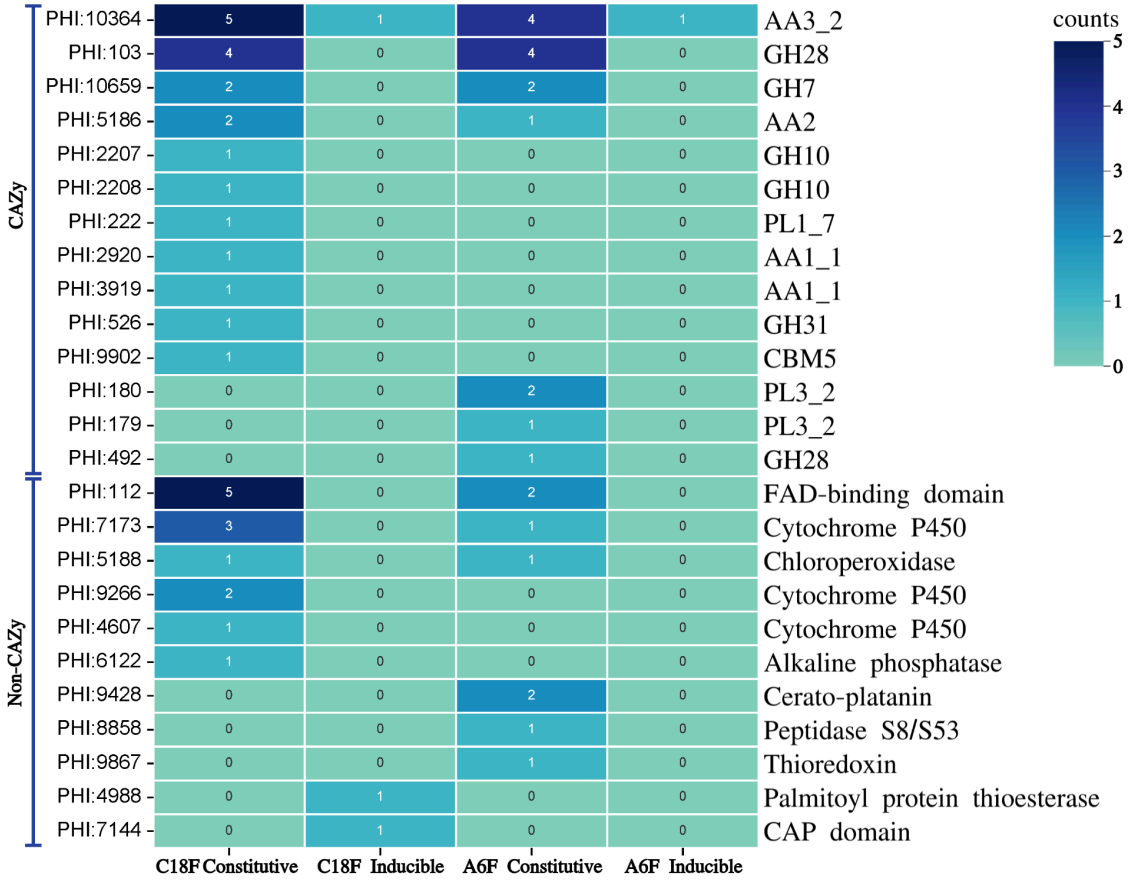

Figure 10. Distribution of PHIbase homologs with reduced virulence across constitutive and inducible pools of *A. ostoyae* (C18F) and *A. borealis* (A6F) incubated in fresh stems.

4.2. Identification of potential wood degrading factors (autoclaved stems)

4.2.1. Stem invasion

Both high and low virulence isolates of *A. ostoyae* and *A. borealis* successfully colonised autoclaved Norway spruce stem segments. Fungal mycelial samples were collected once the mycelial front reached designated openings in the segments.

High virulence *A. ostoyae* isolates again displayed faster colonisation compared to their low virulence counterparts, achieving complete invasion in 11 days on average, compared to 13 days for the low virulence strain. While *A. borealis* isolates could colonise autoclaved wood, their overall invasion times were slower. Both high and low virulence isolates took an average of 15 and 16 days, respectively, to colonise the segments, with the high virulence

strain showing a minimal advantage. Each colonisation time represents the average of three replicates per isolate.

4.2.2. Sequencing results

Similar to the fresh stem analysis, RNA-Seq was performed on three biological replicates for each isolate and condition, including high and low virulence isolates of *A. ostoya*e and *A. borealis* grown in autoclaved stems and controls. Sequencing depth ranged from 20.7 to 88.3 million reads, with an average of 71% and 74% of reads mapping to *A. ostoyae* and *A. borealis* genomes, respectively (Supplementary material 7). As with the fresh stem samples, mapping percentages varied across samples, with controls generally showing higher rates than autoclaved stem samples. Similar to the previous experiment, some differences in mapping percentages were observed between high and low virulence isolates within each species.

4.2.3. Multi-dimensional scaling analysis

MDS again revealed clear clustering of transcriptomic profiles based on species, virulence level, and treatment (control vs. autoclaved stem) (Figure 11). This confirmed distinct transcriptomic signatures associated with these factors.

4.2.4. Differentially expressed genes DEGs

We further investigated genes specifically involved in wood degradation mechanisms of *A. ostoyae* and *A. borealis* by comparing gene expression profiles of high and low virulence isolates grown on autoclaved Norway spruce stem segments to each other, as well as to their respective controls (Figure 12).

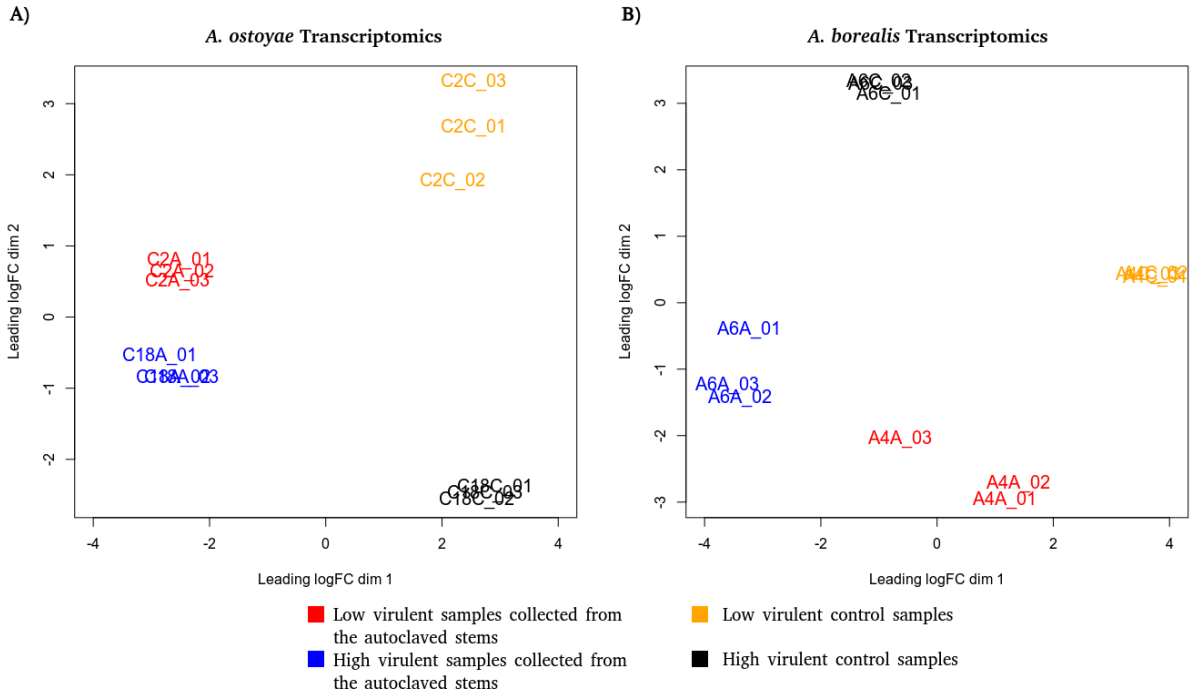

Figure 11. Multidimensional scaling of transcriptomes from *A. ostoyae* (C2: low virulent, C18: high virulent) (A) and *A. borealis* (A4: low virulent, A6: high virulent) (B). Replicates are coloured according to sample types. (C2C/C18C/A4C/A6C: control samples, C2A/C18A/A4A/A6A: samples from under the bark of autoclaved stems)

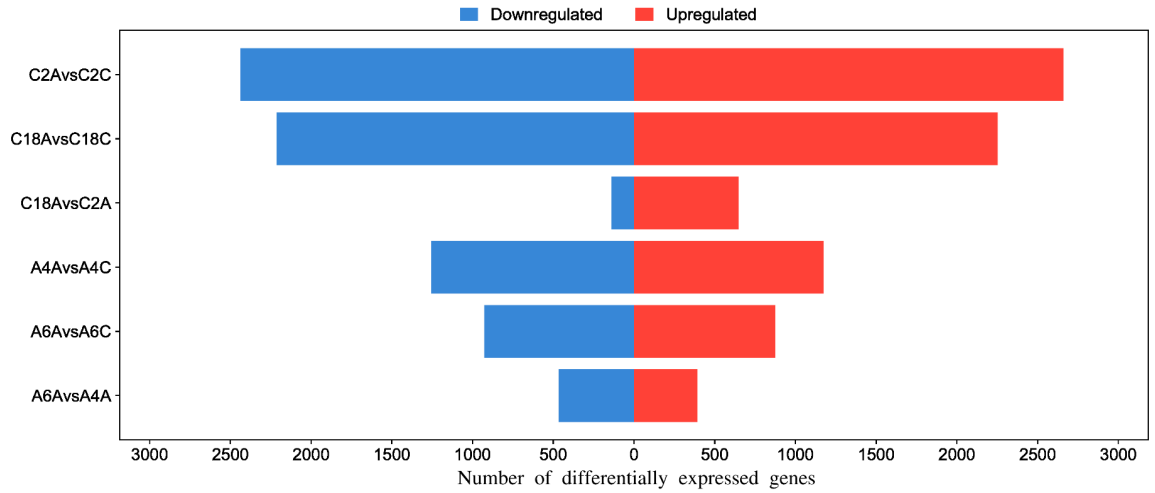

Figure 12. Comparison of up- (red) and down-regulated (blue) DEGs in *A. ostoyae* (C2: low virulent, C18: high virulent) and *A. borealis* (A4: low virulent, A6: high virulent) isolates grown in autoclaved Norway spruce stems (C2A/C18A/A4A/A6A) and their controls (C2C/C18C/A4C/A6C).

4.2.5. Identifying potential wood degrading factors candidates

Similar to the approach used for identifying virulence factors, we investigated potential wood-degrading enzymes produced by fungal cultures grown in autoclaved stems. Focusing on upregulated genes specifically present in highly wood-degrading isolates compared to both low-degrading isolates and their respective controls (Figure 13), we implemented a two-pronged strategy:

1. **Inducible wood degrading candidates**: These genes were exclusively upregulated in highly wood-degrading isolates compared to all other groups, potentially representing enzymes specifically tailored for efficient wood breakdown.
2. **Constitutive wood degrading candidates**: These genes were upregulated in highly wood-degrading isolates compared to their own controls, suggesting roles in general fitness or baseline wood-degrading capabilities.

Within these upregulated genes, we prioritised extracellular enzymes due to their direct interaction with the wood substrate and potential involvement in wood degradation. Similar to the virulence factor analysis, we utilised SignalP and WolfPsort to predict and categorise these enzymes (Table 4).

Table 4. Summary of identified upregulated genes and secreted proteins of interest in highly wood-degrading isolates of *A. ostoyae* and *A. borealis* incubated in autoclaved stems.

Species	Category	Total Upregulated	Secreted proteins
***A. ostoyae* (C18A)**	Constitutive	2249	233
	Inducible	371	23
***A. borealis* (A6A)**	Constitutive	1031	182
	Inducible	300	30

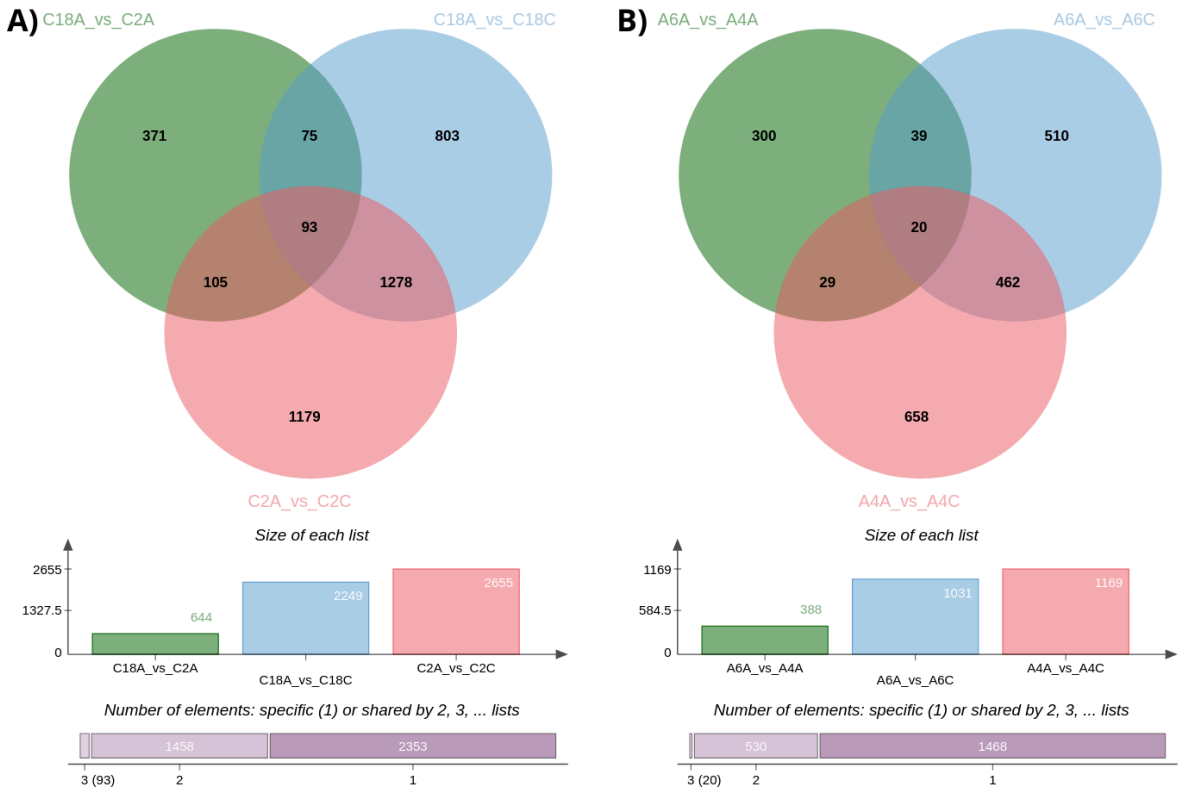

Figure 13. Overlap of upregulated genes specific to highly wood-degrading vs. low wood-degrading and control isolates of *A. ostoyae* (C2: low virulent, C18: high virulent) (A) and *A. borealis* (A4: low virulent, A6: high virulent) (B) incubated in autoclaved stems (A) or control (C) environments, with charts showing the list size and intersection size repartition located underneath the diagram.

4.2.6. Identification and characterization of secreted proteins

Similar to the approach used for identifying virulence factors, we analysed secreted proteins produced by fungal cultures grown in autoclaved stems. Focusing on CAZymes upregulated in highly wood-degrading isolates compared to both low-degrading isolates and their respective controls, we again further classified them into PCWDEs and FCWs.

As highlighted in Figure 14A, the majority of potential genes of interest originated from the constitutive pool in highly wood-degrading isolates of both *A. ostoyae* (C18F) and *A. borealis* (A6F). Both species displayed substantial representation of enzymes targeting cellulose, hemicellulose, lignin, and pectin, key wood components, within the constitutive

group. Notably, *A. ostoyae* exhibited a higher overall abundance of PCWDEs compared to *A. borealis*.

Species-specific signatures were observed in the secreted enzymes. Figure 14B reinforces the higher prevalence of PCWDEs in *A. ostoyae* compared to *A. borealis*, highlighting potential differences in their wood degradation strategies. Figure 14C depicts the ratio of PCWDEs to FCWs for each group. This ratio provides insights into the potential emphasis on wood degradation relative to fungal cell wall modification within each species. Constitutive groups of both species exhibit a higher PCWDE:FCW ratio, while inducible ones show absence of FCWs, suggesting a strong focus on degrading the wood cell wall.

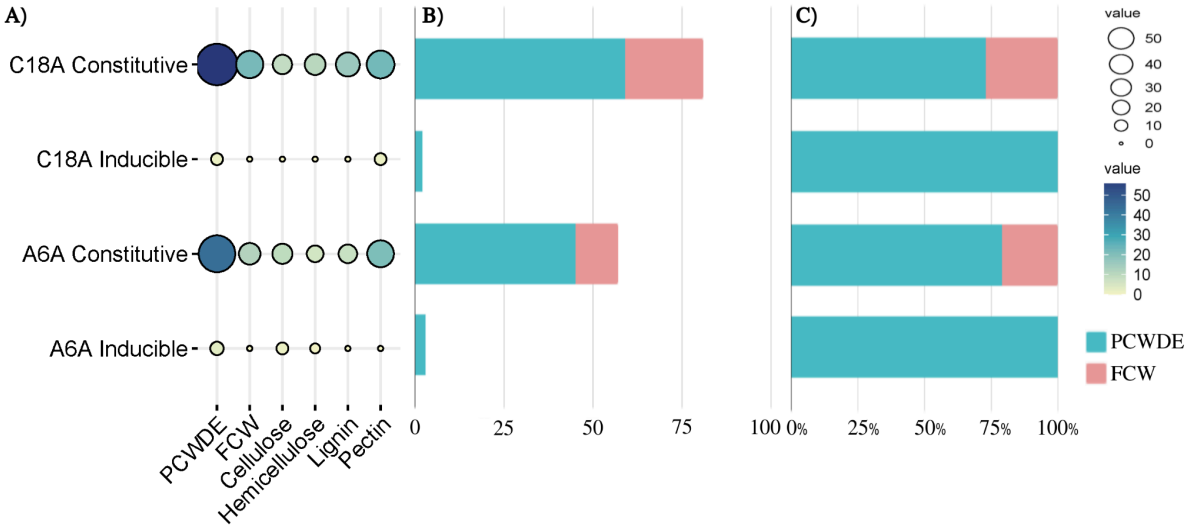

Figure 14. Count distribution of major CAZyme categories (PCWDE and FCW), classified according to Sahu et al. (2023). A) Count distribution of PCWDE, FCW, cellulose, hemicellulose, lignin and pectin degrading CAZymes among upregulated candidate DEGs of highly wood-degrading isolates of *A. ostoyae* (C18A) and *A. borealis* (A6A) incubated in autoclaved stems. B) Total PCWDE and FCW counts in each group. C) PCWDE and FCW ratios in each group.

4.2.7. Specific CAZyme families and their potential roles

Building upon the initial analysis of overall CAZyme profiles, further identification of specific CAZyme families was conducted in order to gain understanding of distinct wood degradation strategies employed *by A. ostoyae* (C18A) and *A. borealis* (A6A). The insights

obtained from Figure 15, which depicted the distribution of CAZyme families across diverse categories and substrates, serve as the cornerstone for this deeper dive.

Cellulose:

- Array of cellulases (GH1, GH3, GH6, GH7, GH12) was present in both fungal species.
- Both species had one species-specific constitutive enzyme present, AA16 for *A. ostoyae* (C18A), and GH5_5 for *A. borealis* (A6A).
- *A. borealis* (A6A) possesses two unique inducible cellulases (AA9).

Hemicellulose:

- A diverse range of hemicellulases (CE16, GH10, GH31, GH35, GH51,) targeting various hemicellulose components like xylan, arabinoxylan, and glucuronoxylan were found in both fungal species, with only GH29 being specific to *A. ostoyae* (C18A), and GH93 to *A. borealis* (A6A).

Lignin:

- Lignin-modifying enzymes (AA1_1, AA2, AA3_2) were identified in both fungi.
- *A. ostoyae* (C18A) exhibits higher abundance of these enzymes, particularly AA1_1 and AA3_2, compared to *A. borealis* (A6A).
- *A. ostoyae* (C18A) shows species-specific constitutive expression of AA5_1.

Pectin:

- Both fungal species possess enzymes targeting pectin (CE8, CE12, GH28, GH78, GH88,).
- *A. ostoyae* (C18A) displays a wider range of constitutive pectinases (CBM67, GH53, GH105, PL1_7, PL26) compared to *A. borealis* (A6A) (PL4_1).
- *A. ostoyae* (C18A) possesses unique inducible pectinases (PL14_4).

Fungal cell wall modifying enzymes (FCWs):

- Enzymes potentially involved in fungal cell wall maintenance or adaptation during wood colonisation were identified in both fungi, including chitinases (GH18, GH20, CBM50), glucanases (GH16, GH55, GH128), and mannanases (GH92).

- *A. ostoyae* (C18A) exhibits a higher abundance of constitutive GH16 glucanase and GH18 chitinase compared to *A. borealis* (A6A).
- *A. ostoyae* (C18A) also possesses unique constitutive mannanase GH76, chitinase CBM5, and glucanase GH30_3.

The analysis of CAZyme profiles revealed distinct enzyme sets employed by *A. ostoyae* (C18A) and *A. borealis* (A6A) for wood degradation. *A. ostoyae* exhibits a broader array of constitutive enzymes across various categories, potentially reflecting a more aggressive and broad-spectrum wood degradation approach. *A. borealis* possesses unique enzymes and inducible responses, suggesting a potentially niche-oriented strategy targeting specific wood components.

Despite these differences, both fungi share a significant portion of their CAZyme repertoire, highlighting convergent strategies for tackling key wood components like cellulose, hemicellulose, lignin, and pectin.

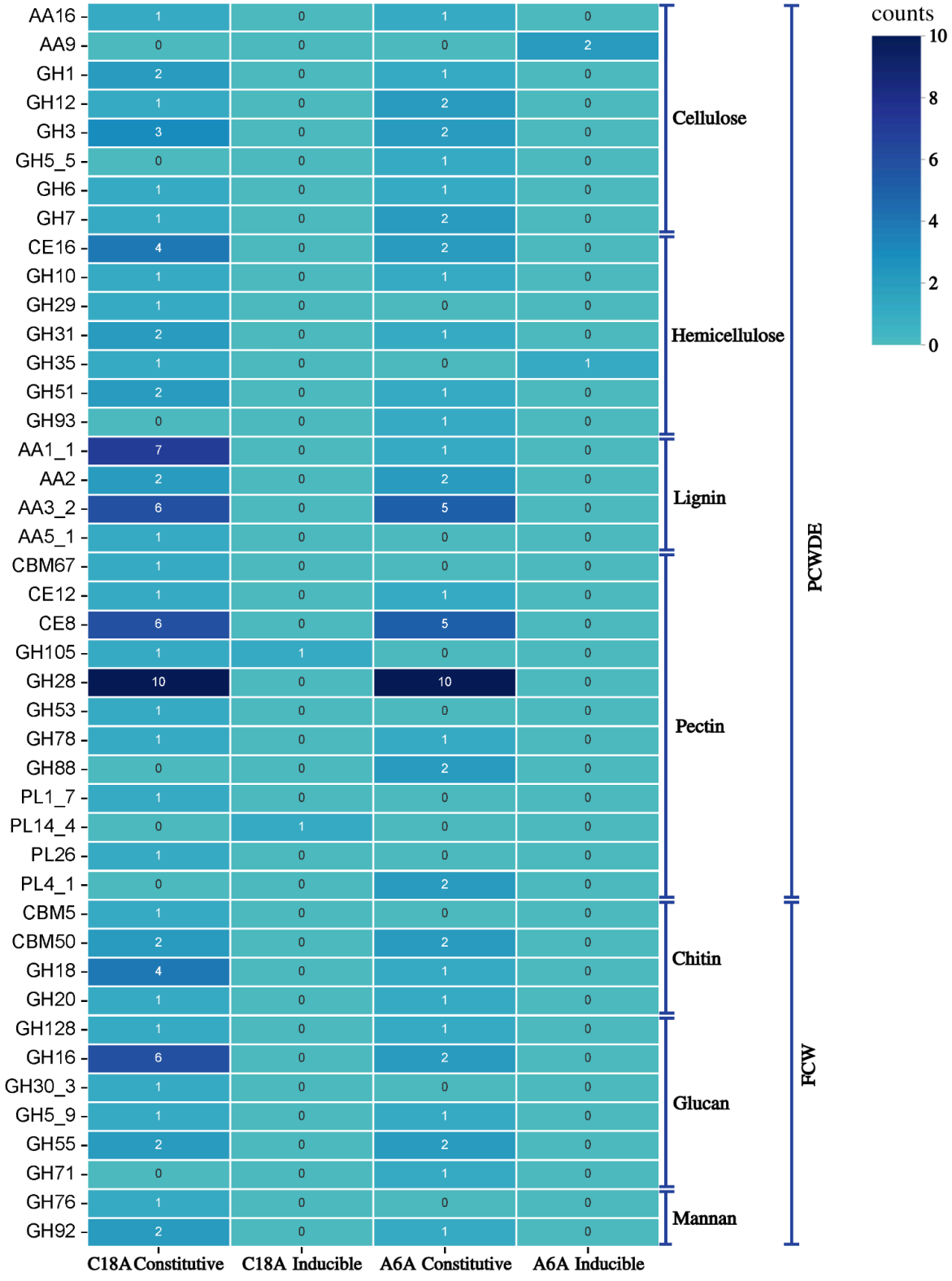

Figure 15. Distribution and abundance of CAZyme families in *A. ostoyae* (C18A) and *A. borealis* (A6A) incubated in autoclaved stems.

4.2.8. Non-CAZyme secretory wood degrading candidates

While CAZymes play a central role in breaking down wood components, non-CAZyme secretory candidates identified through InterPro annotation analysis represent a diverse array of functionalities that might complement and support CAZyme activity during this process.

The analysis revealed a distribution and abundance of these candidates categorised based on their predicted functions annotated by InterPro.

A total of 67 unique InterPro domains were detected across the identified non-CAZyme secretory proteins (Figure 16). Focusing on annotations relevant to wood degradation, the figure highlights several key categories:

Cell wall-degrading enzymes:

- Alpha/beta hydrolase (IPR000073): Found in *A. ostoyae* C18A constitutive pool.
- Endonuclease/exonuclease/phosphatase (IPR005135): Present in both *A. ostoyae* C18A constitutive and *A. borealis* A6A inducible pools.
- Fungal lipase-like domain (IPR002921): Specific to the *A. ostoyae* C18A constitutive pool where it appears three times.
- Intradiol ring-cleavage dioxygenase (IPR000627): Showing up multiple times in both *A. ostoyae* C18A and *A. borealis* A6A constitutive pools.

Other enzymes potentially contributing to wood degradation:

- Carboxylesterase (IPR002018): Two constitutively expressed non-CAZymes in *A. ostoyae* C18A.
- Cytochrome P450 (IPR001128): Highly present in constitutive pools of both species.
- Calcineurin-like phosphoesterase domain (IPR004843): With one copy in both species' constitutive pools.
- Lysine-specific metallo-endopeptidase (IPR029463): Also with one copy in both species' constitutive pools.
- Tyrosinase copper-binding domain (IPR002227): With two copies in *A. ostoyae* C18A constitutive and one in both *A. borealis* A6A constitutive and inducible pools.

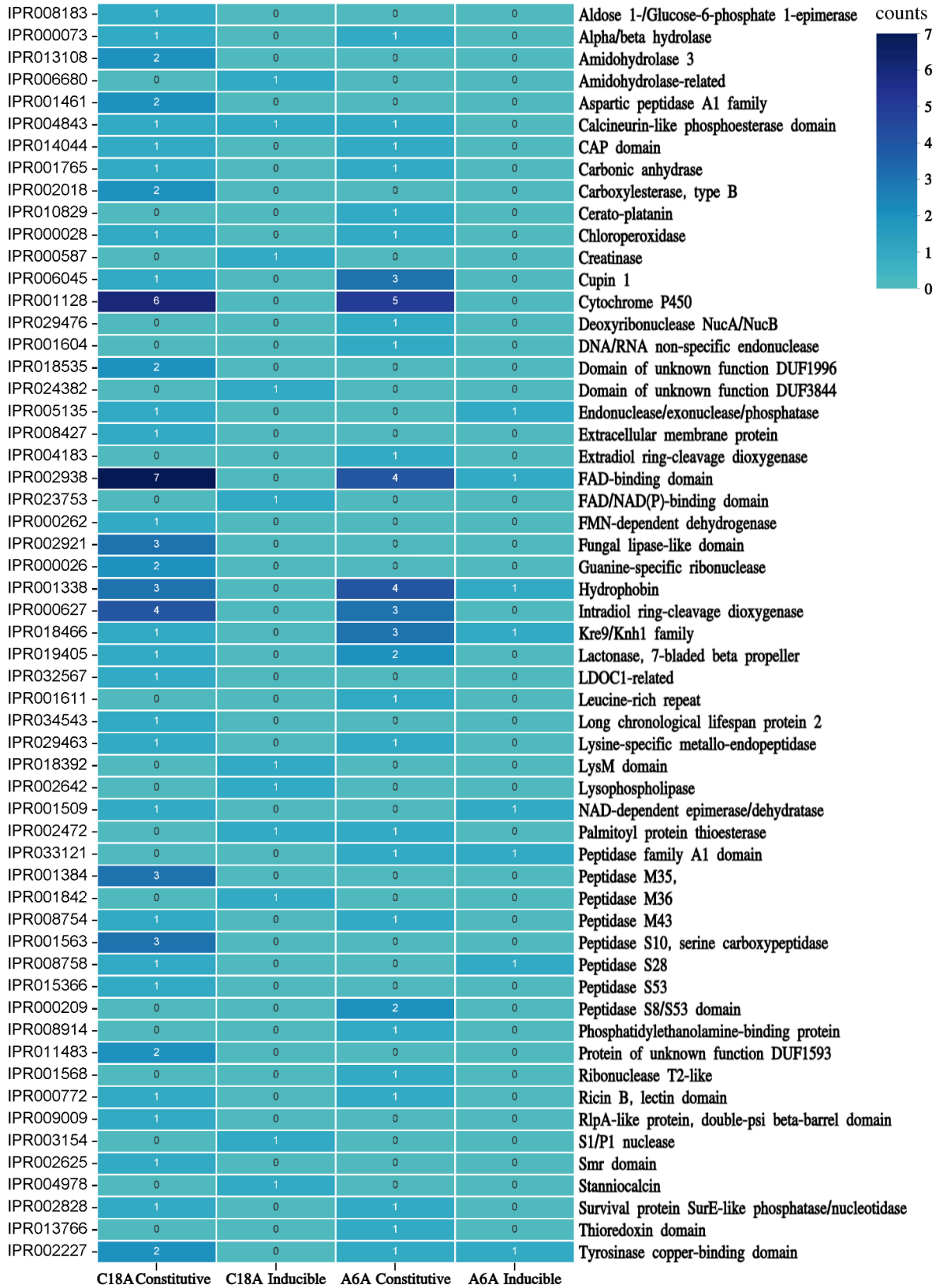

Figure 16. Distribution and abundance of non-CAZyme secretory candidates in *A. ostoyae* (C18A) and *A. borealis* (A6A) incubated in autoclaved stems.

4.3. Mycoremediation potential of *A. ostoyae* and *A. borealis*

Comparing the genetic makeup of *Armillaria* species with other fungal genomes reveals that these species exhibit a higher prevalence of genes involved in degrading various monocyclic aromatic compounds compared to their fungal counterparts (Supplementary material 8 and 9). This includes enzymes like homogentisate 1,2-dioxygenase (HGD), maleylacetate reductase, arylesterase/paraoxonase, nitrilase, and 3-carboxy-cis,cis-muconate cycloisomerase. These enzymes work together to break down various single-ringed aromatic molecules, potentially contributing to the bioremediation potential of these fungi.

One particularly noteworthy finding is the abundance of HGD genes among all *Armillaria* spp. compared to other basidiomycetes, with both *A. ostoyae* and *A. borealis* having four copies each (Supplementary material 8). HGD plays a crucial role in degrading homogentisate, a key intermediate in the breakdown of several aromatic compounds. This finding suggests a potentially enhanced capacity for these *Armillaria* species to tackle various aromatic substrates.

Additionally, all armillarioid species possess maleylacetate reductase and 3-carboxy-cis,cis-muconate cyclase genes, unlike most other basidiomycetes but similar to some ascomycetes (Supplementary material 7). These enzymes contribute to specific steps within the degradation pathway of certain monocyclic aromatics, further illustrating the unique enzymatic machinery possessed by these *Armillaria* species. Also, arylesterase/paraoxonase gene, which plays a role in degrading specific aromatic compounds like aminobenzoate, is present in higher copy numbers among *Armillaria*s compared to other fungi, suggesting a potential advantage in handling these substrates.

While genes associated with polycyclic aromatic hydrocarbons (PAH) degradation were identified in armillarioids, their copy numbers were generally lower compared to other basidiomycete species. This suggests that other basidiomycete fungi might be more efficient in degrading PAH pollutants.

Among the enzymes involved in PAH breakdown, salicylate hydroxylase and manganese peroxidase (MnP), were present in higher numbers in *A. ostoyae* and *A. borealis* compared to ascomycetes but lower compared to other basidiomycetes. Soluble epoxide hydrolase which degrades benzo[a]pyrene, had more copies in *A. ostoyae* and *A. borealis*s compared to most ascomycetes, suggesting a potential for degrading this specific PAH.

RNA-sequencing data revealed that over 95% in *A. ostoyae* and 87% in *A. borealis* of the identified genes potentially involved in mycoremediation were actively expressed in both species, regardless of their virulence (Table 5).

Table 5. Expression analysis of the mycoremediation-related genes.

	A. ostoyae (expressed/total in genome)	*A. borealis* (expressed/total in genome)
Mycoremediation related genes	130/137 (95%)	126/145 (87%)
Monocyclic aromatics degraders	9/12 (75%)	10/11 (91%)
Homogentisate 1,2-dioxygenase [EC:1.13.11.5]	4/4	4/4
Maleylacetate reductase [EC:1.3.1.32]	1/1	1/1
Arylesterase/paraoxonase [EC:3.1.1.2 3.1.8.1]	2/2	2/2
Nitrilase [EC:3.5.5.1]	3/3	2/2
3-carboxy-cis,cis-muconate cycloisomerase [EC:5.5.1.2]	0/1	1/1
Carboxy-cis,cis-muconate cyclase [EC:5.5.1.5]	0/2	0/1
PAH degraders	15/20 (75%)	21/23 (91%)
Salicylate hydroxylase [EC:1.14.13.1]	7/8	9/9
Manganese peroxidase [EC:1.11.1.13]	4/7	7/8
Soluble epoxide hydrolase/lipid-phosphate phosphatase [EC:3.3.2.10 3.1.3.76]	4/5	5/6

Further analysis of HGD gene expression revealed upregulation in both *A. ostoyae* and *A. borealis* during plant stem invasion experiments. Their comparative analysis of gene expression revealed that 3 out of the 8 genes, similarly to benzoate-4-monooxygenases, exhibited upregulation during plant-invasive conditions, while the remaining genes either remained inactive or displayed altered expression patterns. Additionally, the gene expression profiles of salicylate hydroxylases and MnPs, which are associated with the breakdown of PAHs and commonly found in Basidiomycota, differed from those of benzoate monooxygenase and HGD genes, as their levels of expression tended to rise when cultivated on nutrient-rich media (Figure 17).

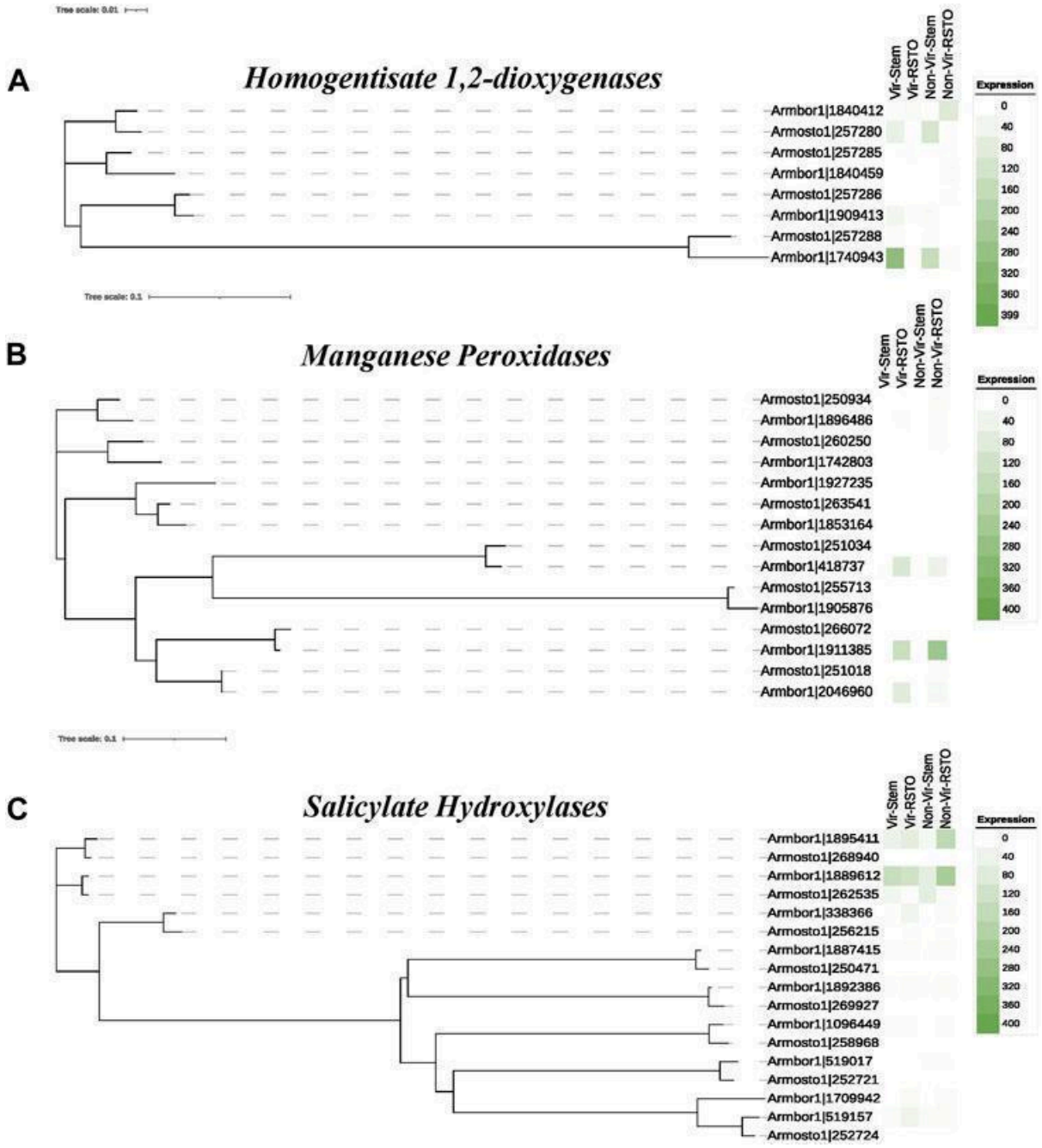

Figure 17. Heatmaps of the expression of HGD (A), manganese peroxidase (B) and salicylate-hydroxylase (C) genes. High ("Vir") and low virulent ("Non-Vir") *A. ostoyae* and *A. borealis* isolate pairs were used in the *in vitro* stem invasion assays, and "Stem" indicating mycelia isolated from the underbark tissue of stem segments and "RSTO" being the control mycelia growing on rich media.

5. DISCUSSION

Forests are crucial ecosystems facing threats from various pathogens, including the aggressive fungal pathogens. Plants defend themselves with physical barriers like cell walls and activate immune responses upon pathogen invasion (Jones and Dangl, 2006; Wang et al., 2019). To overcome these defences, necrotrophic fungi, including *A. ostoyae* and *A. borealis*, deploy an arsenal of PCWDEs that facilitate breaching and nutrient acquisition (Hématy et al., 2009). This study aimed to elucidate the molecular mechanisms underlying their virulence and wood degradation by identifying putative virulence factors among differentially expressed genes (DEGs) during infection.

The two *Armillaria* species were selected due to their overlapping occurrences in Europe, mostly in central and eastern Europe and southern Scandinavia. Additionally, both species have been known for showing affinities towards coniferous trees, and being associated with Norway spruce (Keca and Solheim, 2011; Heinzelmann et al., 2017). However, where these species do differ are their pathogenicity and virulence levels. Previous studies report *A. borealis* as being mostly saprotrophic, with some limited pathogenicity and virulence levels, usually as a secondary pathogen, infecting already weakened trees (Gregory and Watling, 1985; Keca and Solheim, 2011; Pavlov, 2015). On the other hand, *A. ostoyae* is a species with a high pathogenicity and virulence potential and is recognized as a very aggressive primary pathogen which can infect a wide range of tree species (Omdal et al., 1995; Prospero et al., 2004; Heinzelmann et al., 2017).

5.1. Virulence candidates

Our findings demonstrate a clear correlation between faster colonisation and higher virulence in *A. ostoyae*, supporting observations from previous studies (Prospero et al., 2004; Heinzelmann et al., 2017). Additionally, transcriptomic profiles revealed distinct responses to the host environment based on species, virulence level, and treatment. Differential gene expression (DEG) analysis identified a significant upregulation of genes associated with plant cell wall degradation (PCWD) in both *A. ostoyae* and *A. borealis*. This finding aligns with established knowledge in phytopathogenic fungi, where PCWDEs have been linked to fungal virulence, highlighting the importance of this strategy in overcoming plant defences (Espino et

al., 2005; Brito et al., 2006; Kema et al., 2008; Fernández‐Acero et al., 2010; Mathioni et al., 2011; Martínez-Soto et al., 2013).

Focusing on DEGs specifically present in the stem-invasive mycelia of highly virulent isolates (Figures 8-9), we identified potential virulence factor candidates. Among these, carbohydrate-active enzymes (CAZymes) emerged as a prominent group, with *A. ostoyae* exhibiting a higher abundance of PCWDEs compared to both its low virulence counterpart and *A. borealis* isolates. This suggests a potentially more aggressive strategy for breaching the cell wall, contributing to its observed higher virulence. Species-specific differences were also evident in the overall enzyme profiles. Interestingly, both species shared a significant portion of their CAZyme repertoire, suggesting convergent strategies for tackling common cell wall components. However, observed differences in abundance and inducible expression suggest unique nuances in their approaches to overcoming host defences.

To gain further insights into potential virulence factors, we identified homologs of DEGs within the PHIbase database. This *in silico* approach allowed us to leverage existing knowledge about fungal virulence factors in other pathogens and explore their potential presence in *A. ostoyae* and *A. borealis*. Analysis of PHIbase homologs (Supplementary material 5 and 6) revealed homologs for numerous candidates in both fungi. Generally, a higher number of PHIbase homologs were found for *A. ostoyae* virulence factors, where we focused on ones associated with reduced virulence phenotypes. This suggests that many *A. ostoyae* virulence factors may play essential roles in overcoming host defences, while some *A. borealis* virulence factors might contribute to less critical aspects of the infection process. These findings not only provide insights into *A. ostoyae's* potential virulence strategies but also contribute to our understanding of the commonalities and variations in how necrotrophic fungi overcome host defences.

5.1.1. CAZyme virulence candidates

Among the CAZymes, a homolog identified across all four groups encodes a **glucose-methanol-choline oxidoreductase** (**GMC oxidoreductase**), previously characterised in *Botrytis cinerea* (PHI:10364), where this enzyme plays a crucial role in host infection (Zhang et al., 2020). The PHIbase analysis revealed five homologs in *A. ostoyae* constitutive pool (ARMOST_14728, ARMOST_17626, ARMOST_01984, ARMOST_04029,

ARMOST_16408) and one in inducible (ARMOST_20378), compared to four (jgi|Armbor1|1744029, jgi|Armbor1|1699834, jgi|Armbor1|1987737, jgi|Armbor1|1941457) among *A. borealis* constitutive candidates and one (jgi|Armbor1|1926153) among inducible ones. This suggests that GMC oxidoreductase might be more prevalent in armillarioid virulence.

The identification of GMC oxidoreductase homologs aligns with existing knowledge about the functional diversity of this enzyme family in fungal degradation of plant cell wall components (Sutzl et al., 2019). In polypore fungi, GMC oxidoreductases are known to generate hydrogen peroxide (H_2O_2), which plays a critical role in both white-rot and brown-rot decay (Ferreira et al., 2015). While the specific role of GMC oxidoreductases in *A. ostoyae* and *A. borealis* virulence remains to be investigated, the presence of homologs associated with reduced virulence suggests their potential importance in overcoming host defences. Future functional validation studies are necessary to confirm the specific roles of these candidate virulence factors in fungal pathogenesis.

The PHIbase analysis also revealed homologs for a putative **endopolygalacturonase (glycoside hydrolase family 28 (GH28))** in both *A. ostoyae* (ARMOST_17334, ARMOST_17320, ARMOST_17350, ARMOST_17277) and *A. borealis* (jgi|Armbor1|2082336, jgi|Armbor1|1904159, jgi|Armbor1|577390, jgi|Armbor1|583912) constitutive fractions. These homologs share sequence similarity with Bcpg1 from *Botrytis cinerea* (PHI:103), an endopolygalacturonase enzyme known to be essential for full virulence in tomato infection (Have et al., 1998). Endopolygalacturonases are enzymes known to degrade plant cell wall components and have been linked to fungal virulence in various necrotrophs. They contribute to the breakdown of plant cell wall components, facilitating fungal penetration and nutrient acquisition (Kubicek et al., 2014). The presence of homologs in both *A. ostoyae* and *A. borealis* with constitutive expression suggests that this enzyme might be a shared virulence factor employed by these fungi.

Focusing specifically on *A. borealis*, PHIbase identified a single homolog (PHI:492) encoding a **GH28** protein in the constitutive pool (jgi|Armbor1|123718). The study by Kars et al. (2005) using *B. cinerea* provides insights into the potential function of the endopolygalacturonase homolog in *A. borealis*. In that study, five BcPG (*Botrytis cinerea* polygalacturonase) enzymes were identified and characterised, including BcPG2, an endopolygalacturonase enzyme essential for full virulence in *B. cinerea*. Deletion of the

BcPG2 gene in *B. cinerea* resulted in significantly reduced virulence on tomato and broad bean plants. In *A. borealis*, the presence of a putative GH28 homolog suggests its potential involvement in early stages of infection. Similar to BcPG2, the *A. borealis* GH28 might contribute to pectin degradation and play a role in breaching the plant cell wall, promoting fungal invasion and symptom development.

Further analysis of PHIbase homologs revealed candidates encoding **cellobiohydrolases (glycoside hydrolase family 7 (GH7))** in the constitutive pools of both *A. ostoyae* (ARMOST_17072, ARMOST_17156) and *A. borealis* (jgi|Armbor1|1277186, jgi|Armbor1|1739286). In *Phytophthora sojae*, a similar GH7, PsGH7a (PHI:10659) has been demonstrated to be essential for full virulence on soybeans. PsGH7a promotes fungal invasion by hydrolyzing β-1,4-glucan bonds in cellulose, facilitating the breaching of plant cell walls (Tan et al., 2020). The identification of GH7 homologs in *A. ostoyae* and *A. borealis* with constitutive expression suggests that GH7s might play a vital role in their early stages of infection.

Our analysis of PHIbase homologs identified putative peroxidases in constitutive pools of both *A. ostoyae* (ARMOST_18738, ARMOST_17524) and *A. borealis* (jgi|Armbor1|1356237). These homologs included **haem peroxidases (auxiliary activity family - AA2)** (PHI:5186) within the CAZy fraction. Additionally, one homolog encoding a putative **chloroperoxidase** (PHI:5188) was identified in the non-CAZy fraction of both species' constitutive pools (ARMOST_12912, jgi|Armbor1|1466796). Peroxidases are versatile enzymes involved in various cellular processes, including mitigating oxidative stress during infection. Studies in *Magnaporthe oryzae* have demonstrated that multiple peroxidase genes are essential for full virulence. Deletion mutants exhibited reduced peroxidase activity, increased sensitivity to hydrogen peroxide (H_2O_2), and compromised ability to infect rice (Mir et al., 2015). The presence of homologs in both *A. ostoyae* and *A. borealis* suggests that peroxidases might also play a role in their virulence strategies.

PHIbase analysis revealed homologs (PHI:2207 and PHI:2208) encoding putative **endo-1,4-beta-xylanases (glycoside hydrolase family 10 - GH10)** within the constitutive group of *A. ostoyae* (ARMOST_08096, ARMOST_13039). Xylanases are enzymes that degrade xylan, a major component of plant cell walls. In *Magnaporthe oryzae*, functional studies have demonstrated that xylanase genes are essential for full virulence. Silencing xylanase genes in *M. oryzae* resulted in reduced pathogenicity, including decreased numbers of

lesions, penetration rates, and the extent of infected plant cells (Nguyen et al., 2011). These findings suggest that xylanases play a critical role in both the vertical penetration and horizontal expansion of the fungus within the host plant tissue. The identification of xylanase homologs in *A. ostoyae*, but not *A. borealis*, suggests a potential importance in early stages of infection.

A homolog (PHI:222) encoding a **putative pectate lyase (PL1_7)** in the constitutive fraction of *A. ostoyae* (ARMOST_13458). Pectate lyases are enzymes that degrade pectin, a major component of the middle lamella in plant cell walls. In *Colletotrichum gloeosporioides*, a necrotrophic fungal pathogen, studies have shown that a pectate lyase B (pelB) is an important virulence factor. *C. gloeosporioides* mutants lacking pelB displayed a significant reduction in their ability to cause disease on avocado fruit (Yakoby et al., 2001). While the specific plant cell wall composition of *A. ostoyae* hosts may differ from avocado, pectate lyase could still contribute to pathogenesis by aiding in the breakdown of host cell wall components during early stages of infection.

PHIbase analysis revealed two homologs (PHI:2920 and PHI:3919) **encoding putative multicopper oxidases (AA1_1)** in the constitutive pool of *A. ostoyae* (ARMOST_20610, ARMOST_21416, ARMOST_16697, ARMOST_02569). Multicopper oxidases are enzymes involved in iron acquisition, a vital process for fungal pathogens. Studies in *Colletotrichum graminicola* and *Ustilago maydis*, maize fungal pathogens, have demonstrated the importance of multicopper oxidases (FET3-2 and fer1, respectively) for full virulence (Eichhorn et al., 2006; Albarouki and Deising, 2013). These enzymes function by converting ferrous iron (Fe^{2+}) to ferric iron (Fe^{3+}), a form that's easier to assimilate by fungi. Deletion of the genes encoding these multicopper oxidases in *C. graminicola* and *U. maydis* resulted in reduced virulence, with defects in appressorial penetration, cell wall integrity, and biotrophic development (Eichhorn et al., 2006; Albarouki and Deising, 2013). The identification of multicopper oxidase homologs in *A. ostoyae* suggests a potential role for iron acquisition in its virulence strategies. Iron availability within the host plant environment plays a complex role in fungal-plant interactions. Plants often employ iron-withholding mechanisms to limit pathogen access to this essential nutrient (Ye et al., 2014). The presence of multicopper oxidase homologs in *A. ostoyae* suggests it may possess mechanisms to acquire iron efficiently, potentially influencing both its ability to establish infection and counteract host defence responses.

A homolog encoding a putative glucosidase belonging to **glycoside hydrolase family 31 (GH31)** was identified in the constitutive fraction of *A. ostoyae* (ARMOST_15648) (PHI:526). In the corn smut fungus *Ustilago maydis*, a gene encoding an endoplasmic reticulum (ER) glucosidase (GAS1) was found to be essential for full virulence on maize. Deletion of GAS1 did not affect fungal growth or appressorium formation but resulted in a block in pathogenic development soon after penetration into the host plant tissue. Mutant *U. maydis* lacking GAS1 displayed defects in septum formation and cell wall organisation at the infection site (Schirawski et al*.,* 2005). The identification of an ER glucosidase homolog in *A. ostoyae* suggests a potential role for protein N-glycosylation in its virulence strategies. While the specific contribution of ER glucosidase to *A. ostoyae* pathogenesis remains to be confirmed, it might be important for proper protein folding and function during early stages of infection, particularly for proteins involved in host cell wall degradation, nutrient acquisition, and effector molecule secretion.

PHIbase analysis revealed a homolog (PHI:9902) encoding a **carbohydrate-binding module family 5 (CBM5)** domain in the constitutive fraction of *A. ostoyae* (ARMOST_11243). While the specific function of this CBM domain is unknown, it's interesting to note the crucial role subtilisin-like proteases play in fungal virulence, as exemplified by Bcser2 in *Botrytis cinerea* (Liu et al., 2020). Bcser2 deletion in *B. cinerea* resulted in severe defects in pathogenesis, potentially due to its interaction with carbohydrates on the host plant cell wall. In *A. ostoyae*, the CBM5 domain might be associated with an enzyme or protein with a similar virulence-related function, but it's important to consider that CBM domains can bind to various carbohydrates. The specific role of this CBM domain in *A. ostoyae* could involve recognition of fungal cell wall components, interaction with signalling molecules, or binding to carbohydrates on the host during infection.

Among the constitutive pool of *A. borealis* three homologs encoding **pectate lyases (PL3_2)** were present (jgi|Armbor1|1467293, jgi|Armbor1|1999178, jgi|Armbor1|1777836). Two of these homologs (PHI:180) share similarity to pectate lyase A (pelA) sequences, while the third homolog (PHI:179) resembles pectate lyase D (pelD). The importance of both pelA and pelD for full virulence has been demonstrated in the fungal pathogen *Fusarium solani*. There, the disruption of either pelA or pelD alone did not significantly affect virulence, but deletion of both genes resulted in a drastic reduction in virulence (Rogers et al., 2000). These findings highlight the concept of functional redundancy, where multiple enzymes with similar

functions can compensate for each other's loss and contribute to overall virulence (Nowak et al., 1997). In *A. borealis*, the presence of two pelA homologs and a single pelD homolog suggests potential for pectin degradation during early stages of infection. Similar to *F. solani*, *A. borealis* might rely on the combined activity of these PL isoforms to effectively degrade plant cell wall components and establish infection. This redundancy could also provide *A. borealis* with an advantage in overcoming potential host defences that target specific PL isoforms.

5.1.2. Non-CAZyme virulence candidates

While CAZymes are central to fungal pathogenesis by breaking down plant cell walls, non-CAZyme secretory proteins offer a broader range of functionalities crucial for successful colonisation and virulence. These proteins encompass diverse categories, including:

- **Adhesins:** Facilitate attachment to host tissues, aiding in initial colonisation.
- **Transporters:** Essential for nutrient acquisition from the host environment.
- **Oxidoreductases:** Play a role in detoxifying host defence compounds and modifying the surrounding environment to benefit fungal growth.
- **Hydrolases:** Contribute to degrading host cell wall components and potentially modulating the immune response.

Analysis of non-CAZyme candidates revealed multiple homologs encoding **FAD-binding domains** (PHI:112) in both *A. ostoyae* (ARMOST_05711, ARMOST_04588, ARMOST_05456, ARMOST_05454, ARMOST_04595) and *A. borealis* (jgi|Armbor1|2008440, jgi|Armbor1|107486). FAD-binding domains are associated with proteins that utilise flavin adenine dinucleotide (FAD) as a cofactor in various enzymatic reactions, including those involved in detoxification. In some fungal pathogens, proteins containing these domains are known to play a role in detoxifying plant defence compounds called phytoalexins. The study by Enkerli et al. (1998) demonstrates how the FAD-binding domain containing protein MAK1 contributes to the virulence of *F. solani* by detoxifying maackiain, a phytoalexin produced by the chickpea plant. Disruption of the MAK1 gene in*F. solani* reduced its virulence, highlighting the role of detoxification in fungal pathogenesis. The higher number of homologs in *A. ostoyae* compared to *A. borealis* might indicate functional

redundancy in its detoxification pathway. Alternatively, the multiple homologs in *A. ostoyae* could suggest broader substrate specificity for detoxification, enabling it to inactivate a wider range of phytoalexins produced by their conifer hosts compared to *A. borealis*.

The PHIbase analysis identified several homologs encoding **cytochrome P450** enzymes in *A. ostoyae* and one in *A. borealis*. Cytochrome P450s are a diverse group of enzymes found in all living organisms and play a crucial role in various metabolic processes. They metabolise a wide range of compounds, both internally produced (endogenous) and externally encountered (exogenous). Endogenous substrates include steroids, fatty acids, and hormones, while exogenous compounds encompass plant secondary metabolites, pesticides, and mutagens. These metabolic processes contribute to various vital functions in organisms, such as growth, development, nutrition, and detoxification of foreign chemicals (Xu et al., 2015).

Several examples from other fungal pathogens highlight this connection. In *Verticillium dahliae* (PHI:7173), a cytochrome P450 (HiC-15) is critical for hyphal growth, and its disruption significantly reduces virulence in cotton plants (Zhang et al., 2016a). The HiC-15 homolog has three copies in *A. ostoyae* (ARMOST_21614, ARMOST_07521, ARMOST_00213) and one in *A. borealis* (jgi|Armbor1|1154540). This difference in homolog numbers might indicate functional redundancy in the detoxification pathway of *A. ostoyae*, allowing it to compensate for the loss of one homolog. Alternatively, the multiple homologs could suggest a broader substrate specificity for detoxification in *A. ostoyae* compared to *A. borealis*. This could potentially contribute to *A. ostoyae* having a higher tolerance towards a wider range of defence compounds.

Another example comes from *Fusarium proliferatum* (PHI:9266), where a cytochrome P450 (FUM6) is responsible for fumonisin biosynthesis, a mycotoxin essential for its virulence in rice (Sun et al., 2019). Similarly, the two cytochrome P450s homologs in *A. ostoyae* (ARMOST_15491, ARMOST_06306) could be involved in the biosynthesis of virulence factors required for infection.

The final homolog identified from the *A. ostoyae* (ARMOST_03637) constitutive pool possesses a conserved **alkaline phosphatase**, suggesting its potential role in phosphate acquisition (PHI:6122). This homolog shares similarity with FGSG_06610 in *Fusarium graminearum*, where mutants lacking this protein exhibit significantly reduced virulence on maize, with lesions reaching only half the size compared to wild-type infections (Zhang et al.,

2016b). They function as alkaline phosphatases, liberating free phosphate from organic compounds within the host tissue. This finding suggests that the *A. ostoyae* homolog might play a similar role by acquiring phosphate from organic sources in hosts, facilitating nutrient uptake and promoting successful colonisation.

Two homologs present in the *A. borealis* constitutive pool (jgi|Armbor1|1736842, jgi|Armbor1|1896746) belong to the **cerato-platanin family** and share similarities with SsSm1 (PHI:9428), a protein elicitor from *Sclerotinia sclerotiorum*. SsSm1 plays a role in regulating *S. sclerotiorum* growth and development, influencing mycelial growth and sclerotium formation. Silencing the gene encoding SsSm1 significantly reduced fungal growth, infection cushion formation, and sclerotia production, ultimately decreasing the virulence (Pan et al., 2018). Similar to SsSm1, the *A. borealis* homologs might act as virulence factors, manipulating the host's defence mechanisms to promote fungal growth and colonisation.

A single homolog identified in the *A. borealis* constitutive pool (jgi|Armbor1|1741355) possesses a **Peptidase S8/S53** domain (PHI:8858), suggesting its role as a protease. This homolog shares similarities with VdSSEP1, a protease from *Verticillium dahliae*. VdSSEP1 functions by degrading chitinase enzyme (Chi28) involved in the plant's defence response. Mutants lacking VdSSEP1 displayed reduced virulence on cotton plants, with significantly lower disease severity (Han et al., 2019). The *A. borealis* homolog might act similarly to VdSSEP1, targeting and degrading specific proteins within the host apoplast to suppress plant defence responses and promote fungal colonisation.

The PHIbase analysis identified a single homolog in *A. borealis* (jgi|Armbor1|1706119) possessing a **thioredoxin domain** (PHI:9867). This domain is characteristic of protein disulfide isomerases (PDIs), enzymes that play a crucial role in protein folding within the ER. Proper protein folding is essential for protein function, and PDI activity is critical for various cellular processes. Similar to this thioredoxin domain in *A. borealis* is Pdi1, a PDI in *U. maydis*, essential for its virulence on maize. Deletion of Pdi1 resulted in significant virulence reduction and growth defects, likely due to its role in facilitating proper protein folding within the ER, which is essential for fungal growth, development, and virulence (Marín-Menguiano et al., 2019).

The final two *Armillaria* virulence candidates were identified within the inducible pool of *A. ostoyae*. The first homolog (ARMOST_09930) shares similarity with **palmitoyl protein**

thioesterase Ppt1 (PHI:4988), a protein essential for virulence in fungal plant pathogens *Cochliobolus* necrotrophs*, C. heterostrophus,* and *C. miyabeanus*. Ppt1 activates enzymes involved in synthesising various secondary metabolites, including host-selective toxins and pigments like melanin. Deletion of the Ppt1 gene in *Cochliobolus* species resulted in reduced virulence, inability to produce toxins, and defects in stress tolerance and development (Zainudin et al., 2015). This suggests that the *A. ostoyae* homolog might play a similar role, with its potential involvement in secondary metabolite biosynthesis contributing to *A. ostoyae* virulence.

The final homolog identified in *A. ostoyae*'s inducible pool (ARMOST_06352) shares similarity with FvScp1 (PHI:7144), a SCP-like extracellular protein belonging to the **cysteine-rich secretory protein** superfamily, essential for virulence in the fungal maize pathogen *Fusarium verticillioides*. FvScp1 interacts with other proteins, forming a complex that helps regulate virulence. Deletion of FvScp1 in *F. verticillioides* leads to mislocalization of a key virulence regulator protein and a decrease in fungal virulence (Zhang et al., 2018). The *A. ostoyae* homolog possesses a similar CAP domain as FvScp1, suggesting it might be part of a similar protein complex that regulates virulence factors or fungal processes crucial for successful infection.

Overall, the PHIbase analysis identified several potential virulence factors in *A. ostoyae* and *A. borealis*. Future research is necessary to understand specific functions of these homologs and their actual contribution to pathogenicity.

5.1.3. Limitations and future directions

While this study provides valuable insights into the putative virulence factors employed by *A. ostoyae* and *A. borealis*, some limitations need to be acknowledged. Relying solely on *in silico* analysis for predicting virulence factors necessitates further functional validation. Future research should focus on experimental approaches like gene deletion or overexpression experiments coupled with virulence assays on susceptible hosts to confirm the roles of these candidate genes. Additionally, for the specific contributions to the pathogenesis of each fungal species, investigation of the expression patterns of these genes during different stages of infection should be conducted.

The observed similarities and differences in virulence strategies between *A. ostoyae* and *A. borealis* likely extend beyond the identified virulence factors. Future studies should explore other potential contributors to virulence, such as differences in secondary metabolite production or defence response manipulation. Additionally, investigating the interplay between these virulence factors and wood degrading enzymes during different stages of infection would provide a more complete picture of the pathogenic processes employed by these fungi.

5.2. Wood degrading repertoire

Armillaria fungi possess not only virulence factors that compromise host defences but also require a robust arsenal of wood-degrading enzymes to break down and utilise the complex polysaccharides within the host cell wall. Understanding the repertoire of these enzymes in *A. ostoyae* and *A. borealis* is crucial for a comprehensive understanding of their pathogenic mechanisms. The discussion follows the magnitude of observed DEGs (Figures 15-16).

5.2.1. Cellulose degradation

Cellulose, the most abundant polysaccharide in wood, presents a formidable barrier for fungi seeking to access nutrients within the host cell wall. White-rot (WR) fungi, including *Armillaria* species, overcome this challenge by employing a diverse arsenal of cellulases.

The presence of five GH families (GH1, GH3, GH6, GH7, GH12) in both *A. ostoyae* and *A. borealis* suggests a coordinated approach to cellulose breakdown, with each family likely contributing to a specific enzymatic activity (Nagy et al., 2016; Hage and Rosso, 2021):

- **GH1, GH3, and GH6:** These families encompass endoglucanases, enzymes that act like molecular scissors, cleaving cellulose chains internally at various points. This creates new chain ends, making cellulose more susceptible to further degradation.
- **GH7:** Enzymes belonging to GH7 likely function as cellobiohydrolases, progressively cleaving cellobiose (a dimer of β-glucose) units from the newly created ends generated by endoglucanases.
- **GH12:** Similar to GH1, GH3, and GH6, GH12 might also encompass endoglucanases, further contributing to cellulose fragmentation.

The synergistic action of these GH families is essential for efficient cellulose degradation. Endoglucanases create new access points, while cellobiohydrolases steadily break down cellulose from the ends (Zerillo et al., 2013; Riley et al., 2014). This coordinated effort allows *Armillaria* to access nutrients within the plant cell wall fueling fungal growth during infection.

While both *Armillaria* species share a core set of cellulases, the presence of unique enzymes hints at potential variations in their wood degradation strategies:

- ***A. ostoyae*:** The presence of the **AA16** enzyme suggests a possible role in disrupting the crystalline structure of cellulose, making it more accessible to other cellulases (Filiatrault-Chastel et al., 2019). This could enhance the overall efficiency of cellulose breakdown in *A. ostoyae*.
- ***A. borealis*:** The presence of a unique β-1,4-endoglucanase (**GH5_5**) and two inducible lytic polysaccharide monooxygenase (LPMO) (**AA9**) enzymes suggests a potentially distinct or adaptable strategy. While the specific function of GH5_5 in *A. borealis* needs further investigation, AA9 (formerly GH61) enzymes are known to loosen cellulose microfibrils (Vaaje-Kolstad et al., 2010; Hu et al., 2013), similar to AA16 in *A. ostoyae*. The inducible nature of the AA9 enzymes in *A. borealis* might indicate their role in targeting specific forms of cellulose during different stages of wood colonisation.

5.2.2. Hemicellulose degradation

Hemicellulose is the second most abundant polysaccharide within the plant cell wall that holds cellulose fibres together and hinders access to the nutrients locked within. Analysis of CAZy families reveals a diverse array of hemicellulases (CE16, GH10, GH31, GH35, GH51) present in both *A. ostoyae* and *A. borealis*. These enzymes target various hemicellulose components, including xylan, arabinoxylan, and glucuronoxylan. This shared repertoire suggests a well-coordinated strategy for depolymerizing hemicellulose polymers, a crucial step in unlocking the nutrients they encapsulate (van den Brink and de Vries, 2011; Rytioja et al., 2014; Nagy et al., 2016; Hage and Rosso, 2021).

- **CE16:** Acetylxylan esterase prepares the xylan backbone for degradation by endoxylanases by removing acetyl residues from xylan chains.
- **GH10:** Endoxylanase targets xylan, a major hemicellulose component.

- **GH51:** α-l-arabinofuranosidase cleaves the arabinose substitution of xylan and works synergistically with other hemicellulases for complete degradation.
- **GH31 and GH35:** These enzymes tackle more specific hemicellulose types: α-xylosidase (GH31) breaks down xyloglucan, and β-galactosidases (GH35) target galactomannan.

This shared enzymatic toolbox suggests a common strategy employed by both *Armillaria* species to effectively dismantle the hemicellulose matrix and access the nutrients it conceals.

Although, a core set of hemicellulases is shared, the presence of unique enzymes in each species hints at potential variations in their degradation strategies:

- ***A. ostoyae*:** The presence of α-fucosidases (**GH29**) suggests a unique enzymatic capability not found in *A. borealis*, probably connected to realising l-fucose residues in xyloglucan branches (van den Brink and de Vries, 2011).
- ***A. borealis*:** The presence of endo-α-1,5-arabinanase (**GH93**) suggests a unique enzymatic tool specific to *A. borealis*. Similar to GH29 in *A. ostoyae*, further research is needed to determine its precise role in *A. borealis'* hemicellulose breakdown strategy (Hage and Rosso, 2021).

5.2.3. Lignin degradation

Lignin is a complex aromatic polymer that encases cellulose and hemicellulose within the plant cell wall, forming a major barrier to fungal nutrient acquisition. The identification of lignin-modifying enzymes (AA1_1, AA2, AA3_2) in both fungal species aligns with previous findings by Sipos et al. (2017) and Champramary et al. (2022). Both studies reported a high abundance of lignin-degrading genes for these enzymes in armillarioid fungi, suggesting a strong potential for lignocellulose decomposition and lignin mineralization.

However, ***A. ostoyae*** exhibits a higher abundance of laccases (**AA1_1**) and aryl-alcohol oxidases (**AA3_2**). Laccases are 'blue' copper oxidases that oxidise various phenolic compounds, including lignin components, while aryl-alcohol oxidases generate hydrogen peroxide (H_2O_2) - a key component in lignin degradation by class II peroxidases (Levasseur et al., 2013). This suggests a potentially stronger capacity for lignin breakdown and could provide *A. ostoyae* with a selective advantage allowing for faster degradation of the plant cell

wall. Furthermore, *A. ostoyae* displays species-specific constitutive expression of the glyoxal oxidase **AA5_1** enzyme, another H_2O_2-generating enzyme, known to facilitate the oxidative cleavage of lignin by peroxidases. The presence of this enzyme in *A. ostoyae* highlights a potential advantage for more efficient lignin degradation (Floudas et al., 2012; Andberg et al., 2017).

5.2.4. Pectin degradation

Following lignin breakdown, another major plant cell wall component, pectin, comes into play. Both *A. ostoyae* and *A. borealis* upregulate enzymes targeting pectin (CE8, CE12, GH28, GH78, GH88), highlighting their ability to soften the cell wall and access the nutrients locked within this complex polymer.

A. ostoyae displays a wider range of constitutively expressed pectinases (CBM67, GH53, GH105, PL1_7, PL26) compared to *A. borealis* (PL4_1) suggesting a potentially stronger and more efficient pectin degradation capability. Constitutive expression implies these enzymes are always "on" and ready to function, allowing *A. ostoyae* to readily break down pectin encountered during wood decay.

Pectinolytic enzyme functions (Martens-Uzunova and Schaap, 2009, Van den Brink and de Vries, 2011; Rytioja et al., 2014; Sipos et al., 2017):

- **Carbohydrate esterases (CE):** CE8 and CE12 families initiate pectin degradation by de-acetylating or de-esterifying the molecule, making it more susceptible to further breakdown by other enzymes.
- **Glycoside hydrolases (GH):** This diverse group contains GH28, GH78, and GH88 enzymes. They act as the primary pectin-degrading enzymes, cleaving the glycosidic bonds within the pectin backbone. GH28 enzymes have been linked to the necrotrophic lifestyle of pathogenic *Armillaria* species. This family encompasses enzymes like polygalacturonases and rhamnogalacturonan hydrolases, targeting different regions of the pectin backbone. GH78 and GH88 families also play a crucial role in pectin backbone hydrolysis by removing specific side chains, further aiding in its disassembly.

- **Polysaccharide lyases (PL):** These enzymes (PL1_7, PL4_1, and PL14_4) cleave pectin chains through a different mechanism compared to GHs. They operate via a β-elimination reaction, resulting in a more random breakdown of the pectin structure.
- **Carbohydrate-binding Modules (CBM):** While not directly involved in degradation, rhamnose-binding modules (CBM67) help target and bind pectin molecules, bringing the GH and PL enzymes in close proximity for efficient breakdown.

The observed expansion of pectinolytic enzyme families in *Armillaria* species is particularly noteworthy. Compared to other white-rot fungi, *Armillaria* exhibits a significant enrichment of enzymes belonging to families GH28, GH78, GH88, PL1, PL4, CE8, and CBM67 (Sipos et al., 2017; Champramary et al., 2022). This enrichment further highlights the unique pectinolytic repertoire of *Armillaria* species compared to typical white-rot fungi.

The inducible PL14_4 enzyme identified specifically in *A. ostoyae* further strengthens the idea of niche adaptation for pectin degradation. The presence of this unique enzyme suggests *A. ostoyae* might be particularly adept at targeting specific pectin structures potentially abundant in living plant tissues.

Interestingly, studies on the PL1_7 gene family in *Clonostachys rosea*, a fungus with similar ecological strategies to *A. ostoyae*, suggest that PL1_7 enzymes might play a role beyond pectin degradation, potentially influencing root colonisation and plant health in *A. ostoyae* as well (Mesny et al., 2021).

This unusual emphasis on pectin degradation enzymes in *A. ostoyae* might be linked to their ability to act as both powerful wood decayers and necrotrophic pathogens. The extensive PCWDE repertoire allows the fungi to gain access to wood resources while potentially damaging live trees (Sipos et al., 2017; Champramary et al., 2022). This strategy provides *A. ostoyae* a competitive edge by overcoming competition from other microbes and facilitating access to nutrients.

5.2.5. Beyond CAZymes

While CAZymes represent the core enzymatic machinery for wood breakdown, the analysis of non-CAZyme secretory candidates reveals an intriguing dimension to this process. These proteins, identified through InterPro analysis, lack the characteristic carbohydrate-active

enzyme domains but possess functionalities that likely complement and support CAZyme activity during wood degradation.

The identified non-CAZyme candidates encompass a diverse array of predicted functions categorised by InterPro. Focusing on annotations relevant to wood breakdown highlights several key categories:

Cell wall-degrading enzymes:

- **Alpha/beta hydrolase (IPR000073):** Found in *A. ostoyae*'s constitutive pool, these enzymes have also identified in secretomes of other filamentous fungi, such as *Piptoporus betulinus*, *Aspergillus terreus*, and *Pleurotus ostreatus* (Meng et al., 2012; Fernández-Fueyo et al., 2016; Arntzen et al., 2020). This widespread presence across diverse wood-decaying fungi underscores the potential importance of these enzymes. Although their specific functionalities within these fungi might vary depending on the presence of additional domains or their overall protein structure, their activity could act synergistically with CAZymes targeting specific hemicellulose and pectin components.
- **Endonuclease/exonuclease/phosphatase (IPR005135):** Present in both *A. ostoyae* and *A. borealis*, these enzymes offer the potential to break down various cell wall polysaccharides, including hemicellulose and pectin (Wymelenberg et al., 2006; Zhu et al., 2023). Their presence alongside CAZymes suggests a multifaceted approach to polysaccharide deconstruction within the fungal cell wall arsenal.
- **Fungal lipase-like domain (IPR002921):** This domain, specific to *A. ostoyae*'s constitutive pool, but also present in *P. chrysosporium and A. terreus,* might be involved in deacylation of plant cell walls (Arntzen et al., 2020).
- **Intradiol ring-cleavage dioxygenase (IPR000627):** Belonging to the catechol dioxygenase (CDO) family, play a critical role in aromatic compounds degradation by cleaving their carbon-carbon bonds (Ferraroni et al., 2004; Vaillancourt et al., 2006). Their presence alongside lignin-modifying CAZymes strengthens the concept of a coordinated ligninolytic machinery in *Armillaria* species. Interestingly, studies on fungal lifestyles reveal a potential link between the number of CDO genes and a fungus's pathogenic behaviour (Soal et al., 2022). These studies observed that necrotrophic pathogens, like *A. ostoyae*, typically possess four CDO genes, while mildly pathogenic species harbour two to three genes, and saprophytic fungi, which primarily target dead and degraded wood,

possess only a single CDO gene. In our study, this trend holds true. *A. ostoyae*, the necrotrophic pathogen, exhibits four CDO genes, whereas *A. borealis*, with a milder pathogenic character, displays three CDO genes. This alignment suggests a potential adaptation for more efficient lignin degradation in necrotrophic fungi like *A. ostoyae*. The ability to break down lignin might be less critical for saprophytes that target readily available, decomposed wood sources. Conversely, necrotrophs that can infect living trees might benefit from a more robust ligninolytic machinery for successful wood colonisation.

Other enzymes potentially contributing to wood degradation:

- **Carboxylesterase (IPR002018):** A constitutively expressed non-CAZyme found in *A. ostoyae,* has also been identified in other wood-decaying fungi belonging to the *Polyporales* order (Hage et al., 2021). These enzymes can potentially modify lignin structure by hydrolyzing ester bonds, enhancing accessibility for other lignin-degrading enzymes to act on the modified substrate (Fernández-Fueyo et al., 2016). This highlights a collaborative effort between enzymatic classes in lignin breakdown, while the widespread presence of carboxylesterase across diverse wood-decaying fungi reinforces the notion that these enzymes play a significant role in lignin biodegradation.
- **Cytochrome P450 (CYP450) (IPR001128):** The high abundance of CYP450 enzymes in both *A. ostoyae* and *A. borealis* suggests their multifaceted roles in wood decay. While the precise roles of many CYP450s remain elusive, some are thought to play a role in detoxifying diverse compounds, including secondary metabolites generated during lignin degradation and xenobiotics encountered in the environment (Syed et al., 2014; Nagy et al., 2106, 2017; Sahu et al., 2021). By altering the structure of lignin and cellulose, CYP450s might enhance their accessibility for subsequent enzymatic degradation by other enzymes. Interestingly, a broader analysis of fungal genomes revealed an enrichment of CYP450 genes within Agaricomycetes and Dacrymycetes compared to other fungal classes (Nagy et al., 2016). This expansion of CYP450s seems to be correlated with the diversification patterns observed for CAZymes, which are directly involved in wood breakdown. In contrast, no significant reduction in CYP450 numbers was observed within brown-rot or mycorrhizal fungal lineages, suggesting their potential importance across various wood-decay strategies. A closer look at *A. ostoyae* and *A. cepistipes* reveals dynamic regulation of CYP450 genes during different stages of fungal growth (Sahu et al., 2021). Transcriptomic and proteomic data suggest that a subset of CYP450s are

upregulated in invasive mycelia compared to non-invasive counterparts. This upregulation suggests their potential role in promoting wood decay during fungal invasion.

- **Calcineurin-like phosphoesterase domain (IPR004843) and lysine-specific metallo-endopeptidase (IPR029463):** The presence of these enzymes, with one copy each in both species, suggests their potential roles in acquiring essential nutrients like phosphates released during wood breakdown and degrading cell wall proteins, respectively (Healy et al., 1999; Lin et al., 2020). These seemingly peripheral functions contribute to the overall efficiency of the wood degradation process.

The identification of these non-CAZyme candidates underscores the complexity of the wood-degrading arsenal in *Armillaria* species. Their diverse functionalities likely act in concert with CAZymes to achieve efficient wood deconstruction and nutrient acquisition during fungal colonisation. Future research efforts aimed at functionally characterising these non-CAZyme candidates would provide valuable insights into their specific contributions to the wood degradation process.

5.2.6. Limitations and future directions

This study has provided valuable insights into the enzymatic repertoire employed by *Armillaria* species for wood breakdown. The analysis of CAZyme and non-CAZyme candidates has shed light on the diverse enzymatic functionalities at play during this process. However, some limitations are worth considering:

As with virulence candidates, functional validation remains a crucial next step. While the identified enzymes possess functionalities suggestive of their roles in wood breakdown, their specific contributions need further elucidation. Future studies employing functional characterization techniques, such as enzyme activity assays and gene deletion experiments, would be crucial to validate their predicted functions during wood degradation.

Another limitation lies in our understanding of substrate specificity. The analysis focused on predicted enzyme functionalities, but the specific types of wood components targeted by these enzymes remain unclear. Future studies could involve *in vitro* degradation assays using well-defined wood polysaccharide substrates. This would help determine the precise target specificities of the identified enzymes.

The current study provides a snapshot of the enzymatic profile, lacking information on temporal and spatial expression. Investigating the temporal and spatial expression patterns of these enzymes during fungal growth and wood colonisation would offer a more comprehensive understanding of their roles. Techniques like RNA-seq analysis and enzyme activity assays at different stages of wood decay could provide valuable insights.

By addressing these limitations, future research can significantly enhance our understanding of the intricate enzymatic mechanisms employed by *Armillaria* species for efficient wood deconstruction. Additionally, exploring the potential synergistic interactions between CAZymes and non-CAZyme candidates would provide a more holistic view of the wood-degradation process in these fungi.

5.3. Mycoremediation potential of *Armillaria* species

This study investigated the mycoremediation potential of *A. ostoyae* and *A. borealis* through a comparative genomic analysis. The results revealed promising capabilities for degrading various monocyclic aromatic compounds, while suggesting limitations for polycyclic aromatic hydrocarbons (PAH) degradation compared to other basidiomycetes.

Both *A. ostoyae* and *A. borealis* possess a richer genetic repertoire for degrading various **monocyclic aromatic hydrocarbons** compared to other fungal counterparts. This is evident in the abundance of genes encoding enzymes like homogentisate 1,2-dioxygenase (HGD), maleylacetate reductase, and arylesterase/paraoxonase (Champramary et al., 2023). Notably, the presence of four HGD gene copies in each *Armillaria* species is significantly higher compared to other basidiomycetes. HGD plays a crucial role in breaking down homogentisate, a key intermediate in the degradation pathway for numerous aromatic compounds (Mori et al., 2016; Fernández‐González et al., 2018). This suggests a potentially enhanced capacity for these *Armillaria* species to tackle a wider range of aromatic substrates in contaminated environments. Additionally, the higher copy number of arylesterase genes in *Armillaria* compared to other fungi might provide an advantage in degrading specific aromatic compounds like aminobenzoate.

While genes associated with PAH degradation were identified in *Armillaria* species, their overall abundance was lower compared to other basidiomycetes. This suggests that other

basidiomycete fungi might be more efficient in degrading PAH pollutants. However, *A. ostoyae* and *A. borealis* exhibited a higher number of soluble epoxide hydrolase genes compared to most ascomycetes. Soluble epoxide hydrolase plays a role in degrading benzo[a]pyrene, a specific PAH pollutant, suggesting a potential role for these *Armillaria* species in remediating environments contaminated with this specific PAH.

RNA-sequencing data revealed encouraging results, with over 85% of the identified mycoremediation-related genes actively expressed in both *A. ostoyae* and *A. borealis*, regardless of their virulence. This highlights the inherent capability of these fungi to perform biodegradation functions. Furthermore, the upregulation of HGD genes during plant stem invasion experiments suggests their potential role in natural environments where these fungi encounter various aromatic compounds. Interestingly, salicylate hydroxylase and MnP genes, involved in PAH degradation, displayed different expression patterns compared to other genes, with their expression levels tending to increase on rich media. This warrants further investigation to understand the environmental factors that influence their expression during mycoremediation processes.

5.3.1. Future applications and research directions

Based on the identified genetic makeup and observed gene expression patterns, *A. ostoyae* and *A. borealis* hold significant promise for bioremediation of environments contaminated with monocyclic aromatic compounds. Future research efforts should focus on:

- Validating *in vitro* findings: Conducting field studies to assess the efficacy of these fungi in real-world scenarios and validate the laboratory findings.
- Optimising environmental conditions: Investigating the specific environmental conditions (e.g., substrate composition, presence of co-contaminants) that might optimise the mycoremediation potential of these *Armillaria* species.
- Exploring enzyme applications: Researching the potential of identified enzymes, particularly HGD and arylesterase, for biocatalysis applications in the targeted degradation of specific aromatic pollutants.
- Large-scale mycoremediation: Developing strategies to optimise factors like temperature, pH, and pollutant concentration for efficient biodegradation in large-scale mycoremediation applications.

This study highlights the potential of *A. ostoyae* and *A. borealis* for bioremediation, particularly for monocyclic aromatic compounds. Further research efforts are crucial to translate these promising findings into practical applications for environmental cleanup.

6. SUMMARY

Armillaria fungi, like *A. ostoyae* and *A. borealis*, are notorious plant pathogens responsible for significant economic losses in forestry and agriculture. They infect living trees and possess a formidable ability to decompose wood, contributing to forest decline. Understanding the intricate mechanisms employed by *Armillaria* species for both plant infection and wood decay is crucial for developing effective management strategies.

However, our current knowledge about the specific virulence factors and wood-degrading enzymes utilised by these fungi remains incomplete. This gap in knowledge hinders the development of targeted approaches to control their spread and mitigate their destructive impact.

This study addresses this critical gap by investigating the distinct enzymatic profiles of *A. ostoyae* and *A. borealis*. By employing a two-pronged approach of transcriptome analysis and homology searches against known virulence factors, we aimed to identify key players involved in their pathogenic strategies and wood degradation capabilities.

Focusing on highly virulent isolates, we identified DEGs with potential roles in virulence, with CAZymes emerging as a prominent group. Notably, *A. ostoyae* exhibited a significantly higher abundance of PCWDEs compared to both its less-virulent counterpart and *A. borealis* isolates, suggesting a more aggressive strategy for breaching the host cell wall. While some of the CAZyme repertoire is shared between the fungi, species-specific differences were also observed, highlighting unique enzymatic profiles.

The high abundance of PCWDEs observed in *A. ostoyae* suggests a well-developed enzymatic arsenal for dismantling plant cell walls. Key players include endopolygalacturonase, responsible for breaking down cell wall components, and cellobiohydrolases, adept at breaching plant defences. Peroxidases mitigate oxidative stress during infection, while xylanases facilitate fungal spread within the host. Pectate lyase further contributes by dismantling pectin, while multicopper oxidases secure vital iron required by the fungus. The presence of a glucosidase suggests a potential role in early infection stages, possibly influencing protein folding. The function of the CBM5 domain remains to be elucidated but may be linked to virulence.

A. ostoyae also possesses a broader array of virulence factor candidates beyond CAZymes. FAD-binding domain proteins may function in detoxifying host defences, while cytochrome P450 enzymes could be involved in either detoxification or virulence factor biosynthesis. An alkaline phosphatase homolog suggests the fungus might target the host's phosphate resources, and a palmitoyl protein thioesterase Ppt1 homolog hints at potential involvement in secondary metabolite biosynthesis, which could contribute to virulence. Finally, a FvScp1 homolog might be part of a complex regulating virulence factors.

While *A. borealis* shares some CAZymes with *A. ostoyae*, such as endopolygalacturonase and pectate lyases, it also possesses a distinct set of virulence factors. A GH28 protein homolog might contribute to pectin degradation. Similar to *A. ostoyae*, specific FAD-binding domain proteins and a cytochrome P450 enzyme homolog are present, suggesting potential roles in detoxification. Cerato-platanin family homologs may manipulate the host's defences, while a peptidase S8/S53 domain homolog might target and degrade specific host proteins, suppressing their defence mechanisms. Finally, a thioredoxin domain homolog highlights its potential importance for virulence by ensuring proper protein folding.

Armillaria fungi are not just equipped to compromise host defences, they possess an arsenal of wood-degrading enzymes to break down and utilise the complex polysaccharides within the plant cell wall. The analysis of wood-degrading enzyme profiles in *A. ostoyae* and *A. borealis* reveals an interplay between shared and unique enzymatic capabilities. This tailored enzyme machinery allows both species to efficiently deconstruct the complex plant cell wall, but *A. ostoyae* appears to possess a potentially stronger lignin and pectin degradation arsenal.

Both *A. ostoyae* and *A. borealis* employ a diverse array of cellulases (GH families 1, 3, 6, 7, 12) for a coordinated attack with each family likely contributing to a specific enzymatic activity. This synergy is essential for efficient degradation. Endoglucanases create access points, while cellobiohydrolases steadily break down cellulose from the ends. While both species share this core set, *A. ostoyae* possesses the AA16 enzyme, potentially disrupting cellulose structure for other cellulases to access. *A. borealis*, on the other hand, has a unique β-1,4-endoglucanase (GH5_5) and inducible LPMOs (AA9) enzymes, suggesting a potentially distinct or adaptable strategy.

Analysis reveals a diverse array of hemicellulases (CE16, GH10, GH31, GH35, GH51) present in both species, targeting various hemicellulose components like xylan, arabinoxylan, and glucuronoxylan. This shared repertoire suggests a well-coordinated strategy for depolymerizing hemicellulose polymers, a crucial step in unlocking the nutrients they encapsulate. However, *A. ostoyae* possesses α-fucosidases (GH29), suggesting a unique enzymatic capability, while *A. borealis* has a unique endo-α-1,5-arabinanase (GH93), highlighting potential variations in their degradation strategies.

The identification of lignin-modifying enzymes (AA1_1, AA2, AA3_2) in both fungal species aligns with previous findings. However, *A. ostoyae* exhibits a higher abundance of laccases (AA1_1) and aryl-alcohol oxidases (AA3_2), enzymes that break down lignin components. This suggests a potentially stronger capacity for lignin breakdown, providing *A. ostoyae* with a selective advantage for faster cell wall degradation. Furthermore, *A. ostoyae* displays constitutive expression of the glyoxal oxidase AA5_1 enzyme, another H_2O_2-generating enzyme known to facilitate lignin breakdown by peroxidases.

Both species upregulate pectin-targeting enzymes (CE8, CE12, GH28, GH78, GH88), highlighting their ability to soften the cell wall and access nutrients. However, *A. ostoyae* displays a wider range of constitutively expressed pectinases compared to *A. borealis*, suggesting a potentially stronger and more efficient pectin degradation capability.

While CAZymes are the core wood-breakdown machinery, non-CAZyme secretory candidates reveal an intriguing dimension. This study identified a suite of non-CAZyme secretory candidates with diverse predicted functions, potentially acting synergistically with CAZymes to deconstruct wood components.

These candidates include enzymes like alpha/beta hydrolases (potentially aiding in hemicellulose and pectin breakdown), endonucleases/exonucleases/phosphatases (for various polysaccharide degradation), and fungal lipase-like domains (potentially involved in plant cell wall deacylation in *A. ostoyae*). Notably, the presence of intradiol ring-cleavage dioxygenases suggests a ligninolytic strategy, with *A. ostoyae*, the necrotroph, exhibiting more genes compared to the milder pathogen *A. borealis*.

Furthermore, enzymes like carboxylesterases (potentially modifying lignin structure in *A. ostoyae*) and cytochrome P450s (with multifaceted roles in detoxification and wood component modification) contribute to the overall degradation process. Additionally,

calcineurin-like phosphoesterase domains and lysine-specific metallo-endopeptidases likely play supporting roles in nutrient acquisition and protein degradation, respectively.

These non-CAZyme candidates highlight the complexity of the wood-degrading arsenal in *Armillaria* species. Their diverse functionalities likely act together with CAZymes to achieve efficient wood deconstruction and nutrient acquisition during fungal colonisation.

This study also investigated the mycoremediation potential of *A. ostoyae* and *A. borealis* through a comparative genomic analysis. The results revealed promising capabilities for degrading various monocyclic aromatic compounds, while suggesting limitations for PAH degradation compared to other basidiomycetes.

Both *A. ostoyae* and *A. borealis* possess a richer genetic repertoire for degrading various monocyclic aromatic hydrocarbons compared to other fungal counterparts. This suggests a potentially enhanced capacity for these *Armillaria* species to tackle a wider range of aromatic substrates in contaminated environments. While genes associated with PAH degradation were identified, their overall abundance was lower compared to other basidiomycetes. Future research should focus on validating these findings in field studies, optimising environmental conditions for mycoremediation, exploring enzyme applications, and developing strategies for large-scale mycoremediation applications.

This research provides valuable insights into the variations in pathogenic strategies of *Armillaria* species, laying the foundation for developing targeted approaches to control these destructive pathogens. Additionally, the study highlights the potential of *A. ostoyae* and *A. borealis* for bioremediation, particularly for monocyclic aromatic compounds. Further research efforts are crucial to translate these promising findings into practical applications for environmental cleanup. Understanding these mechanisms paves the way for a more comprehensive approach to managing *Armillaria* species in both agricultural and environmental contexts.

7. FINANCIAL SUPPORT

This research was funded by the Hungarian Government and the European Union within the frames of the Széchenyi 2020 Program (GINOP-2.3.2-15-2016-00052), as well as by National Research, Development and Innovation Office of Hungary and their support for Hungarian participation in the Hungarian-Turkish applied research and development cooperation program (2022-1.2.6-TÉT-IPARI-TR-2022-00009).

Participation in this PhD program was made possible by the “Tempus Public Foundation” which provided financial assistance by awarding “Stipendium Hungaricum Scholarship”.

8. LIST OF PUBLICATIONS

MTMT ID: 10072794

Journal articles:

- Champramary, Simang, **Boris Indic**, Attila Szűcs, Chetna Tyagi, Omar Languar, KM Faridul Hasan, András Szekeres, Csaba Vágvölgyi, László Kredics, and György Sipos. "The mycoremediation potential of the armillarioids: a comparative genomics analysis." *Frontiers in Bioengineering and Biotechnology* 11 (2023): 1189640. (IF 2023 : 6.1)
- Chen, Liqiong, Simang Champramary, Neha Sahu, **Boris Indic**, Attila Szűcs, Gábor Nagy, Gergely Maróti et al. "Dual RNA-Seq profiling unveils mycoparasitic activities of *Trichoderma atroviride* against haploid *Armillaria ostoyae* in antagonistic interaction assays." *Microbiology Spectrum* 11, no. 3 (2023): e04626-22. (IF 2023: 9.0)
- Sahu, Neha, **Boris Indic**, Johanna Wong-Bajracharya, Zsolt Merényi, Huei-Mien Ke, Steven Ahrendt, Tori-Lee Monk et al. "Vertical and horizontal gene transfer shaped plant colonization and biomass degradation in the fungal genus *Armillaria*." *Nature microbiology* 8, no. 9 (2023): 1668-1681. (IF 2023 : 31.0)
- Kedves, Orsolya, Danish Shahab, Simang Champramary, Liqiong Chen, **Boris Indic**, Bettina Bóka, Viktor Dávid Nagy, Csaba Vágvölgyi, László Kredics, and György Sipos. "Epidemiology, biotic interactions and biological control of armillarioids in the northern hemisphere." *Pathogens* 10, no. 1 (2021): 76. (IF 2021: 3.5)
- Chen, Liqiong, Bettina Bóka, Orsolya Kedves, Viktor Dávid Nagy, Attila Szűcs, Simang Champramary, Róbert Roszik, Zoltán Patocskai, Martin Münsterkötte, Thu Huynh, **Boris Indic**, Csaba Vágvölgyi, György Sipos, and László Kredics. "Towards the biological control of devastating forest pathogens from the genus *Armillaria*." *Forests* 10, no. 11 (2019): 1013. (IF 2019: 2.2)

Cumulative impact factor (IF) of the publications related to the thesis: 51.8

Accepted, but not yet published articles:

- **Boris Indic**, and György Sipos. "Developing an experimental protocol to test *Armillaria* specific genes for their potential role in pathogenicity and virulence." *Acta Biologica Szegediensis*

- **Boris Indic**, and György Sipos. "Kárpát-medencei fehérkorhasztó gombák faanyag-bontó képességeinek genomikai szintű összehasonlító vizsgálata." *Erdészeti Tudományos Konferencia*

Conference papers:

- Champramary, Simang, **Boris Indic**, László Kredics, and György Sipos. "A comparison of the wood decay abilities of common white-rot fungi from the Carpathian Basin." (2022): 188-193.
- Chen, Liqiong, Danish Shahab, Orsolya Kedves, Simang Champramary, **Boris Indic**, Viktor Dávid Nagy, Csaba Vágvölgyi, László Kredics, and György Sipos. "Armillarioid root rot invasion: possibilities of silvicultural and chemical control." *9th Hardwood Proceedings− Part II.* (2021): 90.

Books:

- Sipos, György ; Kredics, László ; Chen, Liqiong ; Sahu, Neha ; Prasanna, Arun ; Champramary, Simang ; Kedves, Orsolya ; **Indic, Boris** ; Raj, Garima ; Nyikos, Bendegúz Richárd et al. "Az erdészeti kártevő *Armillaria* (tuskógomba) nemzetség patológiája és a biológiai védekezés lehetőségei." (2021). Soproni Egyetem Kiadó

Conference abstracts:

- Kedves Orsolya, Champramary Simang, Lange Enyedi Nóra Tünde, Tüh Annamária, **Indic Boris**, Horváth Márton, Bányi Árpád, Vágvölgyi Csaba, Danesh Younes Rezaee, Sipos György, Kredics László. “The future of walnut production challenged by the walnut husk fly and microbial pathogens.” In: Magyar Mikrobiológiai Társaság 2024. évi Nagygyűlése/ Hungarian Society for Microbiology General Meeting 2024. - Absztraktok/ Abstracts. Siofok, Hungary (2024) 97 p. pp. 13-14. , 2 p.
- Omar Languar, Orsolya Kedves, Simang Champramary, Nóra Tünde Lange-Enyedi, **Boris Indic**, Csaba Vágvölgyi, András Szekeres, László Kredics, György Sipos. “Interactions between Trichoderma and Armillaria mediated by volatile organic compounds in the light of biocontrol strategies.” In: Magyar Mikrobiológiai Társaság 2024. évi Nagygyűlése/ Hungarian Society for Microbiology General Meeting 2024. - Absztraktok/ Abstracts. Siofok, Hungary (2024) 97 p. p. 15 , 1 p.

- Omar Languar, Orsolya Kedves, Simang Champramary, Nóra T. Lange-Enyedi, **Boris Indic**, Csaba Vágvölgyi, László Kredics, András Szekeres, György Sipos. “Volatile compound-mediated interactions between *Armillaria* and *Trichoderma*: implications for biocontrol strategies.” In: 1st Annual Conference of the MiCropBiomes COST Action: Exploiting Plant-Microbiomes Networks and Synthetic Communities to Improve Crops Fitness (2024) 106 p. pp. 54-55., 2 p.
- Sipos, György ; Champramary, Simang ; Lakatos, Ferenc ; Folcz, Ádám ; Király, Géza ; **Indic, Boris. “**A Sopron környéki erdeifenyő pusztulások hátterének genomszintű mikrobiológiai vizsgálata” In: Czimber, Kornél (eds.) Erdészeti Tudományos Konferencia Sopron, 2024. február 5-6. : Kivonatok Kötete, Sopron, Hungary : Soproni Egyetem Erdőmérnöki Kar (2024) 75 p. p. 40
- Liqiong, Chen ; Simang, Champramary ; Neha, Sahu ; **Boris, Indic** ; Attila, Szűcs ; Gábor, Nagy ; Gergely, Maróti ; Bernadett, Pap ; Csaba, Vágvölgyi ; László, Nagy et al. “In Vitro Transcriptome Level Interactions Between Mycoparasitic Trichoderma Atroviride And Haploid Armillaria Ostoyae Uncovered By Dual Rna-Seq Profiling”. Acta Microbiologica Et Immunologica Hungarica 70 : Supplement1 Pp. 11-11. , 1 P. (2023)
- Simang, Champramary ; **Boris, Indic** ; Attila, Szűcs ; Omar, Languar ; Faridul, K. M. Hasan ; András, Szekeres ; Csaba, Vágvölgyi ; László, Kredics ; György, Sipos. “Comparative genomics and transcriptomics analyses confirm the distinctive mycoremediation potential of armillarioid species”. Acta Microbiologica Et Immunologica Hungarica 70 : Supplement1 Pp. 59-60. , 1 P. (2023)
- **Boris, Indic**; Simang, Champramary; Liqiong, Chen; Huynh, Thu; Orsolya, Kedves; Ferenc, Lakatos; Csaba, Vágvölgyi; László, Kredics; György, Sipos “Phylogenetic analysis shows contrasting genetic diversity among various Armillarioid species in Pannonian forests” In: Róbert, Németh; Christian, Hansmann; Peter, Rademacher; Miklós, Bak; Mátyás, Báder (eds.) 10TH Hardwood Conference Proceedings : Sopron, Hungary, 12-14 October 2022, Sopron, Hungary : University Of Sopron Press (2022) 323 P. P. 203 , 1 P.
- Liqiong, Chen ; Simang, Champramary ; Neha, Sahu ; **Boris, Indic** ; Attila, Szűcs ; Gábor, Nagy ; Gergely, Maróti ; Bernadett, Pap ; Csaba, Vágvölgyi ; László, Nagy et al. “In vitro transcriptome level interactions between mycoparasitic *Trichoderma atroviride* and haploid *Armillaria ostoyae* uncovered by dual RNA-seq profiling” in: a Magyar

Mikrobiológiai Társaság 2022. évi Nagygyűlése és a XV. Fermentációs Kollokvium : absztraktfüzet (2022) 54 p. p. 12 , 1 p.

- **Indic, Boris**; Münsterkötter, M. ; Kredics, L. ; Sipos, Gyoergy “The genome of the pathogenic white rot fungus *Armillaria ostoyae* encodes a distinctive genetic potential to degrade aromatic compounds” In: Piotr, Mleczko (eds.) Abstract Book, XVIIII Congress of European Mycologists Warszawa, Varsó, Poland : Polish Mycological Society (2019) pp. 71-71. , 1 p.

9. LIST OF REFERENCES

Akhtar, N., and Mannan, M. A. U. (2020). Mycoremediation: expunging environmental pollutants. Biotechnology reports, 26, e00452.

Akulova, V. S., Sharov, V. V., Aksyonova, A. I., Putintseva, Y. A., Oreshkova, N. V., Feranchuk, S. I., ... and Krutovsky, K. V. (2020). De novo sequencing, assembly and functional annotation of *Armillaria borealis* genome. BMC genomics, 21(7), 1-8.

Albarouki, E., and Deising, H. B. (2013). Infection structure-specific reductive iron assimilation is required for cell wall integrity and full virulence of the maize pathogen *Colletotrichum graminicola*. Molecular Plant-Microbe Interactions, 26(6), 695-708.

Almagro Armenteros, J. J., Sønderby, C. K., Sønderby, S. K., Nielsen, H., and Winther, O. (2017). DeepLoc: prediction of protein subcellular localization using deep learning. Bioinformatics, 33(21), 3387-3395.

Almagro Armenteros, J.J., Tsirigos, K.D., Sønderby, C.K., Petersen, T.N., Winther, O., Brunak, S., von Heijne, G. and Nielsen, H. (2019). SignalP 5.0 improves signal peptide predictions using deep neural networks. Nature Biotechnology, 37(4), pp.420-423.

Andberg, M., Mollerup, F., Parikka, K., Koutaniemi, S., Boer, H., Juvonen, M., ... and Kruus, K. (2017). A novel Colletotrichum graminicola raffinose oxidase in the AA5 family. Applied and Environmental Microbiology, 83(20), e01383-17.

Anderson, J. B., and Kohn, L. M. (1995). Clonality in soilborne, plant-pathogenic fungi. Annual Review of Phytopathology, 33(1), 369-391.

Andrews, S. (2017). FastQC: a quality control tool for high throughput sequence data. 2010. https://www.bioinformatics.babraham.ac.uk/projects/fastqc/

Aramaki, T., Blanc-Mathieu, R., Endo, H., Ohkubo, K., Kanehisa, M., Goto, S., and Ogata, H. (2020). KofamKOALA: KEGG Ortholog assignment based on profile HMM and adaptive score threshold. Bioinformatics, 36(7), 2251-2252.

Arntzen, M. Ø., Bengtsson, O., Várnai, A., Delogu, F., Mathiesen, G., and Eijsink, V. G. (2020). Quantitative comparison of the biomass-degrading enzyme repertoires of five filamentous fungi. Scientific Reports, 10(1), 20267.

Atanasova, L., Dubey, M., Grujić, M., Gudmundsson, M., Lorenz, C., Sandgren, M., ... and Karlsson, M. (2018). Evolution and functional characterization of pectate lyase PEL12, a member of a highly expanded *Clonostachys rosea* polysaccharide lyase 1 family. BMC microbiology, 18(1), 1-19.

Bailey, T. L., Johnson, J., Grant, C. E., and Noble, W. S. (2015). The MEME suite. Nucleic acids research, 43(W1), W39-W49.

Balla, A., Silini, A., Cherif-Silini, H., Chenari Bouket, A., Moser, W. K., Nowakowska, J. A. Oszako, T., Benia, F., and Belbahri, L. (2021). The threat of pests and pathogens and the potential for biological control in forest ecosystems. Forests, 12(11), 1579.

Barr, D. P., and Aust, S. D. (1994). Pollutant degradation by white rot fungi. Reviews of Environmental Contamination and Toxicology: Continuation of Residue Reviews, 49-72.

Bass, A. J., Robinson, D. G., and Storey, J. D. (2019). Determining sufficient sequencing depth in RNA-Seq differential expression studies. bioRxiv, 635623.

Baumgartner, K. (2004). Root collar excavation for postinfection control of *Armillaria* root disease of grapevine. Plant Disease, 88(11), 1235-1240.

Baumgartner, K., Coetzee, M. P., and Hoffmeister, D. (2011). Secrets of the subterranean pathosystem of *Armillaria*. Molecular Plant Pathology, 12(6), 515-534.

Bauters, L., Stojilković, B., and Gheysen, G. (2021). Pathogens pulling the strings: effectors manipulating salicylic acid and phenylpropanoid biosynthesis in plants. Molecular Plant Pathology, 22(11), 1436-1448.

Blanchette, R. A. (1991). Delignification by wood-decay fungi. Annual Review of Phytopathology, 29(1), 381-403.

Bolger, A. M., Lohse, M., and Usadel, B. (2014). Trimmomatic: a flexible trimmer for Illumina sequence data. Bioinformatics, 30(15), 2114-2120.

Bradley, E. L., Ökmen, B., Doehlemann, G., Henrissat, B., Bradshaw, R. E., and Mesarich, C. H. (2022). Secreted glycoside hydrolase proteins as effectors and invasion patterns of plant-associated fungi and Oomycetes. Frontiers in Plant Science, 13, 853106.

Brazee, N. J., Hulvey, J. P., and Wick, R. L. (2011). Evaluation of partial tef1, rpb2, and nLSU sequences for identification of isolates representing *Armillaria calvescens* and *Armillaria gallica* from northeastern North America. Fungal Biology, 115(8), 741-749.

Brazee, N. J., Ortiz-Santana, B., Banik, M. T., and Lindner, D. L. (2012). *Armillaria altimontana*, a new species from the western interior of North America. Mycologia, 104(5), 1200-1205.

Brito, N., Espino, J. J., and González, C. (2006). The endo-β-1, 4-xylanase Xyn11A is required for virulence in *Botrytis cinerea*. Molecular Plant-Microbe Interactions, 19(1), 25-32.

Bruhn, J. N., Wetteroff Jr, J. J., Mihail, J. D., Kabrick, J. M., and Pickens, J. B. (2000). Distribution of *Armillaria* species in upland Ozark Mountain forests with respect to site, overstory species composition and oak decline. Forest Pathology, 30(1), 43-60.

Campbell, W. G. (1932). The chemistry of the white rots of wood: The effect on wood substance of *Ganoderma applanatum* (Pers.) Pat., *Fomes fomentarius* (Linn.) Fr., *Polyporus adustus* (Willd.) Fr., *Pleurotus ostreatus* (Jacq.) Fr., *Armillaria mellea* (Vahl.) Fr., *Trametes pini* (Brot.) Fr., and *Polystictus abietinus* (Dicks.) Fr. Biochemical Journal, 26(6), 1829.

Champramary, S., Indic, B., Kredics, L., and Sipos, G. (2022). A comparison of the wood decay abilities of common white-rot fungi from the Carpathian Basin.

Champramary, S., Indic, B., Szűcs, A., Tyagi, C., Languar, O., Hasan, K.F., Szekeres, A., Vágvölgyi, C., Kredics, L. and Sipos, G. (2023). The mycoremediation potential of the armillarioids: a comparative genomics analysis. Frontiers in Bioengineering and Biotechnology, 11, 1189640

Chen, L., Bóka, B., Kedves, O., Nagy, V. D., Szűcs, A., Champramary, S., Roszik, R., Patocskai, Z., Münsterkötter, M., Huynh, T., Indic, B., Vágvölgyi, C., Sipos, G., and Kredics, L. (2019). Towards the biological control of devastating forest pathogens from the genus *Armillaria*. Forests, 10(11), 1013.

Chen, Y., Lun, A. T., and Smyth, G. K. (2016). From reads to genes to pathways: differential expression analysis of RNA-Seq experiments using Rsubread and the edgeR quasi-likelihood pipeline. F1000Research, 5.

Cleary, M. R., Van Der Kamp, B. J., and Morrison, D. J. (2012). Effects of wounding and fungal infection with *Armillaria ostoyae* in three conifer species. II. Host response to the pathogen. Forest Pathology, 42(2), 109-123.

Coetzee, M. P., Wingfield, B. D., and Wingfield, M. J. (2018). Armillaria root-rot pathogens: species boundaries and global distribution. Pathogens, 7(4), 83.

Collins, C., Hurley, R., Almutlaqah, N., O'Keeffe, G., Keane, T. M., Fitzpatrick, D. A., and Owens, R. A. (2017). Proteomic characterization of *Armillaria mellea* reveals oxidative stress response mechanisms and altered secondary metabolism profiles. Microorganisms, 5(3), 60.

Collins, C., Keane, T. M., Turner, D. J., O'Keeffe, G., Fitzpatrick, D. A., and Doyle, S. (2013). Genomic and proteomic dissection of the ubiquitous plant pathogen, *Armillaria mellea*: toward a new infection model system. Journal of proteome research, 12(6), 2552-2570.

Daou, M., Bisotto, A., Haon, M., Oliveira Correia, L., Cottyn, B., Drula, E., ... and Faulds, C. B. (2021). A putative lignin copper oxidase from *Trichoderma reesei*. Journal of Fungi, 7(8), 643.

de Vries, R. P., and Visser, J. A. A. P. (2001). Aspergillus enzymes involved in degradation of plant cell wall polysaccharides. Microbiology and molecular biology reviews, 65(4), 497-522.

Dettman, J. R., and van der Kamp, B. J. (2001). The population structure of *Armillaria ostoyae* in the southern interior of British Columbia. Canadian Journal of Botany, 79(5), 612-620.

Devkota, P., and Hammerschmidt, R. (2020). The infection process of *Armillaria mellea* and *Armillaria solidipes*. Physiological and Molecular Plant Pathology, 112, 101543.

Ding, S., Liu, X., Hakulinen, N., Taherzadeh, M. J., Wang, Y., Wang, Y., ... and Tu, T. (2022). Boosting enzymatic degradation of cellulose using a fungal expansin: Structural insight into the pretreatment mechanism. Bioresource Technology, 358, 127434.

Dobin, A., Davis, C.A., Schlesinger, F., Drenkow, J., Zaleski, C., Jha, S., Batut, P., Chaisson, M. and Gingeras, T.R., (2013). STAR: ultrafast universal RNA-seq aligner. Bioinformatics, 29(1), pp.15-21.

Eichhorn, H., Lessing, F., Winterberg, B., Schirawski, J., Kamper, J., Muller, P., and Kahmann, R. (2006). A ferroxidation/permeation iron uptake system is required for virulence in *Ustilago maydis*. The Plant Cell, 18(11), 3332-3345.

Ellis, L. B., Roe, D., and Wackett, L. P. (2006). The University of Minnesota biocatalysis/biodegradation database: the first decade. Nucleic Acids Research, 34(suppl_1), D517-D521.

Enkerli, J., Bhatt, G., and Covert, S. F. (1998). Maackiain detoxification contributes to the virulence of *Nectria haematococca* MP VI on chickpea. Molecular plant-microbe interactions, 11(4), 317-326.

Espino, J. J., Brito, N., Noda, J., and González, C. (2005). Botrytis cinerea endo-ß-1, 4-glucanase Cel5A is expressed during infection but is not required for pathogenesis. Physiological and molecular plant pathology, 66(6), 213-221.

Fernández-Fueyo, E., Ruiz-Dueñas, F. J., López-Lucendo, M. F., Pérez-Boada, M., Rencoret, J., Gutiérrez, A., ... and Martínez, A. T. (2016). A secretomic view of woody and nonwoody lignocellulose degradation by *Pleurotus ostreatus*. Biotechnology for biofuels, 9, 1-18.

Fernández‐Acero, F. J., Colby, T., Harzen, A., Carbu, M., Wieneke, U., Cantoral, J. M., and Schmidt, J. (2010). 2‐DE proteomic approach to the *Botrytis cinerea* secretome induced with different carbon sources and plant‐based elicitors. Proteomics, 10(12), 2270-2280.

Fernández‐González, A. J., Valette, N., Kohler, A., Dumarçay, S., Sormani, R., Gelhaye, E., and Morel‐Rouhier, M. (2018). Oak extractive‐induced stress reveals the involvement of new enzymes in the early detoxification response of *Phanerochaete chrysosporium*. Environmental microbiology, 20(10), 3890-3901.

Ferraroni, M., Solyanikova, I. P., Kolomytseva, M. P., Scozzafava, A., Golovleva, L., and Briganti, F. (2004). Crystal structure of 4-chlorocatechol 1, 2-dioxygenase from the chlorophenol-utilizing gram-positive *Rhodococcus opacus* 1CP. Journal of Biological Chemistry, 279(26), 27646-27655.

Ferreira, P., Carro, J., Serrano, A., and Martínez, A. T. (2015). A survey of genes encoding H_2O_2-producing GMC oxidoreductases in 10 *Polyporales* genomes. Mycologia, 107(6), 1105-1119.

Filiatrault-Chastel, C., Navarro, D., Haon, M., Grisel, S., Herpoël-Gimbert, I., Chevret, D., ... and Berrin, J. G. (2019). AA16, a new lytic polysaccharide monooxygenase family identified in fungal secretomes. Biotechnology for Biofuels, 12, 1-15.

Floudas, D., Binder, M., Riley, R., Barry, K., Blanchette, R. A., Henrissat, B., ... and Hibbett, D. S. (2012). The Paleozoic origin of enzymatic lignin decomposition reconstructed from 31 fungal genomes. Science, 336(6089), 1715-1719.

Floudas, D., Held, B. W., Riley, R., Nagy, L. G., Koehler, G., Ransdell, A. S., ... and Hibbett, D. S. (2015). Evolution of novel wood decay mechanisms in Agaricales revealed by the genome sequences of *Fistulina hepatica* and *Cylindrobasidium torrendii*. Fungal Genetics and Biology, 76, 78-92.

Ford, K. L., Baumgartner, K., Henricot, B., Bailey, A. M., and Foster, G. D. (2015). A reliable in vitro fruiting system for *Armillaria mellea* for evaluation of *Agrobacterium tumefaciens* transformation vectors. Fungal Biology, 119(10), 859-869.

Fox, E. M., and Howlett, B. J. (2008). Secondary metabolism: regulation and role in fungal biology. Current Opinion in Microbiology, 11(6), 481-487.

Fox, R. T. (2000). Armillaria root rot: biology and control of honey fungus. 1st ed, Andover: Intercept Ltd., p.113–136.

Gao, D., Du, L., Yang, J., Wu, W. M., and Liang, H. (2010). A critical review of the application of white rot fungus to environmental pollution control. Critical Reviews in Biotechnology, 30(1), 70-77.

Garbelotto, M., 2004. Root and butt rot diseases. Encycl. For. Sci. 750–758.

Girard, V., Dieryckx, C., Job, C., and Job, D. (2013). Secretomes: the fungal strike force. Proteomics, 13(3-4), 597-608.

Gonthier, P. (2010). Controlling root and butt rot diseases in Alpine European forests. In Management of fungal plant pathogens (pp. 345-361). Wallingford UK: CABI.

Goodell, B., Qian, Y., and Jellison, J. (2008). Fungal decay of wood: soft rot—brown rot—white rot.

Goodell, B., Winandy, J. E., and Morrell, J. J. (2020). Fungal degradation of wood: Emerging data, new insights and changing perceptions. Coatings, 10(12), 1210.

Gregory, S. C., and Watling, R. (1985). Occurrence of *Armillaria borealis* in Britain. Transactions of the British Mycological Society, 84(1), 47-55.

Gruber, S., Vaaje-Kolstad, G., Matarese, F., López-Mondéjar, R., Kubicek, C. P., and Seidl-Seiboth, V. (2011). Analysis of subgroup C of fungal chitinases containing chitin-binding and LysM modules in the mycoparasite *Trichoderma atroviride*. Glycobiology, 21(1), 122-133.

Guo, T., Wang, H. C., Xue, W. Q., Zhao, J., and Yang, Z. L. (2016). Phylogenetic analyses of Armillaria reveal at least 15 phylogenetic lineages in China, seven of which are associated with cultivated Gastrodia elata. PLoS One, 11(5), e0154794.

Hage, H., and Rosso, M. N. (2021). Evolution of fungal carbohydrate-active enzyme portfolios and adaptation to plant cell-wall polymers. Journal of Fungi, 7(3), 185.

Hage, H., Miyauchi, S., Virágh, M., Drula, E., Min, B., Chaduli, D., ... and Rosso, M. N. (2021). Gene family expansions and transcriptome signatures uncover fungal adaptations to wood decay. Environmental Microbiology, 23(10), 5716-5732.

Hallgren, J., Tsirigos, K.D., Pedersen, M.D., Almagro Armenteros, J.J., Marcatili, P., Nielsen, H., Krogh, A. and Winther, O. (2022). DeepTMHMM predicts alpha and beta transmembrane proteins using deep neural networks. BioRxiv, pp.2022-04.

Han, L. B., Li, Y. B., Wang, F. X., Wang, W. Y., Liu, J., Wu, J. H., ... and Xia, G. X. (2019). The cotton apoplastic protein CRR1 stabilizes chitinase 28 to facilitate defense against the fungal pathogen *Verticillium dahliae*. The Plant Cell, 31(2), 520-536.

Hanna, J. W., Klopfenstein, N. B., Kim, M. S., McDonald, G. I., and Moore, J. A. (2007). Phylogeographic patterns of *Armillaria ostoyae* in the western United States. Forest Pathology, 37(3), 192-216.

Harrington, T. C., and Wingfield, B. D. (1995). A PCR-based identification method for species of *Armillaria*. Mycologia, 87(2), 280-288.

Have, A. T., Mulder, W., Visser, J., and van Kan, J. A. (1998). The endopolygalacturonase gene Bcpg1 is required for full virulence of *Botrytis cinerea*. Molecular Plant-Microbe Interactions, 11(10), 1009-1016.

Healy, V., O'Connell, J., McCarthy, T. V., and Doonan, S. (1999). The lysine-specific proteinase from *Armillaria mellea* is a member of a novel class of metalloendopeptidases located in Basidiomycetes. Biochemical and Biophysical Research Communications, 262(1), 60-63.

Heinzelmann, R., Dutech, C., Tsykun, T., Labbé, F., Soularue, J. P., and Prospero, S. (2019). Latest advances and future perspectives in *Armillaria* research. Canadian Journal of Plant Pathology, 41(1), 1-23.

Heinzelmann, R., Prospero, S., and Rigling, D. (2017). Virulence and stump colonization ability of *Armillaria borealis* on Norway spruce seedlings in comparison to sympatric *Armillaria* species. Plant Disease, 101(3), 470-479.

Hématy, K., Cherk, C., and Somerville, S. (2009). Host–pathogen warfare at the plant cell wall. Current Opinion in Plant Biology, 12(4), 406-413.

Hess, J., Skrede, I., Chaib De Mares, M., Hainaut, M., Henrissat, B., and Pringle, A. (2018). Rapid divergence of genome architectures following the origin of an ectomycorrhizal symbiosis in the genus *Amanita*. Molecular Biology and Evolution, 35(11), 2786-2804.

Hood, I. A., Horner, I. J., Gardner, J. F., and Sandberg, C. J. (2002). *Armillaria* root disease of *Pinus radiata* in New Zealand. 1: Basidiospore dispersal. New Zealand Journal of Forestry Science, 32(1), 94-102.

Horton, P., Park, K. J., Obayashi, T., Fujita, N., Harada, H., Adams-Collier, C. J., and Nakai, K. (2007). WoLF PSORT: protein localization predictor. Nucleic Acids Research, 35(suppl_2), W585-W587.

Hu, J., Arantes, V., Pribowo, A., and Saddler, J. N. (2013). The synergistic action of accessory enzymes enhances the hydrolytic potential of a “cellulase mixture” but is highly substrate specific. Biotechnology for Biofuels, 6, 1-12.

Jombart, T., Balloux, F., and Dray, S. (2010). Adephylo: new tools for investigating the phylogenetic signal in biological traits. Bioinformatics, 26(15), 1907-1909.

Jones, J. D., and Dangl, J. L. (2006). The plant immune system. Nature, 444(7117), 323-329.

Jones, P., Binns, D., Chang, H.Y., Fraser, M., Li, W., McAnulla, C., McWilliam, H., Maslen, J., Mitchell, A., Nuka, G. and Pesseat, S. (2014). InterProScan 5: genome-scale protein function classification. Bioinformatics, 30(9), pp.1236-1240.

Kanehisa, M., and Goto, S. (2000). KEGG: kyoto encyclopedia of genes and genomes. Nucleic Acids Research, 28(1), 27-30.

Kars, I., Krooshof, G. H., Wagemakers, L., Joosten, R., Benen, J. A., and Van Kan, J. A. (2005). Necrotizing activity of five *Botrytis cinerea* endopolygalacturonases produced in *Pichia pastoris*. The Plant Journal, 43(2), 213-225.

Katoh, K., and Standley, D. M. (2013). MAFFT multiple sequence alignment software version 7: improvements in performance and usability. Molecular Biology and Evolution, 30(4), 772-780.

Keča, N., and Solheim, H. (2011). Ecology and distribution of *Armillaria* species in Norway. Forest Pathology, 41(2), 120-132.

Keča, N., Bodles, W. J. A., Woodward, S., Karadžić, D., and Bojović, S. (2006). Molecular‐based identification and phylogeny of *Armillaria* species from Serbia and Montenegro. Forest Pathology, 36(1), 41-57.

Kedves, O., Shahab, D., Champramary, S., Chen, L., Indic, B., Bóka, B., Nagy, V.D., Vágvölgyi, C., Kredics, L., and Sipos, G. (2021). Epidemiology, biotic interactions and biological control of armillarioids in the Northern Hemisphere. Pathogens, 10(1), 76.

Kelvin, S. H. P., Richard, T. C., and Yves, B. (2015). Routledge handbook of forest ecology (pp. 281-96). London: Routledge Press.

Kema, G. H., van der Lee, T. A., Mendes, O., Verstappen, E. C., Lankhorst, R. K., Sandbrink, H., ... and Waalwijk, C. (2008). Large-scale gene discovery in the septoria tritici blotch fungus *Mycosphaerella graminicola* with a focus on in planta expression. Molecular Plant-Microbe Interactions, 21(9), 1249-1260.

Kim, M. S., Heinzelmann, R., Labbé, F., Ota, Y., Elías-Román, R. D., Pildain, M. B., Stewart, J.E., Woodward, S., and Klopfenstein, N. B. (2022). *Armillaria* root diseases of diverse trees in wide-spread global regions. In Forest Microbiology (pp. 361-378). Academic Press.

Kirk, T. K., and Cullen, D. (1998). Enzymology and molecular genetics of wood degradation by white-rot fungi. Environmentally Friendly Technologies for the Pulp and Paper Industry. Wiley, New York, 273-307.

Koch, R. A., and Herr, J. R. (2021). Global distribution and richness of *Armillaria* and related species inferred from public databases and amplicon sequencing datasets. Frontiers in Microbiology, 12, 733159.

Koch, R. A., Wilson, A. W., Séné, O., Henkel, T. W., and Aime, M. C. (2017). Resolved phylogeny and biogeography of the root pathogen *Armillaria* and its gasteroid relative, *Guyanagaster*. BMC Evolutionary Biology, 17, 1-16.

Koo, C. D., Kim, J. G., Lee, H. Y., Park, Y. W., and Lee, H. S. (2017). Significance of *Armillaria* species in taxonomy, forest ecology and plant pathology. The Korean Journal of Mycology, 45(1), 1-13.

Korhonen, K., and Hintikka, V. (1974). Cytological evidence for somatic diploidization in dikaryotic cells of *Armillariella mellea*. Archives of Microbiology, 95, 187-192.

Koschorreck, K., Alpdagtas, S., and Urlacher, V. B. (2022). Copper-radical oxidases: a diverse group of biocatalysts with distinct properties and a broad range of biotechnological applications. Engineering Microbiology, 100037.

Krijger, J. J., Thon, M. R., Deising, H. B., and Wirsel, S. G. (2014). Compositions of fungal secretomes indicate a greater impact of phylogenetic history than lifestyle adaptation

Krizsán, K., Almási, É., Merényi, Z., Sahu, N., Virágh, M., Kószó, T., ... and Nagy, L. G. (2019). Transcriptomic atlas of mushroom development reveals conserved genes behind complex multicellularity in fungi. Proceedings of the National Academy of Sciences, 116(15), 7409-7418.

Kubiak, K., Żółciak, A., Damszel, M., Lech, P., and Sierota, Z. (2017). *Armillaria* pathogenesis under climate changes. Forests, 8(4), 100.

Kubicek, C. P., Starr, T. L., and Glass, N. L. (2014). Plant cell wall–degrading enzymes and their secretion in plant-pathogenic fungi. Annual Review of Phytopathology, 52, 427-451.

Kulshreshtha, S., Mathur, N., and Bhatnagar, P. (2014). Mushroom as a product and their role in mycoremediation. AMB express, 4, 1-7.

Levasseur, A., Drula, E., Lombard, V., Coutinho, P. M., and Henrissat, B. (2013). Expansion of the enzymatic repertoire of the CAZy database to integrate auxiliary redox enzymes. Biotechnology for Biofuels, 6, 1-14.

Li, B., and Dewey, C. N. (2011). RSEM: accurate transcript quantification from RNA-Seq data with or without a reference genome. BMC Bioinformatics, 12, 1-16.

Li, T., Cui, L., Song, X., Cui, X., Wei, Y., Tang, L., Mu, Y., and Xu, Z. (2022). Wood decay fungi: An analysis of worldwide research. Journal of Soils and Sediments, 22(6), 1688-1702.

Lin, S., Zhou, C., Zhang, H., and Cai, Z. (2020). Expression, purification and characterization of 5′-nucleotidase from caterpillar fungus by efficient genome-mining. Protein Expression and Purification, 168, 105566.

Liu, X., Xie, J., Fu, Y., Jiang, D., Chen, T., and Cheng, J. (2020). The subtilisin-like protease Bcser2 affects the sclerotial formation, conidiation and virulence of *Botrytis cinerea*. International Journal of Molecular Sciences, 21(2), 603.

Liu, Y., Wu, Y., Zhang, Y., Yang, X., Yang, E., Xu, H., ... and Yan, J. (2019). Lignin degradation potential and draft genome sequence of *Trametes trogii* S0301. Biotechnology for Biofuels, 12, 1-13.

Loix, C., Huybrechts, M., Vangronsveld, J., Gielen, M., Keunen, E., and Cuypers, A. (2017). Reciprocal interactions between cadmium-induced cell wall responses and oxidative stress in plants. Frontiers in Plant Science, 8, 286473.

Lundell, T. K., Mäkelä, M. R., de Vries, R. P., and Hildén, K. S. (2014). Genomics, lifestyles and future prospects of wood-decay and litter-decomposing basidiomycota. In Advances in Botanical Research (Vol. 70, pp. 329-370). Academic Press.

Lyu, X., Shen, C., Fu, Y., Xie, J., Jiang, D., Li, G., and Cheng, J. (2015). Comparative genomic and transcriptional analyses of the carbohydrate-active enzymes and secretomes of

phytopathogenic fungi reveal their significant roles during infection and development. Scientific Reports, 5(1), 15565.

M'Barek, S. B., Cordewener, J. H., Ghaffary, S. M. T., van der Lee, T. A., Liu, Z., Gohari, A. M., ... and Kema, G. H. (2015). FPLC and liquid-chromatography mass spectrometry identify candidate necrosis-inducing proteins from culture filtrates of the fungal wheat pathogen *Zymoseptoria tritici*. Fungal Genetics and Biology, 79, 54-62.

Mansora, A. M., Lima, J. S., Anib, F. N., Hashima, H., and Hoa, W. S. (2019). Characteristics of cellulose, hemicellulose and lignin of MD2 pineapple biomass. Chemical Engineering, 72(1), 79-84.

Maphosa, L., Wingfield, B. D., Coetzee, M. P. A., Mwenje, E., and Wingfield, M. J. (2006). Phylogenetic relationships among *Armillaria* species inferred from partial elongation factor 1-alpha DNA sequence data. Australasian Plant Pathology, 35, 513-520.

Marín-Menguiano, M., Moreno-Sánchez, I., Barrales, R. R., Fernández-Álvarez, A., and Ibeas, J. I. (2019). N-glycosylation of the protein disulfide isomerase Pdi1 ensures full *Ustilago maydis* virulence. PLoS pathogens, 15(11), e1007687.

Martínez-Soto, D., Robledo-Briones, A. M., Estrada-Luna, A. A., and Ruiz-Herrera, J. (2013). Transcriptomic analysis of Ustilago maydis infecting *Arabidopsis* reveals important aspects of the fungus pathogenic mechanisms. Plant Signaling and Behavior, 8(8), e25059.

Martinez, D., Larrondo, L. F., Putnam, N., Gelpke, M. D. S., Huang, K., Chapman, J., Helfenbein, K.G., Ramaiya, P., Detter, J.C., Larimer, F., and Rokhsar, D. (2004). Genome sequence of the lignocellulose degrading fungus *Phanerochaete chrysosporium* strain RP78. Nature Biotechnology, 22(6), 695-700.

Matheny, P. B., Wang, Z., Binder, M., Curtis, J. M., Lim, Y. W., Nilsson, R. H., Hughes, K.W., Hofstetter, V., Ammirati, J.F., Schoch, C.L., Langer, E., and Hibbett, D. S. (2007). Contributions of rpb2 and tef1 to the phylogeny of mushrooms and allies (Basidiomycota, Fungi). Molecular Phylogenetics and Evolution, 43(2), 430-451.

Mathioni, S. M., Beló, A., Rizzo, C. J., Dean, R. A., and Donofrio, N. M. (2011). Transcriptome profiling of the rice blast fungus during invasive plant infection and in vitro stresses. Bmc Genomics, 12, 1-20.

Meng, F., Liu, X., and Wang, Q. (2012). Identification of wood decay related genes from *Piptoporus betulinus* (bull. Fr.) karsten using differential display reverse transcription pcr (ddrt-pcr). Biotechnology and Biotechnological Equipment, 26(3), 2961-2965.

Mesny, F., Miyauchi, S., Thiergart, T., Pickel, B., Atanasova, L., Karlsson, M., ... and Hacquard, S. (2021). Genetic determinants of endophytism in the *Arabidopsis* root mycobiome. Nature Communications, 12(1), 7227.

Mihail, J. D., Bruhn, J. N., and Leininger, T. D. (2002). The effects of moisture and oxygen availability on rhizomorph generation by *Armillaria tabescens* in comparison with *A. gallica* and *A. mellea*. Mycological Research, 106(6), 697-704.

Mir, A. A., Park, S. Y., Sadat, M. A., Kim, S., Choi, J., Jeon, J., and Lee, Y. H. (2015). Systematic characterization of the peroxidase gene family provides new insights into fungal pathogenicity in *Magnaporthe oryzae*. Scientific Reports, 5(1), 11831.

Miyauchi, S., Kiss, E., Kuo, A., Drula, E., Kohler, A., Sánchez-García, M., ... and Martin, F. M. (2020). Large-scale genome sequencing of mycorrhizal fungi provides insights into the early evolution of symbiotic traits. Nature Communications, 11(1), 5125.

Miyauchi, S., Rancon, A., Drula, E., Hage, H., Chaduli, D., Favel, A., ... and Rosso, M. N. (2018). Integrative visual omics of the white-rot fungus *Polyporus brumalis* exposes the biotechnological potential of its oxidative enzymes for delignifying raw plant biomass. Biotechnology for Biofuels, 11, 1-14.

Mori, T., Koyama, G., Kawagishi, H., and Hirai, H. (2016). Effects of homologous expression of 1, 4-benzoquinone reductase and homogentisate 1, 2-dioxygenase genes on wood decay in hyper-lignin-degrading fungus *Phanerochaete sordida* YK-624. Current Microbiology, 73, 512-518.

Nagy, L. G., Riley, R., Bergmann, P. J., Krizsán, K., Martin, F. M., Grigoriev, I. V., ... and Hibbett, D. S. (2017). Genetic bases of fungal white rot wood decay predicted by phylogenomic analysis of correlated gene-phenotype evolution. Molecular biology and evolution, 34(1), 35-44.

Nagy, L. G., Riley, R., Tritt, A., Adam, C., Daum, C., Floudas, D., ... and Hibbett, D. S. (2016). Comparative genomics of early-diverging mushroom-forming fungi provides insights

into the origins of lignocellulose decay capabilities. Molecular Biology and Evolution, 33(4), 959-970.

Nagy, L. G., Vonk, P. J., Künzler, M., Földi, C., Virágh, M., Ohm, R. A., ... and Merényi, Z. (2023). Lessons on fruiting body morphogenesis from genomes and transcriptomes of Agaricomycetes. Studies in Mycology.

Nguyen, Q. B., Itoh, K., Van Vu, B., Tosa, Y., and Nakayashiki, H. (2011). Simultaneous silencing of endo‐β‐1, 4 xylanase genes reveals their roles in the virulence of *Magnaporthe oryzae*. Molecular Microbiology, 81(4), 1008-1019.

Nowak, M. A., Boerlijst, M. C., Cooke, J., and Smith, J. M. (1997). Evolution of genetic redundancy. Nature, 388(6638), 167-171.

O'Connell, R. J., Thon, M. R., Hacquard, S., Amyotte, S. G., Kleemann, J., Torres, M. F., ... and Vaillancourt, L. J. (2012). Lifestyle transitions in plant pathogenic *Colletotrichum fungi* deciphered by genome and transcriptome analyses. Nature Genetics, 44(9), 1060-1065.

Omdal, D. W., Shaw III, C. G., Jacobi, W. R., and Wager, T. C. (1995). Variation of pathogenicity and virulence of isolates of *Armillaria ostoyae* on eight tree species. Plant Disease, 79(9), 939-944.

Pan, Y., Wei, J., Yao, C., Reng, H., and Gao, Z. (2018). SsSm1, a Cerato-platanin family protein, is involved in the hyphal development and pathogenic process of *Sclerotinia sclerotiorum*. Plant Science, 270, 37-46.

Pavlov, I. N. (2015). Biotic and abiotic factors as causes of coniferous forests dieback in Siberia and Far East. Contemporary Problems of Ecology, 8, 440-456.

Perazzolli, M., Bampi, F., Faccin, S., Moser, M., De Luca, F., Ciccotti, A. M., ... and Moser, C. (2010). *Armillaria mellea* induces a set of defense genes in grapevine roots and one of them codifies a protein with antifungal activity. Molecular Plant-Microbe Interactions, 23(4), 485-496.

Pérez-Sierra, A. N. A., and Henricot, B. (2002). Identification of fungal species beyond morphology. Mycologist, 16(2), 42-46.

Petchayo Tigang, S., Tchotet Tchoumi, J. M., Roux, J., Nguefack, J., Begoude Boyogueno, A. D., Mbenoun, M., ... and Ten Hoopen, G. M. (2020). *Armillaria* root rot threatens Cameroon's Penja pepper (*Piper nigrum L.*). Tropical plant pathology, *45*, 534-543.

Price, M. N., Dehal, P. S., and Arkin, A. P. (2010). FastTree 2–approximately maximum-likelihood trees for large alignments. PloS one, 5(3), e9490.

Prospero, S., Holdenrieder, O., and Rigling, D. (2004). Comparison of the virulence of *Armillaria cepistipes* and *Armillaria ostoyae* on four Norway spruce provenances. Forest Pathology, 34(1), 1-14.

Rees, H. J., Bashir, N., Drakulic, J., Cromey, M. G., Bailey, A. M., and Foster, G. D. (2021). Identification of native endophytic *Trichoderma* spp. for investigation of in vitro antagonism towards *Armillaria mellea* using synthetic‐and plant‐based substrates. Journal of Applied Microbiology, 131(1), 392-403.

Rigling, D., Günthardt-Goerg, M. S., Blauenstein, H., and Frey, B. (2006). Accumulation of heavy metals into *Armillaria* rhizomorphs from contaminated soils. Forest Snow and Landscape Research, 80(2), 213-220.

Riley, R., Salamov, A. A., Brown, D. W., Nagy, L. G., Floudas, D., Held, B. W., ... and Grigoriev, I. V. (2014). Extensive sampling of basidiomycete genomes demonstrates inadequacy of the white-rot/brown-rot paradigm for wood decay fungi. Proceedings of the National Academy of Sciences, 111(27), 9923-9928.

Rishbeth, J. (1985). Infection cycle of *Armillaria* and host response. European Journal of Forest Pathology, 15(5‐6), 332-341.

Ritchie, M. E., Phipson, B., Wu, D. I., Hu, Y., Law, C. W., Shi, W., and Smyth, G. K. (2015). limma powers differential expression analyses for RNA-sequencing and microarray studies. Nucleic acids research, 43(7), e47-e47.

Robinson, R. (2010). Detection, recognition and management options for *Armillaria* root disease in urban environments. In Proceedings of The International Symposium on Symbolic and Algebraic Computation (ISSAC) (pp. 1-11). South Australia: Adelaide.

Robinson, R. M., and Smith, R. H. (2001). Fumigation of regrowth karri stumps with metham-sodium to control *Armillaria luteobubalina*. Australian Forestry, 64(4), 209-215.

Rogers, L. M., Kim, Y. K., Guo, W., González-Candelas, L., Li, D., and Kolattukudy, P. E. (2000). Requirement for either a host-or pectin-induced pectate lyase for infection of *Pisum sativum* by *Nectria hematococca*. Proceedings of the National Academy of Sciences, 97(17), 9813-9818.

Roll‐Hansen, F. (1985). The *Armillaria* species in Europe: a literature review. European journal of forest pathology, 15(1), 22-31.

Ross‐Davis, A. L., Stewart, J. E., Hanna, J. W., Kim, M. S., Knaus, B. J., Cronn, R., Rai, H., Richardson, B.A., McDonald, G.I., and Klopfenstein, N. B. (2013). Transcriptome of an *Armillaria* root disease pathogen reveals candidate genes involved in host substrate utilization at the host–pathogen interface. Forest Pathology, 43(6), 468-477.

Rytioja, J., Hildén, K., Yuzon, J., Hatakka, A., De Vries, R. P., and Mäkelä, M. R. (2014). Plant-polysaccharide-degrading enzymes from basidiomycetes. Microbiology and Molecular Biology Reviews, 78(4), 614-649.

Sahu, N., Indic, B., Wong-Bajracharya, J., Merényi, Z., Ke, H. M., Ahrendt, S., ... and Nagy, L. G. (2023). Vertical and horizontal gene transfer shaped plant colonization and biomass degradation in the fungal genus *Armillaria*. Nature Microbiology, 8(9), 1668-1681

Sánchez, C. (2009). Lignocellulosic residues: biodegradation and bioconversion by fungi. Biotechnology Advances, 27(2), 185-194.

Sands, R. (Ed.). (2013). Forestry in a global context. CABI.

Schilling, M., Farine, S., Péros, J. P., Bertsch, C., and Gelhaye, E. (2021). Wood degradation in grapevine diseases. In Advances in Botanical Research (Vol. 99, pp. 175-207). Academic Press.

Schirawski, J., Bohnert, H. U., Steinberg, G., Snetselaar, K., Adamikowa, L., and Kahmann, R. (2005). Endoplasmic reticulum glucosidase II is required for pathogenicity of *Ustilago maydis*. The Plant Cell, 17(12), 3532-3543.

Schwarze, F. W. (2007). Wood decay under the microscope. Fungal biology reviews, 21(4), 133-170.

Shah, F., Nicolás, C., Bentzer, J., Ellström, M., Smits, M., Rineau, F., ... and Tunlid, A. (2016). Ectomycorrhizal fungi decompose soil organic matter using oxidative mechanisms adapted from saprotrophic ancestors. New Phytologist, 209(4), 1705-1719.

Shaw, C. G., and Kile, G. A. (1991). *Armillaria* root disease (No. 691). Forest Service, US Department of Agriculture.

Shaw, C. I., & Roth, L. F. (1976). Persistence and distribution of a clone of *Armillaria [Armillariella] mellea* in a Ponderosa Pine forest. 1210-1213.

Showalter, A. M. (1993). Structure and function of plant cell wall proteins. The Plant Cell, 5(1), 9.

Sicoli, G., Fatehi, J., and Stenlid, J. (2003). Development of species‐specific PCR primers on rDNA for the identification of European *Armillaria* species. Forest Pathology, 33(5), 287-297.

Singh, P. (1983). Armillaria root rot: Influence of soil nutrients and pH on the susceptibility of conifer species to the disease. Forest Pathology, 13(2), 92–101.

Sipos, G., Anderson, J. B., and Nagy, L. G. (2018). *Armillaria*. Current Biology, 28(7), R297-R298.

Sipos, G., Prasanna, A. N., Walter, M. C., O'Connor, E., Bálint, B., Krizsán, K., Kiss, B., Hess, J., Varga, T., Slot, J., Riley, R., and Nagy, L. G. (2017). Genome expansion and lineage-specific genetic innovations in the forest pathogenic fungi *Armillaria*. Nature Ecology and Evolution, 1(12), 1931-1941.

Smith, S. E., and Read, D. J. (2010). Mycorrhizal symbiosis. Academic Press.

Soal, N. C., Coetzee, M. P., van der Nest, M. A., Hammerbacher, A., and Wingfield, B. D. (2022). Phenolic degradation by catechol dioxygenases is associated with pathogenic fungi with a necrotrophic lifestyle in the Ceratocystidaceae. G3, 12(3), jkac008.

Somai-Jemmali, L., Randoux, B., Siah, A., Magnin-Robert, M., Halama, P., Reignault, P., and Hamada, W. (2017). Similar infection process and induced defense patterns during compatible interactions between *Zymoseptoria tritici* and both bread and durum wheat species. European Journal of Plant Pathology, 147, 787-801.

Stokland, J. N., Siitonen, J., and Jonsson, B. G. (2012). Biodiversity in dead wood. Cambridge University Press.

Støpamo, F. G., Røhr, Å. K., Mekasha, S., Petrović, D. M., Várnai, A., and Eijsink, V. G. (2021). Characterization of a lytic polysaccharide monooxygenase from *Aspergillus fumigatus* shows functional variation among family AA11 fungal LPMOs. Journal of Biological Chemistry, 297(6).

Strasser, K., McDonnell, E., Nyaga, C., Wu, M., Wu, S., Almeida, H., ... and Tsang, A. (2015). mycoCLAP, the database for characterized lignocellulose-active proteins of fungal origin: resource and text mining curation support. Database, 2015, bav008.

Sun, L., Chen, X., Gao, J., Zhao, Y., Liu, L., Hou, Y., ... and Huang, S. (2019). Effects of disruption of five FUM genes on fumonisin biosynthesis and pathogenicity in *Fusarium proliferatum*. Toxins, 11(6), 327.

Sützl, L., Foley, G., Gillam, E. M., Bodén, M., and Haltrich, D. (2019). The GMC superfamily of oxidoreductases revisited: analysis and evolution of fungal GMC oxidoreductases. Biotechnology for Biofuels, 12, 1-18.

Sützl, L., Laurent, C. V., Abrera, A. T., Schütz, G., Ludwig, R., and Haltrich, D. (2018). Multiplicity of enzymatic functions in the CAZy AA3 family. Applied microbiology and biotechnology, 102, 2477-2492.

Syed, K., Shale, K., Pagadala, N. S., and Tuszynski, J. (2014). Systematic identification and evolutionary analysis of catalytically versatile cytochrome P450 monooxygenase families enriched in model basidiomycete fungi. PLoS One, 9(1), e86683.

Tan, X., Hu, Y., Jia, Y., Hou, X., Xu, Q., Han, C., and Wang, Q. (2020). A conserved glycoside hydrolase family 7 cellobiohydrolase PsGH7a of *Phytophthora sojae* is required for full virulence on soybean. Frontiers in Microbiology, 11, 538365.

Törönen, P., Medlar, A., and Holm, L. (2018). PANNZER2: a rapid functional annotation web server. Nucleic Acids Research, 46(W1), W84-W88.

Travadon, R., Smith, M. E., Fujiyoshi, P., Douhan, G. W., Rizzo, D. M., and Baumgartner, K. (2012). Inferring dispersal patterns of the generalist root fungus *Armillaria mellea*. New Phytologist, 193(4), 959-969.

Vaaje-Kolstad, G., Westereng, B., Horn, S. J., Liu, Z., Zhai, H., Sørlie, M., and Eijsink, V. G. (2010). An oxidative enzyme boosting the enzymatic conversion of recalcitrant polysaccharides. Science, 330(6001), 219-222.

Vaillancourt, F. H., Bolin, J. T., and Eltis, L. D. (2006). The ins and outs of ring-cleaving dioxygenases. Critical Reviews in Biochemistry and Molecular Biology, 41(4), 241-267.

van den Brink, J., and de Vries, R. P. (2011). Fungal enzyme sets for plant polysaccharide degradation. Applied Microbiology and Biotechnology, 91(6), 1477-1492.

Wang, Y., Tyler, B. M., and Wang, Y. (2019). Defense and counterdefense during plant-pathogenic oomycete infection. Annual Review of Microbiology, 73, 667-696.

Winnenburg, R., Baldwin, T. K., Urban, M., Rawlings, C., Köhler, J., and Hammond-Kosack, K. E. (2006). PHI-base: a new database for pathogen host interactions. Nucleic Acids Research, 34(suppl_1), D459-D464.

Wymelenberg, A. V., Minges, P., Sabat, G., Martinez, D., Aerts, A., Salamov, A., ... and Cullen, D. (2006). Computational analysis of the *Phanerochaete chrysosporium* v2. 0 genome database and mass spectrometry identification of peptides in ligninolytic cultures reveal complex mixtures of secreted proteins. Fungal Genetics and Biology, 43(5), 343-356.

Xu, X. L., Wu, X. Q., Ye, J. R., and Huang, L. (2015). Molecular characterization and functional analysis of three pathogenesis-related cytochrome P450 genes from *Bursaphelenchus xylophilus* (Tylenchida: Aphelenchoidoidea). International Journal of Molecular Sciences, 16(3), 5216-5234.

Xu, Y. H., Brandl, H., Osterwalder, S., Elzinga, E. J., and Huang, J. H. (2019). Vanadium-basidiomycete fungi interaction and its impact on vanadium biogeochemistry. Environment International, 130, 104891.

Yakoby, N., Beno-Moualem, D., Keen, N. T., Dinoor, A., Pines, O., and Prusky, D. (2001). *Colletotrichum gloeosporioides* pelB is an important virulence factor in avocado fruit-fungus interaction. Molecular Plant-Microbe Interactions, 14(8), 988-995.

Ye, F., Albarouki, E., Lingam, B., Deising, H. B., and von Wirén, N. (2014). An adequate Fe nutritional status of maize suppresses infection and biotrophic growth of *Colletotrichum graminicola*. Physiologia plantarum, 151(3), 280-292.

Yildirim, N., Erguven, G. O., and Adar, E. (2018). The chemical and biochemical oxygen demand reduction by *Armillaria tabescens* in malathion supplemented culture medium. Glob Nest J, 20, 529-533.

Zabel, R. A., and Morrell, J. J. (2012). Wood microbiology: decay and its prevention. Academic press.

Zainudin, N. A. I. M., Condon, B., De Bruyne, L., Van Poucke, C., Bi, Q., Li, W., ... and Turgeon, B. G. (2015). Virulence, host-selective toxin production, and development of three *Cochliobolus phytopathogens* lacking the Sfp-type 4′-phosphopantetheinyl transferase Ppt1. Molecular Plant-Microbe Interactions, 28(10), 1130-1141.

Zerillo, M. M., Adhikari, B. N., Hamilton, J. P., Buell, C. R., Lévesque, C. A., and Tisserat, N. (2013). Carbohydrate-active enzymes in *Pythium* and their role in plant cell wall and storage polysaccharide degradation. PLoS One, 8(9), e72572.

Zhan, M., Tian, M., Wang, W., Li, G., Lu, X., Cai, G., Yang, H., Du, G., and Huang, L. (2020). Draft genomic sequence of *Armillaria gallica* 012m: Insights into its symbiotic relationship with *Gastrodia elata*. Brazilian Journal of Microbiology, 51, 1539-1552.

Zhang, H., Mukherjee, M., Kim, J. E., Yu, W., and Shim, W. B. (2018). Fsr1, a striatin homologue, forms an endomembrane‐associated complex that regulates virulence in the maize pathogen *Fusarium verticillioides*. Molecular Plant Pathology, 19(4), 812-826.

Zhang, H., Yohe, T., Huang, L., Entwistle, S., Wu, P., Yang, Z., Busk, P.K., Xu, Y. and Yin, Y. (2018). dbCAN2: a meta server for automated carbohydrate-active enzyme annotation. Nucleic Acids Research, 46(W1), pp.W95-W101.

Zhang, J., Bruton, B. D., and Biles, C. L. (2014). Cell wall-degrading enzymes of *Didymella bryoniae* in relation to fungal growth and virulence in cantaloupe fruit. European Journal of Plant Pathology, 139, 749-761.

Zhang, M. Z., Sun, C. H., Liu, Y., Feng, H. Q., Chang, H. W., Cao, S. N., ... and Qin, Q. M. (2020). Transcriptome analysis and functional validation reveal a novel gene, BcCGF1, that enhances fungal virulence by promoting infection‐related development and host penetration. Molecular Plant Pathology, 21(6), 834-853.

Zhang, T., Zhao, Y. L., Zhao, J. H., Wang, S., Jin, Y., Chen, Z. Q., ... and Guo, H. S. (2016a). Cotton plants export microRNAs to inhibit virulence gene expression in a fungal pathogen. Nature Plants, 2(10), 1-6.

Zhang, Y., He, J., Jia, L. J., Yuan, T. L., Zhang, D., Guo, Y., ... and Tang, W. H. (2016b). Cellular tracking and gene profiling of *Fusarium graminearum* during maize stalk rot disease development elucidates its strategies in confronting phosphorus limitation in the host apoplast. PLoS Pathogens, 12(3), e1005485.

Zhao, L., Poschmann, G., Waldera-Lupa, D., Rafiee, N., Kollmann, M., and Stühler, K. (2019). OutCyte: a novel tool for predicting unconventional protein secretion. Scientific Reports, 9(1), 19448.

Zhu, X., Zhou, Z., Guo, G., Li, J., Yan, H., and Li, F. (2023). Proteomics and metabolomics analysis of the lignin degradation mechanism of lignin-degrading fungus *Aspergillus fumigatus* G-13. Analytical Methods, 15(8), 1062-1076.

Zolciak, A. "Armillaria species in coniferous stands." Acta Mycologica 42, no. 2 (2007).

10. SUPPLEMENTARY MATERIALS

Supplementary material 1. CAZymes list and their putative substrates (Sahu et al., 2023)

CAZy_families	References	Substrate	Category
AA1	Nagy et al. 2015	Lignin	PCWDE
AA1_1	Miyauchi et al. 2020	Lignin	PCWDE
AA1_2	Levasseur et al. 2013, Liu et al. 2019	Lignin	PCWDE
AA1_3	Levasseur et al. 2013	Lignin	PCWDE
AA10	Miyauchi et al. 2020	Cellulose	PCWDE
AA11	Støpamo et al. 2021	Cellulose/Chitin,LPMO	PCWDE, FCW
AA14	Miyauchi et al. 2020	Hemicellulose	PCWDE, FCW
AA15	Miyauchi et al. 2020	Chitin, Cellulose	FCW
AA16	Miyauchi et al. 2020	Cellulose	PCWDE
AA2	Riley et al. 2014, Nagy et al. 2015, Miyauchi et al. 2020	Lignin	PCWDE
AA3	Sützl et al. 2018	Putatively acting on_lignin monomers	PCWDE
AA3_1	Rytioja et al. 2014 , Miyauchi et al. 2018	Cellulose	PCWDE
AA3_2	Sützl et al. 2018	Putatively acting on_lignin monomers	PCWDE
AA3_3	Sützl et al. 2018	Putatively acting on_lignin monomers	PCWDE
AA3_4	Sützl et al. 2018	Putatively acting on_lignin monomers	PCWDE
AA5	Strasser et al. 2015	Lignin	PCWDE
AA5_1	Levasseur et al. 2013, Daou et al. 2021	Putatively acting on_lignin monomers	PCWDE
AA5_2	Levasseur et al. 2013, Koschorreck et al. 2022	Putatively acting on_lignin monomers	PCWDE
AA8	Rytioja et al. 2014 , Miyauchi et al. 2018	Cellulose	PCWDE
AA9	Miyauchi et al. 2020	Cellulose	PCWDE
CBM1	Miyauchi et al. 2020	Cellulose	PCWDE
CBM12	Miyauchi et al. 2020	Chitin	FCW

CBM14	Miyauchi et al. 2020	Chitn	FCW
CBM18	Miyauchi et al. 2020	Chitin	FCW
CBM43	Miyauchi et al. 2020	Glucan	FCW
CBM5	Miyauchi et al. 2020	Chitin	FCW
CBM50	Gruber et al. 2011	Chitin	FCW
CBM63	Miyauchi et al. 2020	Cellulose	PCWDE
CBM67	Miyauchi et al. 2020	Pectin	PCWDE
CE12	Miyauchi et al. 2020	Pectin	PCWDE
CE15	Miyauchi et al. 2020	Hemicellulose	PCWDE
CE16	Floudas et al. 2012, Floudas et al. 2015, Nagy et al. 2016	Hemicellulose	PCWDE
CE4	Krizsan et al. 2019	Chitin	FCW
CE5	Miyauchi et al. 2020	Hemicellulose, Cutin, Suberin	PCWDE
CE8	Miyauchi et al. 2020	Pectin	PCWDE
EXPN	Ding et al. 2022	Cellulose	PCWDE
GH1	Rytioja et al. 2014 , Miyauchi et al. 2018	Cellulose	PCWDE
GH10	Miyauchi et al. 2020	Hemicellulose	PCWDE
GH105	Miyauchi et al. 2020	Pectin	PCWDE
GH106	Miyauchi et al. 2020	Pectin	PCWDE
GH11	Miyauchi et al. 2020	Hemicellulose	PCWDE
GH113	Miyauchi et al. 2020	Hemicellulose	PCWDE
GH115	Miyauchi et al. 2020	Hemicellulose	PCWDE
GH12	Rytioja et al. 2014, Miyauchi et al. 2020	Cellulose, Hemicellulose	PCWDE
GH125	Miyauchi et al. 2020	Mannan	FCW
GH128	Miyauchi et al. 2020	Glucan	FCW
GH131	Miyauchi et al. 2020	Cellulose	PCWDE
GH132	Miyauchi et al. 2020	Glucan	FCW
GH134	Miyauchi et al. 2020	Hemicellulose	PCWDE
GH135	Miyauchi et al. 2020	Galactan	FCW

GH152	Krizsan et al. 2019	Glucan	FCW
GH16	Miyauchi et al. 2020	Glucan	FCW
GH16_2	Krizsan et al. 2019	Glucan	FCW
GH17	Miyauchi et al. 2020	Glucan	FCW
GH18	Miyauchi et al. 2020	Chitin	FCW
GH19	Miyauchi et al. 2020	Chitin	FCW
GH2	Rytioja et al. 2014	Hemicellulose	PCWDE
GH20	Miyauchi et al. 2020	Chitin	FCW
GH23	Miyauchi et al. 2020	Peptidoglycan	FCW
GH24	Miyauchi et al. 2020	Peptidoglycan	FCW
GH25	Miyauchi et al. 2020	Peptidoglycan	FCW
GH26	Rytioja et al. 2014, Miyauchi et al. 2020	Hemicellulose, Mannan	PCWDE, FCW
GH27	Rytioja et al. 2014	Hemicellulose	PCWDE
GH28	Miyauchi et al. 2020	Pectin	PCWDE
GH29	Floudas et al. 2015	Hemicellulose	PCWDE
GH3	Rytioja et al. 2014, Miyauchi et al. 2020	Cellulose, Hemicellulose	PCWDE, FCW
GH30	Miyauchi et al. 2018	Hemicellulose	PCWDE
GH30_3	Miyauchi et al. 2020	Glucan	FCW
GH30_5	Miyauchi et al. 2020	Galactan	FCW
GH30_7	Miyauchi et al. 2020	Hemicellulose	PCWDE
GH31	Rytioja et al. 2014	Hemicellulose	PCWDE
GH35	Rytioja et al. 2014	Hemicellulose	PCWDE
GH36	Rytioja et al. 2014	Hemicellulose	PCWDE
GH43	Rytioja et al. 2014, Miyauchi et al. 2020	Hemicellulose	PCWDE
GH44	Miyauchi et al. 2020	Cellulose	PCWDE
GH45	Miyauchi et al. 2020	Cellulose	PCWDE
GH46	Miyauchi et al. 2020	Chitin	FCW
GH48	Miyauchi et al. 2020	Cellulose	PCWDE

GH5	Rytioja et al. 2014, Miyauchi et al. 2020	Cellulose, Hemicellulose	PCWDE
GH5_1	Miyauchi et al. 2020	Cellulose	PCWDE
GH5_15	Miyauchi et al. 2020	Glucan	FCW
GH5_22	Miyauchi et al. 2020	Cellulose, Hemicellulose	PCWDE
GH5_31	Miyauchi et al. 2020	Mannan	FCW
GH5_4	Miyauchi et al. 2020	Cellulose	PCWDE
GH5_49	Krizsan et al. 2019	Glucan	FCW
GH5_5	Miyauchi et al. 2020	Cellulose	PCWDE
GH5_7	Miyauchi et al. 2020	Hemicellulose	PCWDE
GH5_9	Miyauchi et al. 2020	Glucan	FCW
GH51	Rytioja et al. 2014, Miyauchi et al. 2020	Hemicellulose, Pectin	PCWDE
GH52	Miyauchi et al. 2020	Hemicellulose	PCWDE
GH53	Miyauchi et al. 2020	Pectin	PCWDE
GH54	Rytioja et al. 2014, Miyauchi et al. 2020	Hemicellulose, Pectin	PCWDE
GH55	Miyauchi et al. 2020	Glucan	FCW
GH6	Miyauchi et al. 2020	Cellulose	PCWDE
GH62	Rytioja et al. 2014, Miyauchi et al. 2020	Hemicellulose, Pectin	PCWDE
GH64	Miyauchi et al. 2020	Glucan	FCW
GH67	Miyauchi et al. 2020	Hemicellulose	PCWDE
GH7	Miyauchi et al. 2020	Cellulose	PCWDE
GH71	Miyauchi et al. 2020	Glucan	FCW
GH72	Miyauchi et al. 2020	Glucan	FCW
GH74	Miyauchi et al. 2020	Hemicellulose	PCWDE
GH75	Miyauchi et al. 2020	Chitin	FCW
GH76	Miyauchi et al. 2020	Mannan	FCW
GH78	Miyauchi et al. 2020	Pectin	PCWDE
GH8	Miyauchi et al. 2020	Hemicellulose	PCWDE

GH81	Miyauchi et al. 2020	Glucan	FCW
GH88	Miyauchi et al. 2020	Pectin	PCWDE
GH9	Rytioja et al. 2014, Miyauchi et al. 2020	Cellulose	PCWDE
GH92	Miyauchi et al. 2020	Mannan	FCW
GH93	Miyauchi et al. 2020	Hemicellulose	PCWDE
GH95	Rytioja et al. 2014, Floudas et al. 2015	Hemicellulose	PCWDE
GT18	Nagy et al. 2023	FCW	FCW
GT2	Nagy et al. 2023	FCW	FCW
GT24	Nagy et al. 2023	FCW	FCW
GT48	Nagy et al. 2023	FCW	FCW
GT8	Nagy et al. 2023	FCW	FCW
PL1	Miyauchi et al. 2020	Pectin	PCWDE
PL1_10	Atanasova et al. 2018	Pectin	PCWDE
PL1_4	Atanasova et al. 2018	Pectin	PCWDE
PL1_7	Atanasova et al. 2018	Pectin	PCWDE
PL1_9	Atanasova et al. 2018	Pectin	PCWDE
PL11	Miyauchi et al. 2020	Pectin	PCWDE
PL14_4	Miyauchi et al. 2020	Pectin	PCWDE
PL26	Miyauchi et al. 2020	Pectin	PCWDE
PL3	Miyauchi et al. 2020	Pectin	PCWDE
PL3_2	Atanasova et al. 2018	Pectin	PCWDE
PL4	Miyauchi et al. 2020	Pectin	PCWDE
PL4_1	Atanasova et al. 2018	Pectin	PCWDE
PL4_3	Atanasova et al. 2018	Pectin	PCWDE
PL8_4	Miyauchi et al. 2020	Pectin	PCWDE
PL9	Miyauchi et al. 2020	Pectin	PCWDE
PL9_3	Atanasova et al. 2018	Pectin	PCWDE

Supplementary material 2. List of organisms used for biodegradation prospect comparisons (Champramary *et al.,* 2023)

Organism	ShortName	Number of Proteins	Phylum	JGI Collection Name
Trichoderma citrinoviride	Trici4	9737	Ascomycota	*Trichoderma citrinoviride* TUCIM 6016 v4.0
Aspergillus flavus	Aspfl2_3	13715	Ascomycota	*Aspergillus flavus* NRRL3357
Aspergillus glaucus	Aspgl1	11277	Ascomycota	*Aspergillus glaucus* v1.0
Botryosphaeria dothidea	Botdo1_1	14998	Ascomycota	*Botryosphaeria dothidea*
Cladosporium sphaerospermum	Clasph1	8807	Ascomycota	*Cladosporium sphaerospermum* UM 843
Cochliobolus lunatus	Coclu2	12131	Ascomycota	*Cochliobolus lunatus* m118 v2.0
Dentipellis sp. (KUC8613)	Densp1	14320	Ascomycota	*Dentipellis* sp. KUC8613
Fusarium oxysporum	FoxFo5176	19130	Ascomycota	*Fusarium oxysporum* Fo5176
Geotrichum candidum	Galgeo1	6826	Ascomycota	*Galactomyces geotrichum* Phaff 72-186
Penicillium arizonense	Penar1	12253	Ascomycota	*Penicillium arizonense* CBS 141311
Penicillium chrysogenum	PenchWisc1_1	13671	Ascomycota	*Penicillium chrysogenum* Wisconsin 54-1255
Purpureocillium lilacinum	Purli1	11763	Ascomycota	*Purpureocillium lilacinum* PLFJ-1
Trichoderma harzianum	Trihar1	13932	Ascomycota	*Trichoderma harzianum* TR274 v1.0
Armillaria borealis	Armbor1	19984	Basidiomycota	*Armillaria borealis*
Armillaria cepistipes	Armcep1	23460	Basidiomycota	*Armillaria cepistipes* B5
Desrmillaria ectypa	Armect1	12228	Basidiomycota	*Armillaria ectypa* FPL83.16 v1.0
Armillaria gallica	Armga1	25704	Basidiomycota	*Armillaria gallica* 21-2 v1.0
Armillaria luteobubalina	Armlut1	20318	Basidiomycota	*Armillaria luteobubalina* HWK02 v1.0
Armillaria mellea	Armmel1	15646	Basidiomycota	*Armillaria mellea*
Armillaria solidipes	Armost1	20811	Basidiomycota	*Armillaria solidipes* 28-4 v1.0

Armillaria ostoyae	Armosto1	22705	Basidiomycota	*Armillaria ostoyae C18/9*
Desarmillaria tabescens	Armtab1	19032	Basidiomycota	*Armillaria tabescens* CCBAS 213 v1.0
Guyanagaster necrorhizus	Guyne1	14276	Basidiomycota	*Guyanagaster necrorhizus* MCA 3950 v1.0
Heterobasidion annosum	Hetan2	13405	Basidiomycota	*Heterobasidion annosum* v2.0
Polyporus squamosus	Polsqu1	15283	Basidiomycota	*Polyporus squamosus* CCBS 676 v1.0
Schizophyllum commune	Schco3	16319	Basidiomycota	*Schizophyllum commune* H4-8 v3.0
Bjerkandera adusta	Bjead1_1	15473	Basidiomycota	*Bjerkandera adusta* v1.0
Irpex lacteus	Irplac1	15319	Basidiomycota	*Irpex lacteus* CCBAS Fr. 238 617/93 v1.0
Lentinula edodes	Lenedo1	14079	Basidiomycota	*Lentinula edodes* Le(Bin) 0899 ss11 v1.0
Marasmius fiardii	Marfi1	17098	Basidiomycota	*Marasmius fiardii* PR-910 v1.0
Phanerochaete chrysosporium	Phchr2	13602	Basidiomycota	*Phanerochaete chrysosporium RP-78 v2.2*
Phlebia radiata	Phlrad1	14629	Basidiomycota	*Phlebia radiata* Fr. (isolate 79, FBCC0043)
Pleurotus eryngii	Pleery1	15960	Basidiomycota	*Pleurotus eryngii* ATCC 90797 v1.0
Pleurotus ostreatus	PleosPC9_1	12206	Basidiomycota	*Pleurotus ostreatus* PC9 v1.0
Trametes betulina	Trabet1	13239	Basidiomycota	*Trametes betulina* CIRM-BRFM 1801 v1.0
Trametes versicolor	Trave1	14296	Basidiomycota	*Trametes versicolor* v1.0
Mucor lusitanicus	Muccir1_3	11843	Mucoromycota	*Mucor lusitanicus (circinelloides)* MU402 v1.0

Supplementary material 3. Orthologs based phylogenetic tree. Green coloured letters marking the species belonging to the Mucoromycota phylum, brown for Ascomycota phylum species, and blue ad black letters for the Basidiomycota, with armillarioids being blue coloured (Champramary et al., 2023)

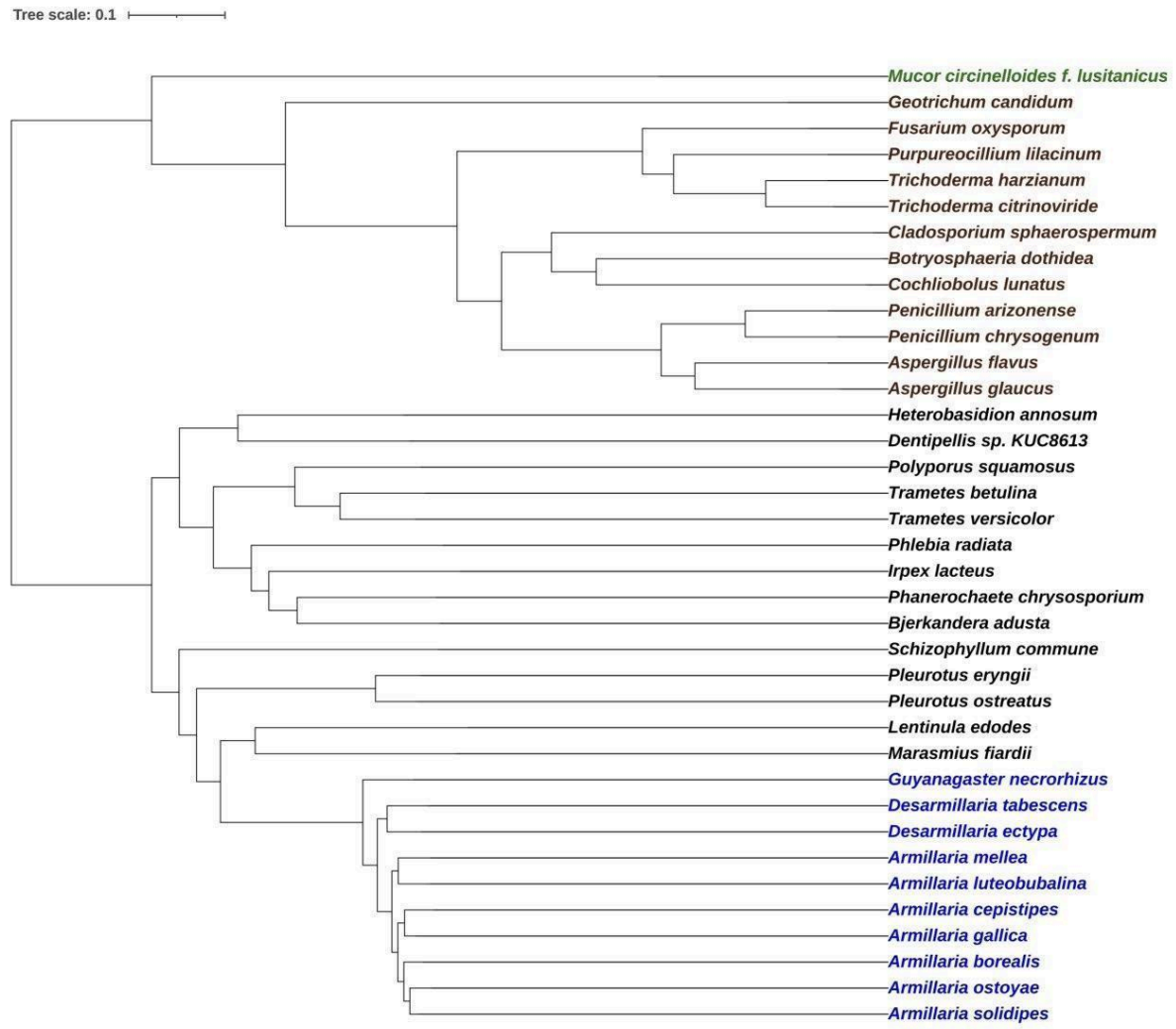

Orthologs-based phylogenetic tree

Supplementary material 4. RNA-Seq mapping statistics for *A. ostoyae* and *A. borealis* growing in the fresh stems

Condition	Organism	Number of input reads	Uniquely mapped reads %	% of reads mapped to multiple loci	Mapping Percentage
C2 Control 1	*A. ostoyae*	23,996,926	28.76%	63.65%	92.41%
C2 Control 2	*A. ostoyae*	20,742,647	15.99%	78.41%	94.40%
C2 Control 3	*A. ostoyae*	25,833,164	52.32%	35.01%	87.33%
C18 Control 1	*A. ostoyae*	24,103,630	64.89%	17.90%	82.79%
C18 Control 2	*A. ostoyae*	24,511,742	49.14%	42.31%	91.45%
C18 Control 3	*A. ostoyae*	22,961,637	44.84%	47.92%	92.76%
C18 Fresh Stems 1	*A. ostoyae*	31,038,216	38.30%	19.67%	57.97%
C18 Fresh Stems 2	*A. ostoyae*	53,808,458	43.91%	9.13%	53.04%
C18 Fresh Stems 3	*A. ostoyae*	44,164,829	43.57%	13.04%	56.61%
C2 Fresh Stems 1	*A. ostoyae*	39,366,220	54.21%	10.22%	64.43%
C2 Fresh Stems 2	*A. ostoyae*	30,191,981	43.43%	14.34%	57.77%
C2 Fresh Stems 3	*A. ostoyae*	56,111,465	16.00%	31.39%	47.39%
A4 Control 1	*A. borealis*	26,501,970	56.64%	12.87%	69.51%
A4 Control 2	*A. borealis*	26,132,116	69.67%	19.12%	88.79%
A4 Control 3	*A. borealis*	27,056,228	42.53%	5.33%	47.86%
A6 Control 1	*A. borealis*	24,980,215	63.74%	15.52%	79.26%
A6 Control 2	*A. borealis*	26,696,080	55.53%	9.29%	64.82%
A6 Control 3	*A. borealis*	25,849,235	48.22%	6.17%	54.39%
A4 Fresh Stems 1	*A. borealis*	75,818,477	51.87%	37.20%	89.07%
A4 Fresh Stems 2	*A. borealis*	76,073,513	15.45%	2.75%	18.20%
A4 Fresh Stems 3	*A. borealis*	71,106,845	39.96%	48.27%	88.23%
A6 Fresh Stems 1	*A. borealis*	92,655,488	53.71%	25.13%	78.84%
A6 Fresh Stems 2	*A. borealis*	93,758,146	42.10%	49.48%	91.58%
A6 Fresh Stems 3	*A. borealis*	85,277,222	58.95%	25.71%	84.66%

Supplementary material 5. *A. ostoyae* genes with putative roles in virulence: functional classification, InterPro domains, and PHIbase homologs.

Group	ProtID	type_of_sec	InterPro ID	Description	PHIbase ID	Pathogen species	Host species	Gene	Gene function
C18F Inducible	ARMOST_20378	Cazy	IPR007867	AA3_2 / GMC oxidoreductase	PHI:10364	*Botrytis cinerea*	*Solanum lycopersicum*	BCIN_03g01540	Choline dehydrogenase
C18F Inducible	ARMOST_09930	Non-Cazy	IPR002472	Palmitoyl protein thioesterase	PHI:4988	*Cochliobolus necrotrophs/ C. heterostrophus /C. miyabeanus*	*Zea mays*	Ppt1	sfp-type 4'-phosphopantetheinyl transferase
C18F Inducible	ARMOST_06352	Non-Cazy	IPR014044	CAP domain	PHI:7144	*Fusarium verticillioide*	*Zea mays*	FvSCP1	SCP-like extracellular protein
C18F Constitutive	ARMOST_07174	Cazy	IPR001117	AA1_1 / Multicopper oxidase	PHI:2920	*Colletotrichum graminicola*	*Zea mays*	FET3-2	Functional ferroxidase
C18F Constitutive	ARMOST_02569	Cazy	IPR001117	AA1_1 / Multicopper oxidase	PHI:3919	*Ustilago maydis*	*Zea mays*	fer1	Iron multicopper oxidase
C18F Constitutive	ARMOST_18738	Cazy	IPR002016	AA2 / Haem peroxidase	PHI:5186	*Magnaporthe oryzae*	*Oryza sativa*	MoAPX2	Class I peroxidase
C18F Constitutive	ARMOST_17524	Cazy	IPR002016	AA2 / Haem peroxidase	PHI:5186	*Magnaporthe oryzae*	*Oryza sativa*	MoAPX2	Class I peroxidase
C18F Constitutive	ARMOST_14728	Cazy	IPR000172	AA3_2 / GMC oxidoreductase	PHI:10364	*Botrytis cinerea*	*Solanum lycopersicum*	BCIN_03g01540	Choline dehydrogenase
C18F Constitutive	ARMOST_17626	Cazy	IPR000172	AA3_2 / GMC oxidoreductase	PHI:10364	*Botrytis cinerea*	*Solanum lycopersicum*	BCIN_03g01540	Choline dehydrogenase
C18F Constitutive	ARMOST_01984	Cazy	IPR000172	AA3_2 / GMC oxidoreductase	PHI:10364	*Botrytis cinerea*	*Solanum lycopersicum*	BCIN_03g01540	Choline dehydrogenase
C18F Constitutive	ARMOST_04029	Cazy	IPR000172	AA3_2 / GMC oxidoreductase	PHI:10364	*Botrytis cinerea*	*Solanum lycopersicum*	BCIN_03g01540	Choline dehydrogenase
C18F Constitutive	ARMOST_16408	Cazy	IPR000172	AA3_2 / GMC oxidoreductase	PHI:10364	*Botrytis cinerea*	*Solanum lycopersicum*	BCIN_03g01540	Choline dehydrogenase
C18F Constitutive	ARMOST_13039	Cazy	IPR001000	GH10 / Glycoside hydrolase family 10	PHI:2208	*Magnaporthe oryzae*	*Hordeum vulgare*	endo-1,4-beta-xylanase	Endo-beta-1,4 xylanase
C18F Constitutive	ARMOST_08096	Cazy	IPR001000	GH10 / Glycoside hydrolase family 10	PHI:2207	*Magnaporthe oryzae*	*Hordeum vulgare*	endo-1,4-beta-xylanase	Endo-beta-1,4 xylanase
C18F Constitutive	ARMOST_17072	Cazy	IPR001722	GH7 / Glycoside hydrolase,	PHI:10659	*Phytophthora sojae*	*Glycine max*	PsGH7a	Glycoside hydrolase, family

				family 7					7
C18F Constitutive	ARMOST_17156	Cazy	IPR001722	GH7 / Glycoside hydrolase, family 7	PHI:10659	*Phytophthora sojae*	*Glycine max*	PsGH7a	Glycoside hydrolase, family 7
C18F Constitutive	ARMOST_13458	Cazy	IPR002022	PL1_7 / Pectate lyase	PHI:222	*Colletotrichum gloeosporioides*	*Persea americana*	PELB	Pectate lyase
C18F Constitutive	ARMOST_11243	Cazy	IPR015500	CBM5 / Peptidase S8, subtilisin-related	PHI:9902	*Botrytis cinerea*	*Arabidopsis thaliana/Solanum lycopersicum*	Bcser2 (Bcin08g02990)	Subtilisin-like protease
C18F Constitutive	ARMOST_15648	Cazy	IPR025887	GH31 / Glycoside hydrolase family 31	PHI:526	*Ustilago maydis*	*Zea mays*	GAS1	Glucosidase 1
C18F Constitutive	ARMOST_17334	Cazy	IPR000743	GH28 / Glycoside hydrolase, family 28	PHI:103	*Botrytis cinerea*	*Solanum lycopersicum*	Bcpg1	Endopolygalacturonase
C18F Constitutive	ARMOST_17320	Cazy	IPR000743	GH28 / Glycoside hydrolase, family 28	PHI:103	*Botrytis cinerea*	*Solanum lycopersicum*	Bcpg1	Endopolygalacturonase
C18F Constitutive	ARMOST_17350	Cazy	IPR000743	GH28 / Glycoside hydrolase, family 28	PHI:103	*Botrytis cinerea*	*Solanum lycopersicum*	Bcpg1	Endopolygalacturonase
C18F Constitutive	ARMOST_17277	Cazy	IPR000743	GH28 / Glycoside hydrolase, family 28	PHI:103	*Botrytis cinerea*	*Solanum lycopersicum*	Bcpg1	Endopolygalacturonase
C18F Constitutive	ARMOST_12912	Non-Cazy	IPR000028	Chloroperoxidase	PHI:5188	*Magnaporthe oryzae*	*Oryza sativa*	MoHPX1	Dye-type peroxidase
C18F Constitutive	ARMOST_15491	Non-Cazy	IPR001128	Cytochrome P450	PHI:9266	*Fusarium proliferatum*	*Oryza sativa*	FUM6	Fumonisin C-14,C15-hydroxylase
C18F Constitutive	ARMOST_21614	Non-Cazy	IPR001128	Cytochrome P450	PHI:7173	*Verticillium dahliae*	*Gossypium hirsutum*	HiC-15	isotrichodermin C-15 hydroxylase
C18F Constitutive	ARMOST_07521	Non-Cazy	IPR001128	Cytochrome P450	PHI:7173	*Verticillium dahliae*	*Gossypium hirsutum*	HiC-15	isotrichodermin C-15 hydroxylase
C18F Constitutive	ARMOST_06306	Non-Cazy	IPR001128	Cytochrome P450	PHI:9266	*Fusarium proliferatum*	*Oryza sativa*	FUM6	Fumonisin C-14,C15-hydroxylase
C18F Constitutive	ARMOST_00213	Non-Cazy	IPR001128	Cytochrome P450	PHI:7173	*Verticillium dahliae*	*Gossypium hirsutum*	HiC-15	Isotrichodermin C-15 hydroxylase
C18F Constitutive	ARMOST_08320	Non-Cazy	IPR001128	Cytochrome P450	PHI:4607	*Bursaphelenchus xylophilus*	*Pinus massoniana*	BxCYP33C9	Cytochrome P450
C18F Constitutive	ARMOST_05711	Non-Cazy	IPR002938	FAD-binding domain	PHI:112	*Fusarium solani*	*Cicer arietinum*	MAK1	Maackiain detoxification

C18F Constitutive	ARMOST_04588	Non-Cazy	IPR002938	FAD-binding domain	PHI:112	*Fusarium solani*	*Cicer arietinum*	MAK1	Maackiain detoxification
C18F Constitutive	ARMOST_05456	Non-Cazy	IPR002938	FAD-binding domain	PHI:112	*Fusarium solani*	*Cicer arietinum*	MAK1	Maackiain detoxification
C18F Constitutive	ARMOST_05454	Non-Cazy	IPR002938	FAD-binding domain	PHI:112	*Fusarium solani*	*Cicer arietinum*	MAK1	Maackiain detoxification
C18F Constitutive	ARMOST_04595	Non-Cazy	IPR002938	FAD-binding domain	PHI:112	*Fusarium solani*	*Cicer arietinum*	MAK1	Maackiain detoxification
C18F Constitutive	ARMOST_03637	Non-Cazy	IPR018946	Alkaline phosphatase D-related	PHI:6122	*Fusarium graminearum*	*Zea mays*	FGSG_06610	Phosphatases

Supplementary material 6. *A. borealis* genes with putative roles in virulence: functional classification, InterPro domains, and PHIbase homologs.

Group	ProtID	type_of_sec	InterPro ID	Description	PHIbase ID	Pathogen species	Host species	Gene	Gene function
A6F Inducible	jgi|Armbor1|1926153	Cazy	IPR000172	AA3_2 / GMC oxidoreductase	PHI:10364	*Botrytis cinerea*	*Solanum lycopersicum*	BCIN_03g01540	Choline dehydrogenase
A6F Constitutive	jgi|Armbor1|1356237	Cazy	IPR002016	AA2 / Haem peroxidase	PHI:5186	*Magnaporthe oryzae*	*Oryza sativa*	MoAPX2	Class I peroxidase
A6F Constitutive	jgi|Armbor1|1744029	Cazy	IPR000172	AA3_2 / GMC oxidoreductase	PHI:10364	*Botrytis cinerea*	*Solanum lycopersicum*	BCIN_03g01540	Choline dehydrogenase
A6F Constitutive	jgi|Armbor1|1699834	Cazy	IPR000172	AA3_2 / GMC oxidoreductase	PHI:10364	*Botrytis cinerea*	*Solanum lycopersicum*	BCIN_03g01540	Choline dehydrogenase
A6F Constitutive	jgi|Armbor1|1987737	Cazy	IPR000172	AA3_2 / GMC oxidoreductase	PHI:10364	*Botrytis cinerea*	*Solanum lycopersicum*	BCIN_03g01540	Choline dehydrogenase
A6F Constitutive	jgi|Armbor1|1941457	Cazy	IPR000172	AA3_2 / GMC oxidoreductase	PHI:10364	*Botrytis cinerea*	*Solanum lycopersicum*	BCIN_03g01540	Choline dehydrogenase
A6F Constitutive	jgi|Armbor1|123718	Cazy	IPR000743	GH28 / Glycoside hydrolase, family 28	PHI:492	*Botrytis cinerea*	*Solanum lycopersicum / Phaseolus vulgaris*	BcPG2	Endopolygalacturonase
A6F Constitutive	jgi|Armbor1|1277186	Cazy	IPR001722	GH7 / Glycoside hydrolase, family 7	PHI:10659	*Phytophthora sojae*	*Glycine max*	PsGH7a	Glycoside hydrolase, family 7
A6F Constitutive	jgi|Armbor1|1739286	Cazy	IPR001722	GH7 / Glycoside hydrolase, family 7	PHI:10659	*Phytophthora sojae*	*Glycine max*	PsGH7a	Glycoside hydrolase, family 7
A6F Constitutive	jgi|Armbor1|1777836	Cazy	IPR004898	PL3_2 / Pectate lyase PlyH/PlyE-like	PHI:179	*Fusarium solani*	*Pisum sativum*	PELD	Pectate lyase
A6F Constitutive	jgi|Armbor1|1467293	Cazy	IPR004898	PL3_2 / Pectate lyase PlyH/PlyE-like	PHI:180	*Fusarium solani*	*Pisum sativum*	PELA	Pectate lyase
A6F Constitutive	jgi|Armbor1|1999178	Cazy	IPR004898	PL3_2 / Pectate lyase PlyH/PlyE-like	PHI:180	*Fusarium solani*	*Pisum sativum*	PELA	Pectate lyase
A6F Constitutive	jgi|Armbor1|2082336	Cazy	IPR000743	GH28 / Glycoside hydrolase, family 28	PHI:103	*Botrytis cinerea*	*Solanum lycopersicum*	Bcpg1	Endopolygalacturonase
A6F Constitutive	jgi|Armbor1|1904159	Cazy	IPR000743	GH28 / Glycoside hydrolase, family 28	PHI:103	*Botrytis cinerea*	*Solanum lycopersicum*	Bcpg1	Endopolygalacturonase

A6F Constitutive	jgi|Armbor1|577390	Cazy	IPR000743	GH28 / Glycoside hydrolase, family 28	PHI:103	*Botrytis cinerea*	*Solanum lycopersicum*	Bcpg1	Endopolygalacturonase
A6F Constitutive	jgi|Armbor1|583912	Cazy	IPR000743	GH28 / Glycoside hydrolase, family 28	PHI:103	*Botrytis cinerea*	*Solanum lycopersicum*	Bcpg1	Endopolygalacturonase
A6F Constitutive	jgi|Armbor1|1466796	Non-Cazy	IPR000028	Chloroperoxidase	PHI:5188	*Magnaporthe oryzae*	*Oryza sativa*	MoHPX1	Dye-type peroxidase
A6F Constitutive	jgi|Armbor1|1741355	Non-Cazy	IPR000209	Peptidase S8/S53 domain	PHI:8858	*Verticillium dahliae*	*Gossypium hirsutum*	VdSSEP1 (VDAG-08100)	Serine endopeptidase
A6F Constitutive	jgi|Armbor1|1154540	Non-Cazy	IPR001128	Cytochrome P450	PHI:7173	*Verticillium dahliae*	*Gossypium hirsutum*	HiC-15	isotrichodermin C-15 hydroxylase
A6F Constitutive	jgi|Armbor1|2008440	Non-Cazy	IPR002938	FAD-binding domain	PHI:112	*Fusarium solani*	*Cicer arietinum*	MAK1	Maackiain detoxification
A6F Constitutive	jgi|Armbor1|107486	Non-Cazy	IPR002938	FAD-binding domain	PHI:112	*Fusarium solani*	*Cicer arietinum*	MAK1	Maackiain detoxification
A6F Constitutive	jgi|Armbor1|1736842	Non-Cazy	IPR010829	Cerato-platanin	PHI:9428	*Sclerotinia sclerotiorum*	*Nicotiana benthamiana / Brassica napus / Glycine max*	SsSm1 (SS1G_10096)	Cerato-platanin family protein
A6F Constitutive	jgi|Armbor1|1896746	Non-Cazy	IPR010829	Cerato-platanin	PHI:9428	*Sclerotinia sclerotiorum*	*Nicotiana benthamiana / Brassica napus / Glycine max*	SsSm1 (SS1G_10096)	Cerato-platanin family protein
A6F Constitutive	jgi|Armbor1|1706119	Non-Cazy	IPR013766	Thioredoxin domain	PHI:9867	*Ustilago maydis*	*Zea mays*	Pdi (UMAG_10156)	Protein disulfide-isomerase

Supplementary material 7. RNA-Seq mapping statistics for *A. ostoyae* and *A. borealis* growing in the autoclaved stems.

Condition	Organism	Number of input reads	Uniquely mapped reads %	% of reads mapped to multiple loci	Mapping Percentage
C2 Control 1	*A. ostoyae*	23,996,926	28.76%	63.65%	92.41%
C2 Control 2	*A. ostoyae*	20,742,647	15.99%	78.41%	94.40%
C2 Control 3	*A. ostoyae*	25,833,164	52.32%	35.01%	87.33%
C18 Control 1	*A. ostoyae*	24,103,630	64.89%	17.90%	82.79%
C18 Control 2	*A. ostoyae*	24,511,742	49.14%	42.31%	91.45%
C18 Control 3	*A. ostoyae*	22,961,637	44.84%	47.92%	92.76%
C2 Autoclaved Stems 1	*A. ostoyae*	51,302,102	24.87%	23.13%	48.00%
C2 Autoclaved Stems 2	*A. ostoyae*	39,294,340	27.54%	26.11%	53.65%
C2 Autoclaved Stems 3	*A. ostoyae*	44,919,246	46.01%	7.41%	53.42%
C18 Autoclaved Stems 1	*A. ostoyae*	39,144,074	30.53%	17.49%	48.02%
C18 Autoclaved Stems 2	*A. ostoyae*	50,261,186	46.88%	8.91%	55.79%
C18 Autoclaved Stems 3	*A. ostoyae*	40,455,649	41.70%	12.36%	54.06%
A4 Control 1	*A. borealis*	26,501,970	56.64%	12.87%	69.51%
A4 Control 2	*A. borealis*	26,132,116	69.67%	19.12%	88.79%
A4 Control 3	*A. borealis*	27,056,228	42.53%	5.33%	47.86%
A6 Control 1	*A. borealis*	24,980,215	63.74%	15.52%	79.26%
A6 Control 2	*A. borealis*	26,696,080	55.53%	9.29%	64.82%
A6 Control 3	*A. borealis*	25,849,235	48.22%	6.17%	54.39%
A4 Autoclaved Stems 1	*A. borealis*	68,981,909	53.84%	37.06%	90.90%
A4 Autoclaved Stems 2	*A. borealis*	78,769,877	52.16%	39.39%	91.55%
A4 Autoclaved Stems 3	*A. borealis*	81,776,100	42.26%	39.16%	81.42%
A6 Autoclaved Stems 1	*A. borealis*	88,301,273	56.83%	17.76%	74.59%
A6 Autoclaved Stems 2	*A. borealis*	71,712,994	62.60%	23.56%	86.16%
A6 Autoclaved Stems 3	*A. borealis*	86,316,046	61.64%	8.69%	70.33%

Supplementary material 8. Heatmap of mycoremediation-related oxidoreductase counts. Fungal species are on the top X-axis, and the enzyme names are listed along the Y-axis. The intensity of the cell colour correlates with the number of counts of a particular enzyme. # Enzyme clusters enriched in armillarioids. # Involved in PAH degradation.

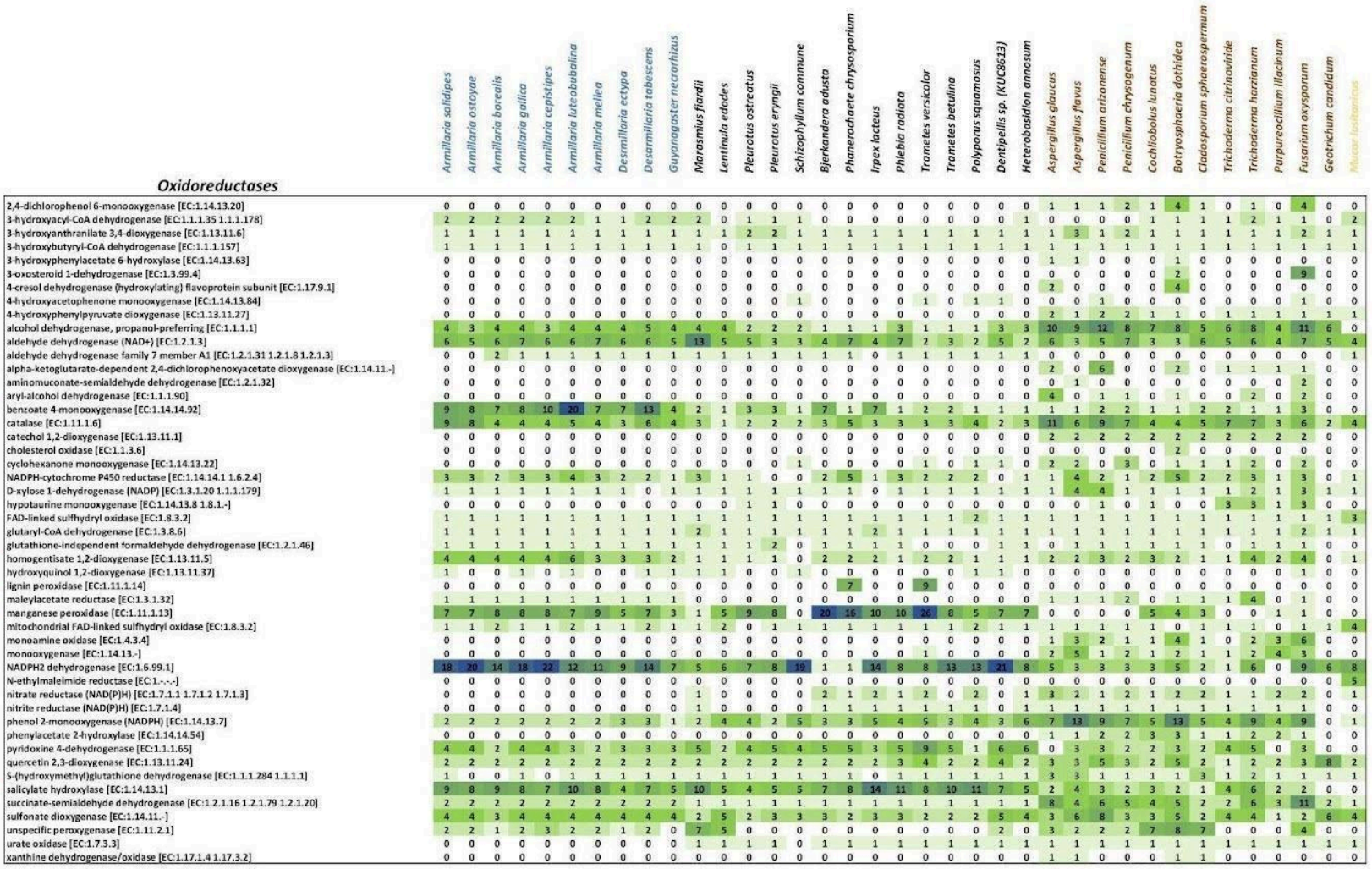

Supplementary material 9. Heatmap of mycoremediation-related hydrolase, transferase, isomerase, ligase and lyase counts. Fungal species are on the top X-axis, and the enzyme names are listed along the Y-axis. The intensity of the cell color correlates with the number of counts of a particular enzyme. # Enzyme clusters enriched in armillarioids. # Involved in PAH degradation.